Lawrence Berkeley Laboratory
UNIVERSITY OF CALIFORNIA

Presented at the International Summer School on Nuclear Astrophysics,
Tianjin, P.R. China, June 17–27, 1991, and to be published in the Proceedings

Rotating Relativistic Neutron Stars

F. Weber and N.K. Glendenning

August 1990

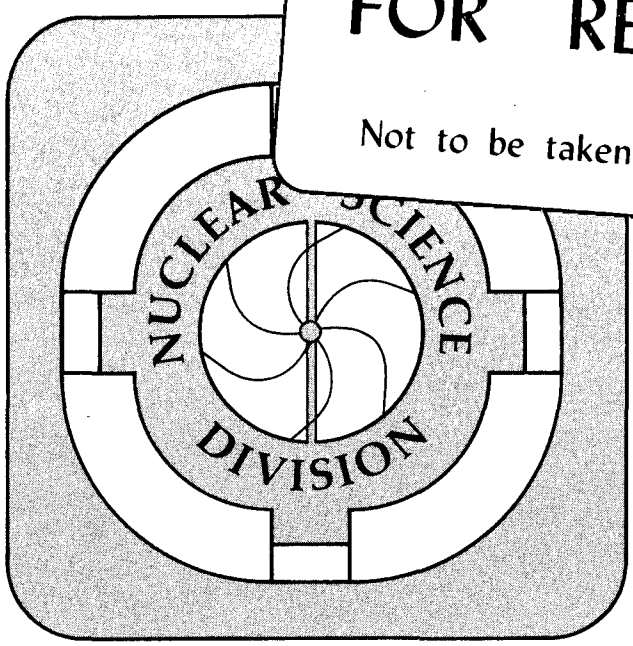

Prepared for the U.S. Department of Energy under Contract Number DE-AC03-76SF00098

DISCLAIMER

LBL - 29106

Rotating Relativistic Neutron Stars*

F. Weber† and N. K. Glendenning

Nuclear Science Division
Lawrence Berkeley Laboratory
University of California
Berkeley, California 94720, U.S.A.

July 21, 1991

Precis of an Invited Course on
Hadronic Matter and Rotating Relativistic Neutron Stars
Held at the
International Summer School on Nuclear Astrophysics
Tianjin, P. R. China, June 17 - 27, 1991
To be published in the Proceedings by World Scientific

*This work was supported by the Director, Office of Energy Research, Office of High Energy and Nuclear Physics, Division of Nuclear Physics, of the U.S. Department of Energy under Contract DE-AC03-76SF00098, and by the Max Kade Foundation of New York.

†Max Kade Foundation Research Fellow. Permanent address: Institute for Theoretical Physics, University of Munich, Theresienstrasse 37/III, D-8000 Munich 2, Federal Republic of Germany.

Contents

Rotating Relativistic Neutron Stars*

F. Weber† and N. K. Glendenning

Nuclear Science Division
Lawrence Berkeley Laboratory
University of California
Berkeley, California 94720, U.S.A.

July 21, 1991

Abstract

Models of rotating neutron stars are constructed in the framework of Einstein's theory of general relativity. For this purpose a refined version of Hartle's method is applied. The properties of these objects, e.g. gravitational mass, equatorial and polar radius, eccentricity, red- and blueshift, quadrupole moment, are investigated for Kepler frequencies of 4000 $s^{-1} \leq \Omega_K \leq$ 9000 s^{-1}. Therefore a self-consistency problem inherent in the determination of Ω_K must be solved. The investigation is based on neutron star matter (electrically charge neutral many-baryon/lepton system at zero temperature) equations of state derived from the relativistic Martin-Schwinger hierarch of coupled Green's functions. By means of introducing the Hartree, Hartree-Fock, and ladder (Λ) approximations, models of the equation of state are derived. A special feature of the latter approximation scheme is the inclusion of dynamical (Brueckner-type) two-particle correlations. These have been calculated from the relativistic T-matrix (effective two-particle interaction in matter) applying both the HEA and Bonn meson-exchange potentials of the nucleon-nucleon force. The nuclear forces of the former two treatments are those of the standard scalar-vector-isovector model of quantum hadron dynamics, with parameters adjusted to the nuclear matter data. An important aspect of this work consists in testing the compatibility of different competing models of the nuclear equation of state with data on pulsar periods. By this the fundamental problem of nuclear physics concerning the behavior of the equation of state at supernuclear densities can be treated.

PACS 11.10.Ef, 21.65.+f, 97.10.Kc, 97.60.Jd

*This work was supported by the Director, Office of Energy Research, Office of High Energy and Nuclear Physics, Division of Nuclear Physics, of the U.S. Department of Energy under Contract DE-AC03-76SF00098, and by the Max Kade Foundation of New York.

†Max Kade Foundation Research Fellow. Permanent address: Institute for Theoretical Physics, University of Munich, Theresienstrasse 37/III, D-8000 Munich 2, Federal Republic of Germany.

Rotating Relativistic Neutron Stars

F. Weber[1] and N. K. Glendenning

July 21, 1991

1 Introduction

The number of observed pulsars has increased rapidly since the discovery of the first one, CP1919, in 1967. The sources of pulsars have been interpreted as rapidly rotating, highly magnetized neutron stars [1]. To date about 500 pulsars are known [2], and the fastest of them have rotational periods in the millisecond range, e.g. pulsars 1937+21 and 1957+20 with periods of P=1.6 msec. At such high rotational frequencies the influence of rotation on the properties of pulsars becomes important [3].

In this article we continue our investigation of the properties of rotating neutron stars in the framework of Einstein's theory of general relativity [4]. The *exact* solution of Einstein's equations for massive rotating objects is known to be a cumbersome and complicated task [3]. An alternative method, which is easier to implement and has proven to be a practical tool for the construction of models of rotating neutron stars [5, 6] is Hartle's perturbative formalism [7, 8]. Within the latter a perturbative solution of the rotating stellar structure equations, based on the Schwarzschild metric, is developed. We perform our investigations in the framework of this method [4].

In Ref. [4] rotating star models have been constructed based on four different relativistic *neutron matter* (electrically charge neutral system of interacting baryons $(p, n, \Sigma^{\pm,0}, \Lambda, \Xi^{0,-}, \Delta^{++,\pm,0,-})$ and leptons in generalized β equilibrium) equations of state. Two of them (denoted by HV and HFV) are calculated for the relativistic Hartree (H) [9] and Hartree-Fock (HF) [10] approximation. The remaining two equations of state contain the influence of "dynamical" (Brueckner-type) two-particle correlations which are connected with a two-body meson-exchange potential. We

[1]Max Kade Foundation Research Fellow. Permanent address: Institute for Theoretical Physics, University of Munich, Theresienstrasse 37/III, D-8000 Munich 2, Federal Republic of Germany.

study these correlations for the so-called Λ^{00} ladder approximation [11] of the scattering (T) matrix by applying the Bonn [12] and HEA [13] meson-exchange potentials. The basic structure of the Λ approximation is similar to the well-known Brueckner approach [14, 15, 16, 17]. An essential difference between the Λ and Hartree-Fock approach is the different behavior of the resulting equations of state at small nuclear densities. This has its origin in the different T matrices in both of these methods. As discussed in detail in Ref. [4], in the framework of the Hartree-Fock method, the T-matrix is simply given in terms of free-meson propagators multiplied with meson-baryon vertex functions. The coupling constants of the HF theory are adjusted to the bulk properties of infinite nuclear matter (saturation density, binding energy, symmetry energy, compression modulus, and effective nucleon mass). This is in contrast to the ladder approximation where an integral equation for T must be solved. The Hartree-Fock "T-matrix" is then just the Born term of this integral equation. The T-matrix of the ladder approximation has *no free parameters* since (as described above) meson-exchange models of the nucleon-nucleon force with parameters determined from nuclear scattering data and the properties of the deuteron serve as an input.

The application of the Λ method is however restricted to not too large nuclear densities ϱ. As discussed in Ref. [4] an upper limit of $\varrho \lesssim 2\varrho_0$ is typical. In neutron star models central densities of $\approx 10\varrho_0$ are typical. Therefore the equation of state of neutron star matter must be determined up to such high densities. To overcome this problem we have combined the equations of state calculated for the Λ approximation with those of the Hartree and Hartree-Fock method. The latter equations of state are calculated for neutron star matter (i.e. nucleons, hyperons, eventually more massive baryons like the Δ resonance, electrons and muons) at zero temperature. In other words our equations of state include all baryon states which relativistic nuclear field theory, treated in the Hartree and Hartree-Fock approximation, predicts. [9, 10].

On a first sight the above described combination scheme may occur rather arbitrary. This is however not the case for the following reason. Since an enormous density range is involved in the determination of the nuclear equation of state, the composition of matter, and by this its complexity, changes considerably. In short the treatment of the many-body problem gets the easier the closer the nuclear density is to ϱ_0 since then neutron star matter consists to a good approximation of neutrons only, and this is when the T-matrix method is applicable.

Our theoretical analysis of the many-body problem is performed in the framework of relativistic Green's functions. These are coupled with each other by the so-called Martin-Schwinger hierarchy [18]. We show how the Hartree, Hartree-Fock, and ladder approximations emerge from the Martin-Schwinger hierarchy.

The article is organized as follows. First, we summarize in Sect. 2 the hierarchy of Hartle's rotating stellar structure equations in a representation which (i) they take on when the metric functions are defined according to the conventions of Friedman, Ipser, and Parker [3], and (ii) is adequate for the numerical treatment. In Sect. 3 we introduce the Lagrangian that governs the dynamics of many-baryon/lepton star matter. We derive the matter equations (i.e. T-matrix, mass-operator, energy-momentum relation of a baryon) as well as the equations of state of the system by introducing the relativistic Green's function method. Furthermore we establish the connection of our treatment with Walecka's $\sigma-\omega$ mean-field approximation [14]. The self-consistent solution of the hierarchy of neutron matter equations is discussed in Sect. 4. In Sect. 6 we, firstly, compare the characteristics of the different equations of state of this work. Secondly, the outcome of rotating neutron star calculations is presented for sequences of stars rotating at their respective Kepler frequencies, $\Omega_{\rm K}$. The self-consistency problem encountered in the determination of $\Omega_{\rm K}$ for these models is described. Important properties of the rotating star models are given in tabulated form. The impact of the pure general relativistic effect of the dragging of local inertial frames is investigated in detail at the end of this section. A summary is given in Sect. 7. Useful relations and mathematical details concerning the many-body Green's function formalism are outlined in the Appendix.

2 Treatment of rotating neutron stars in general relativity

Neutron stars are objects of highly compressed matter so that the geometry of space-time is changed considerably from flat space. Thus for the construction of realistic stellar models of neutron stars one has to resort to Einstein's theory of general relativity. Therein the Einstein curvature tensor $\mathcal{G}_{\mu\nu}$ is coupled to the energy-momentum density tensor $\mathcal{T}_{\mu\nu}$ of matter (G denotes the gravitational constant, cf. Table 1) [19, 20]:

$$\mathcal{G}_{\mu\nu} \;=\; 8\,\pi\,G\,\mathcal{T}_{\mu\nu}\;. \tag{1}$$

The tensor $\mathcal{T}_{\mu\nu}$ is derivable from the star's matter Lagrangian $\mathcal{L}_m$,

$$\frac{\delta \mathcal{L}_m}{\delta \chi} - \partial_\mu \frac{\delta \mathcal{L}_m}{\delta (\partial_\mu \chi)} = 0 , \qquad \text{for each matter field } \chi . \tag{2}$$

From Eq. (1) it follows that the field equations for empty space are

$$\mathcal{R}_{\mu\nu} = 0 . \tag{3}$$

The matter Lagrangian $\mathcal{L}_m$ of Eq. (2) is in the case of neutron star matter a complicated function of various baryon ($p, n, \Sigma^{\pm,0}, \Lambda, \Xi^{0,-}, \Delta^{++,+,0,-}$), meson ($\sigma, \omega, \pi, \varrho, \eta, \delta, \phi$), and lepton ($e^-, \mu^-$) fields. [9, 10, 21]. Nuclear many-particle physics and astrophysics are connected through Eqs. (1) and (2) with each other. We will turn back to the treatment of Eq. (2) in Sect. 3. Before, however, the application of Eq. (1) to rotating neutron stars in the framework of Hartle's method will be discussed. His treatment is based on a perturbation solution on the Schwarzschild metric of a spherically symmetric, static object.

2.1 Non-rotating structure equations

For a static metric describing a spherically symmetric space, the solution of the Einstein equation (1) is known to have the form [22, 23, 19]

$$ds^2 = -e^{2\,\Phi(r)} dt^2 + e^{2\,\Lambda(r)} dr^2 + r^2 \left(d\theta^2 + \sin^2\theta \, d\phi^2\right) , \tag{4}$$

where $\Phi(r)$ and $\Lambda(r)$ are the metric functions. Everywhere outside the star the empty-space Einstein equation (3) holds. The corresponding unique solution of Eq. (3) is known as the Schwarzschild metric. By denoting the (spherical) star's radius and mass by R_s and M_s, respectively, and introducing the abbreviation

$$\Upsilon = \begin{cases} 2\, m\, G \,/\, r & \text{if } r < R_s , \\ 2\, M_s\, G \,/\, r & \text{if } r > R_s , \end{cases} \tag{5}$$

the metric functions of Eq. (4) are then given by

$$e^{2\,\Lambda(r)} = \frac{1}{1 - \Upsilon(r)} , \tag{6}$$

$$e^{2\,\Phi(r)} = e^{-\,2\,\Lambda(r)} = 1 - \Upsilon(r) \qquad \text{(outside the star)} . \tag{7}$$

The structure of spherical neutron stars is determined by the Oppenheimer-Volkoff equations [24, 23] of hydrostatic equilibrium (all quantities denoted by a hat here and in the following are dimensionless; for the conventions, see Table 1):

$$\frac{d\hat{P}}{d\hat{r}} = -\,\hat{G}\,\hat{r}^{-2} \left(\hat{\epsilon}(\hat{r}) + \hat{P}(\hat{r})\right) \left(\hat{m}(\hat{r}) + 4\pi\kappa\hat{r}^3\hat{P}(\hat{r})\right) \left(1 - \Upsilon(\hat{r})\right)^{-1} , \tag{8}$$

Table 1: Key to the dimensionless quantities introduced in Sect. 2.

Quantity	Symbol	Dimensionless notation	Defined in equation
Radial coordinate	r	$\hat{r} = r/r_0$	
Gravitational constant	G †	$\hat{G} = G\,M_\odot/r_0$	
Gravitational mass	M	$\hat{M} = M/M_\odot$	(9)
Baryon mass	M_A	$\hat{M}_A = \hat{m}_n A$	(207), (208)
Proper mass	M_P	$\hat{M}_P = M_P/M_\odot$	(12)
Change of mass due to rotation	ΔM	$\Delta\hat{M} = \Delta M/M_\odot$	(35)
Mass of neutron	m_n	$\hat{m}_n = m_n/m_\odot$	
Monopole mass perturbation function	m_0	$\hat{m}_0 = m_0/M_\odot$	(32), (34)
Quadrupole mass perturbation function	m_2	$\hat{m}_2 = m_2/r_0$	(59)
Monopole stretching function	ξ_0	$\hat{\xi}_0 = \xi_0/r_0$	(61)
Quadrupole stretching function	ξ_2	$\hat{\xi}_2 = \xi_2/r_0$	(62)
Quadrupole moment	Π	$\hat{\Pi} = \Pi/(R_s^2\,M_s)$	(66)
Energy density	ϵ	$\hat{\epsilon} = \epsilon/\epsilon_c$	(162), (164), (181), (195)
Pressure	P	$\hat{P} = P/\epsilon_c$	(179), (180), (196)
Number density	ϱ	$\hat{\varrho} = \varrho\, r_0^3$	(169)
Angular velocity relative to infinity	Ω	$\hat{\Omega} = \Omega\, r_0$	(30)
Angular velocity relative to the local inertial frame	$\bar{\omega}$	$\hat{\bar{\omega}} = \bar{\omega}\, r_0$	(26)
Moment of inertia	I	$\hat{I} = I/(\kappa\, M_\odot\, r_0^2)$ ‡	(31)
Angular momentum	J	$\hat{J} = J/(\kappa\, M_\odot\, r_0)$	(29)
Rotational energy	T	$\hat{T} = T/M_\odot$	(77)
Total gravitational mass	W	$\hat{W} = \hat{M}_P + \hat{T} - \hat{M}$	(78)

† $G = 2.612 \cdot 10^{-40}$ fm^2, fm^{-1} = 197.33 MeV, $M_\odot = 1.116 \cdot 10^{60}$ MeV.

‡ The scaling factor κ is defined by $\kappa \equiv \epsilon_c\, r_0^3\, /\, M_\odot$ ($r_0 \simeq 3 \cdot 10^{19}$ fm).

with the boundary condition $\hat{P}(\hat{r}=0) \equiv \hat{P}(\epsilon_c) \equiv \hat{P}_c$ [24, 25, 26, 9, 27]. The mass contained in a sphere of radius r ($\leq R_s$), denoted by $m(r)$, follows from the energy density $\epsilon(r)$ (for the conversion of ϵ given in units of MeV/fm^3 to g/cm^3, see the footnote of Table 2):

$$\hat{m}(\hat{r}) = 4\pi\kappa \int_0^{\hat{r}} d\hat{r}'\, \hat{r}'^2\, \hat{\epsilon}(\hat{r}')\,. \tag{9}$$

The metric function $\Phi(r)$ satisfies the differential equation

$$\frac{d\Phi(\hat{r})}{d\hat{r}} = -\frac{1}{\hat{\epsilon}(\hat{r}) + \hat{P}(\hat{r})} \frac{d\hat{P}(\hat{r})}{d\hat{r}}\,, \tag{10}$$

with the boundary condition

$$\Phi(\hat{r} = \hat{R}_s) = \frac{1}{2} \ln\left[1 - \Upsilon(\hat{R}_s)\right]. \tag{11}$$

We note that the Oppenheimer-Volkoff equations (8) - (9) can only be solved once the equation of state of neutron matter, $P = P(\epsilon)$, has been specified. Then Eqs. (8) - (10) can be integrated outward from the star's origin at $r = 0$ until the pressure $P(r)$ vanishes. The point at which $P(r) = 0$ is the star's surface, and the value of r there its radius, R_s. The value of $m(r)$ of Eq. (9) at $r = R_s$ defines the star's total gravitational mass energy, i.e. $M_s \equiv m(R_s)$. For later use we define the proper star mass, which is given by

$$M_P = 4\pi \int_0^{\hat{R}_s} d\hat{r}\, \hat{r}^2 \frac{\hat{\epsilon}(\hat{r})}{\sqrt{1 - \Upsilon(\hat{r})}}\,. \tag{12}$$

2.2 Rotating structure equations

In this Section we summarize Hartle's set of rotating stellar structure equations, however rewritten for the metric of Friedmann, Ipser, and Parker. Furthermore, we introduce a notation that is convenient for the numerical treatment (cf. Table 1).

2.2.1 Rotational perturbations

The basic idea in Hartle's treatment is the development of a perturbation solution based on the Schwarzschild metric of Eq. (4). The assumption that under the influence of rotation the star distorts and the pressure, energy density, and baryon number

density change by amounts of ΔP, $\Delta\epsilon$, $\Delta\varrho$, respectively, the energy-momentum density tensor of Eq. (1) changes by $\Delta\mathcal{T}_{\mu\nu}$ and becomes ($g_{\mu\nu} = (-1,1,1,1)\,\delta_{\mu\nu}$) [7, 28]:

$$\mathcal{T}_{\mu\nu} \equiv \mathcal{T}^0_{\mu\nu} + \Delta\mathcal{T}_{\mu\nu}\,, \tag{13}$$

$$\mathcal{T}^0_{\mu\nu} \equiv (\epsilon + P)\,u_\mu\,u_\nu + P\;g_{\mu\nu}\,, \tag{14}$$

$$\Delta\mathcal{T}_{\mu\nu} \equiv (\Delta\epsilon + \Delta P)\,u_\mu\,u_\nu + \Delta P\;g_{\mu\nu}\,. \tag{15}$$

$\mathcal{T}^0_{\mu\nu}$ of Eqs. (13) and (14) denotes the perfect fluid energy-momentum tensor where P, ϵ, and ϱ are measured by an observer in a locally inertial frame co-moving with the fluid at the instant of measurement. From the baryon number density ϱ the total baryon number N_B of the star follows via

$$N_B = 4\pi \int_0^{\hat{R}_s} d\hat{r}\;\hat{r}^2 \frac{\hat{\varrho}(\hat{r})}{\sqrt{1-\Upsilon(\hat{r})}}\,. \tag{16}$$

The normalization of the fluids four-velocity u of Eqs. (14) and (15) is $g^{\mu\nu}\,u_\mu\,u_\nu = -1$. For the distortion functions of Eqs. (13) and (15) a multipole expansion is performed. Assuming aximal symmetry, one can write

$$\Delta P = (\epsilon + P)\;(p_0 + p_2\,P_2(\cos\theta))\,, \tag{17}$$

$$\Delta\epsilon = \Delta P\;\frac{\partial\epsilon}{\partial P}\,, \tag{18}$$

$$\Delta\varrho = \Delta P\;\frac{\partial\varrho}{\partial P}\,. \tag{19}$$

The quantity P_2 of Eq. (17) is the second order Legendre polynomial. The perturbed metric, expanded through second order in the star's rotational velocity, Ω, has in our notation the form [29, 3]

$$ds^2 = -e^{2\,\nu(r)}dt^2 + e^{2\,\psi(r)}\,(d\phi - \omega\,dt)^2 + e^{2\,\mu(r)}\,d\theta^2 + e^{2\,\lambda(r)}dr^2 + O\left(\Omega^3\right)\,. \tag{20}$$

Here, ω is the angular velocity of the local inertial frame and depends on the radial coordinate r. It is proportional to Ω (dragging of the local inertial frame). The velocity Ω is a constant throughout the star's fluid (uniformly rotating configuration). Of major interest in the following discussion is $\bar{\omega} \equiv \Omega - \omega$, the angular velocity of the fluid relative to the local inertial frame in terms of which the fluid inside the star moves. We remark that Hartle and Thorne have performed rotating star calculations

for $\Omega = \Omega_c$, where the latter critical angular velodity is defined by (Newtonian balance of centrifuge and gravity) [7, 8]

$$\Omega_c \equiv \sqrt{\Upsilon_s/(2\,R_s^2)} = 36\,\sqrt{[M_s/M_\odot]/[R_s/\mathrm{km}]^3}\cdot 10^4\ \mathrm{s}^{-1}\,. \tag{21}$$

The metric functions in the disturbed line element of Eq. (20) have the form [7, 8, 30, 3]

$$e^{2\,\nu(r,\Omega)} = e^{2\,\Phi(r)}\,[1 + 2\,(h_0(r,\Omega) + h_2(r,\Omega)\,P_2(\cos\theta))]\,, \tag{22}$$

$$e^{2\,\psi(r,\Omega)} = r^2\,\sin^2\theta\,[1 + 2\,(v_2(r,\Omega) - h_2(r,\Omega))\,P_2(\cos\theta)]\,, \tag{23}$$

$$e^{2\,\mu(r,\Omega)} = r^2\,[1 + 2\,(v_2(r,\Omega) - h_2(r,\Omega))\,P_2(\cos\theta)]\,, \tag{24}$$

$$e^{2\,\lambda(r,\Omega)} = e^{2\,\Lambda(r)}\left(1 + \frac{2}{r}\,\frac{m_0(r,\Omega)\,G + m_2(r,\Omega)\,P_2(\cos\theta)}{1 - \Upsilon(r)}\right)\,, \tag{25}$$

and are independent of time and azimuthal angle ϕ, expressing respectively stationary rotation and axial symmetry about the axis of rotation.

The above defined function $\bar{\omega}(r)$ is the solution of the differential equation

$$\frac{d}{d\hat{r}}\left(\hat{r}^4\,j(\hat{r})\,\frac{d\hat{\bar{\omega}}(\hat{r})}{d\hat{r}}\right) + 4\,\hat{r}^3\,\frac{dj(\hat{r})}{d\hat{r}}\,\hat{\bar{\omega}}(\hat{r}) = 0\,, \quad \hat{r} < \hat{R}_s\,, \tag{26}$$

where

$$j(\hat{r}) = e^{-\Phi(\hat{r})}\,\sqrt{1 - \Upsilon(\hat{r})}\,. \tag{27}$$

Eq. (26) is to be solved subject to the boundary conditions that (i) $\hat{\bar{\omega}}$ is regular at $\hat{r} = 0$ and (ii) $d\hat{\bar{\omega}}/d\hat{r}|_{\hat{r}=0} = 0$. In practice, one integrates Eq. (26) outward from the star's origin, where the boundary condition (i) is imposed by choosing an arbitrary value for $\hat{\bar{\omega}}$ at $\hat{r} = 0$, i.e. $\hat{\bar{\omega}}_c \equiv \hat{\bar{\omega}}(\hat{r} = 0)$ (e.g. Arnett and Bowers [26] use $\bar{\omega} = 1.82342\ \mathrm{s}^{-1}$). Outside the star one has

$$\hat{\bar{\omega}}(\hat{r}) = \hat{\Omega} - \frac{2\,\kappa\,\hat{G}}{\hat{r}^3}\,\hat{J}(\hat{\Omega})\,, \qquad \hat{r} > \hat{R}_s\,, \tag{28}$$

where $\hat{J}(\hat{\Omega})$ is the total angular momentum of the star, defined by

$$\hat{J}(\hat{\Omega}) = \frac{\hat{R}_s^4}{6\,\kappa\,\hat{G}}\,\left(\frac{d\hat{\bar{\omega}}}{d\hat{r}}\right)_{\hat{R}_s}\,. \tag{29}$$

From Eqs. (28) and (29) it follows that the angular velocity Ω - which corresponds to a given boundary value of $\hat{\bar{\omega}}_c$ - is then determined by

$$\hat{\Omega}(\hat{\bar{\omega}}_c) = \hat{\bar{\omega}}(\hat{R}_s) + \frac{2\,\kappa\,\hat{G}}{\hat{R}_s^3}\,\hat{J}(\hat{\Omega})\,. \tag{30}$$

The linearity of the differential equation for $\hat{\bar{\omega}}$ of Eq. (26) implies that a different value of $\hat{\Omega}$, denoted by $\hat{\Omega}^{\rm new}$, can be obtained by rescaling the function $\hat{\bar{\omega}}(\hat{r})$, i.e. $\hat{\bar{\omega}}^{\rm new}(\hat{r})=\hat{\bar{\omega}}^{\rm old}(\hat{r})\ \hat{\Omega}^{\rm new}/\hat{\Omega}^{\rm old}$. The star's momentum of inertia is defined by the ratio J/Ω. An alternative expression for I can be derived by integrating Eq. (26) and substituting $(d\hat{\bar{\omega}}/d\hat{r})|_{\hat{R}_s}$ of Eq. (29) in favor of $\hat{J}(\hat{\Omega})$. One arrives at (using $j(\hat{R}_s)=1$) [31, 32]

$$\hat{I}=\frac{\hat{J}(\hat{\Omega})}{\hat{\Omega}}=\frac{8\,\pi}{3}\int_0^{\hat{R}_s} d\hat{r}\ \hat{r}^4\ \frac{\hat{\epsilon}+\hat{P}}{\sqrt{1-\Upsilon}}\ \frac{\hat{\bar{\omega}}}{\hat{\Omega}}\ e^{-\Phi}\ . \tag{31}$$

2.2.2 Monopole equations

The set of coupled monopole ($l=0$) equations can be integrated once $\hat{\bar{\omega}}(\hat{r})$ is known from Eq. (26). The differential equation for the monopole mass disturbation function $\hat{m}_0$ (cf. Refs. [7, 8, 28, 33]),

$$\frac{d\hat{m}_0}{d\hat{r}}=4\pi\kappa\,\hat{r}^2\frac{d\hat{\epsilon}}{d\hat{P}}\,(\hat{\epsilon}+\hat{P})\cdot p_0+\frac{1}{12\,\hat{G}}\,j^2\,\hat{r}^4\,\left(\frac{d\hat{\bar{\omega}}}{d\hat{r}}\right)^2+\frac{8\pi}{3}\,\kappa\,\hat{r}^4\,j^2\,\frac{\hat{\epsilon}+\hat{P}}{1-\Upsilon}\,\hat{\bar{\omega}}^2\,, \tag{32}$$

is coupled to the monopole pressure perturbation function p_0,

$$\begin{aligned}\frac{dp_0}{d\hat{r}} \;=\; & -\hat{G}\,\frac{1+8\pi\kappa\hat{r}^2\hat{G}\hat{P}}{\hat{r}^2\,(1-\Upsilon)^2}\cdot\hat{m}_0\;-\;4\pi\kappa\hat{G}\,\frac{(\hat{\epsilon}+\hat{P})\,\hat{r}}{1-\Upsilon}\cdot p_0\\ & +\frac{1}{12}\,\frac{\hat{r}^3 j^2}{1-\Upsilon}\,\left(\frac{d\hat{\bar{\omega}}}{d\hat{r}}\right)^2+\frac{1}{3}\,\frac{d}{d\hat{r}}\,\left(\frac{\hat{r}^2 j^2\hat{\bar{\omega}}^2}{1-\Upsilon}\right)\,.\end{aligned} \tag{33}$$

The boundary conditions are that $\hat{m}_0\to 0$ and $p_0\to 0$ for $\hat{r}\to 0$. In the exterior star region $\hat{\bar{\omega}}$ of Eq. (28) can be substituted in Eqs. (32) and (2.33). One finds outside the star

$$\hat{m}_0\;=\;\Delta\hat{M}\;-\;\frac{\kappa^2\,\hat{G}}{\hat{r}^3}\,\hat{J}(\hat{\Omega})^2\,,\qquad\qquad \hat{r}>\hat{R}_s\,, \tag{34}$$

where $\Delta\hat{M}$ is the change in gravitational mass due to rotation. Evaluation of Eq. (34) at the star's surface leads for $\Delta\hat{M}$ to

$$\Delta\hat{M}=\hat{m}_0(\hat{R}_s)\;+\;\frac{\kappa^2\,\hat{G}}{\hat{R}_s^3}\,\hat{J}(\hat{\Omega})^2\,. \tag{35}$$

Here, $\Delta\hat{M}$ is known once the perturbation function $\hat{m}_0$ at the equator has been calculated. Numerical solutions of Eqs. (32) and (2.33) are found by integrating these equations outward from the origin with the boundary conditions

$$p_0(\hat{r})\;\longrightarrow\;\frac{1}{3}\,(j_c\,\hat{\bar{\omega}}_c)^2\,\hat{r}^2\qquad\qquad\text{for}\qquad\hat{r}\;\to\;0 \tag{36}$$

and

$$\hat{m}_0(\hat{r}) \longrightarrow \frac{4\,\pi}{15}\,\kappa\,(\hat{\epsilon}_c + \hat{P}_c)\,\left(2 + \left.\frac{d\hat{\epsilon}}{d\hat{P}}\right|_c\right)\,(j_c\,\hat{\omega}_c)^2\,\hat{r}^5 \quad \text{for} \quad \hat{r} \rightarrow 0\,, \tag{37}$$

respectively. The function h_0 of Eq. (22) can be calculated from the algebraic relations

$$h_0 = -\,p_0 + \frac{\hat{r}^2}{3}\hat{\omega}^2\,e^{-2\,\Phi} + h_{0c}\,, \qquad \hat{r} < \hat{R}_s\,, \tag{38}$$

and

$$h_0 = -\,\frac{\Delta\hat{M}\,\hat{G}}{\hat{r}\,(1-\Upsilon)} + \frac{\kappa^2\,\hat{J}^2\,\hat{G}^2}{\hat{r}^4\,(1-\Upsilon)}\,, \qquad \hat{r} > \hat{R}_s\,, \tag{39}$$

once $\hat{\omega}$, $\Delta\hat{M}$, $\hat{J}$, and p_0 are known. The quantity h_{0c} of Eq. (38) is a constant of integration which is to be specified by demanding that $h_0(\hat{r})$ is continuous across the star's surface.

2.2.3 Quadrupole equations

The $l = 2$ equations determine the shape of the rotating star. The disturbation functions v_2 and h_2 of Eqs. (22) - (24) satisfy the following coupled set of differential equations (cf. Refs. [7, 8, 28]):

$$\frac{dv_2}{d\hat{r}} = -\,2\,\frac{d\Phi}{d\hat{r}}\,\cdot\,h_2 + \left[\frac{1}{\hat{r}} + \frac{d\Phi}{d\hat{r}}\right]\left[-\frac{\hat{r}^3}{3}\,\frac{dj^2}{d\hat{r}}\,\hat{\omega}^2 + \frac{j^2}{6}\,\hat{r}^4\left(\frac{d\hat{\omega}}{d\hat{r}}\right)^2\right] \tag{40}$$

and

$$\begin{aligned}\frac{dh_2}{d\hat{r}} &= \left\{-\,2\,\frac{d\Phi}{d\hat{r}} + \frac{2\,\hat{G}}{1-\Upsilon}\left(\frac{d\Phi}{d\hat{r}}\right)^{-1}\left[2\pi\kappa\,(\hat{\epsilon}+\hat{P}) - \frac{\hat{m}}{\hat{r}^3}\right]\right\}\,\cdot\,h_2 \\ &- \frac{2}{\hat{r}^2\,(1-\Upsilon)}\left(\frac{d\Phi}{d\hat{r}}\right)^{-1}\,\cdot\,v_2 \\ &+ \frac{1}{6}\left[\hat{r}\,\frac{d\Phi}{d\hat{r}} - \frac{1}{2\,\hat{r}\,(1-\Upsilon)}\left(\frac{d\Phi}{d\hat{r}}\right)^{-1}\right]\hat{r}^3\,j^2\left(\frac{d\hat{\omega}}{d\hat{r}}\right)^2 \\ &- \frac{1}{3}\left[\hat{r}\,\frac{d\Phi}{d\hat{r}} + \frac{1}{2\,\hat{r}\,(1-\Upsilon)}\left(\frac{d\Phi}{d\hat{r}}\right)^{-1}\right](\hat{r}\,\hat{\omega})^2\,\frac{dj^2}{d\hat{r}}\,.\end{aligned} \tag{41}$$

Their boundary conditions are $h_2(0) = v_2(0) = 0$ and $h_2(\infty) = v_2(\infty) = 0$. Numerical solutions of Eqs. (40) and (41) can be computed by simultaneously integrating both of these equations outward from the origin. At the origin the solutions must be regular. An examination of Eqs. (40) and (41) for $\hat{r} \rightarrow 0$ leads to the behavior

$$h_2(\hat{r}) \longrightarrow A_2\,\hat{r}^2 \qquad \text{for} \quad \hat{r} \rightarrow 0\,, \tag{42}$$

and

$$v_2(\hat{r}) \longrightarrow B_2\,\hat{r}^4 \qquad \text{for} \quad \hat{r} \to 0\,, \tag{43}$$

where A_2 and B_2 are any dimensionless constants. The latter are related with each other by

$$B_2 + 2\pi\,\kappa\,A_2\,\hat{G}\,(\hat{P}_c + \frac{1}{3}\hat{\epsilon}_c) = -\frac{4\pi}{3}\,\kappa\,\hat{G}\,(\hat{\epsilon}_c + \hat{P}_c)\,(j_c\,\hat{\bar{\omega}}_c)^2\,. \tag{44}$$

Thus if an arbitrary value of B_2 is choosen, A_2 is given by the expression

$$A_2 = \left(B_2 - \frac{4\pi}{3}\,\kappa\,\hat{G}\,(\hat{\epsilon}_c + \hat{P}_c)\,(j_c\,\hat{\bar{\omega}}_c)^2\right)\,\left(2\,\pi\,\kappa\,\hat{G}\,(\hat{P}_c + \frac{\hat{\epsilon}_c}{3})\right)^{-1}\,. \tag{45}$$

The solutions $h_2^{(H)}$ and $v_2^{(H)}$ of the corresponding homogeneous set of differential equations of Eqs. (40) and (41) are for $\hat{r} \to 0$ given by

$$h_2^{(H)}(\hat{r}) \longrightarrow A_2\,\hat{r}^2 \qquad \text{for} \quad \hat{r} \to 0\,, \tag{46}$$

and

$$v_2^{(H)}(\hat{r}) \longrightarrow B_2\,\hat{r}^4 \qquad \text{for} \quad \hat{r} \to 0\,, \tag{47}$$

respectively, with A_2 and B_2 arbitrarily choosen, but now related by

$$B_2 + 2\pi\,\kappa\,A_2\,\hat{G}\,(\hat{P}_c + \frac{1}{3}\hat{\epsilon}_c) = 0\,. \tag{48}$$

The general solutions of Eqs. (40) and (41) are then given as superpositions calculated from the homogeneous and particular solutions in the form

$$v_2 = C_2\,v_2^{(H)} + v_2^{(P)}\,, \tag{49}$$

$$h_2 = C_2\,h_2^{(H)} + h_2^{(P)}\,. \tag{50}$$

The solutions v_2 and h_2 of Eqs. (49) and (50) are to be matched with the exterior solutions of Eqs. (40) and (41), given by

$$v_2^{>} = -\left(\frac{\kappa\,\hat{G}\hat{J}}{\hat{r}^2}\right)^2 + A_2\frac{\Upsilon}{\sqrt{1-\Upsilon}}\,Q_2^1\left(\frac{2}{\Upsilon} - 1\right) \tag{51}$$

and

$$h_2^{>} = \left(\frac{\kappa\,\hat{G}\hat{J}}{\hat{r}^2}\right)^2\left(1 + \frac{2}{\Upsilon}\right) + A_2\,Q_2^2\left(\frac{2}{\Upsilon} - 1\right)\,. \tag{52}$$

Q_2^1 and Q_2^2 occuring in Eqs. (51) and (52) are associated Legendre polynomials of the second kind:

$$Q_2^1(x) = \sqrt{x^2-1}\left[\frac{3x^2-2}{x^2-1} - \frac{3}{2}x\,\ln\frac{x+1}{x-1}\right], \qquad x > 1\,, \tag{53}$$

$$Q_2^2(x) = \left[\frac{3}{2}(x^2-1)\,\ln\frac{x+1}{x-1} - \frac{3x^3-5x}{x^2-1}\right], \qquad x > 1\,. \tag{54}$$

By adjusting the general exterior solution $h_2^>$ of Eq. (52) and its first derivative to the interior solution of Eq. (50) at $\hat{r} = \hat{R}_s$, i.e.

$$h_2^<(\hat{R}_s) = h_2^>(\hat{R}_s)\,, \tag{55}$$

$$\frac{d}{d\hat{r}}h_2^<(\hat{R}_s) = \frac{d}{d\hat{r}}h_2^>(\hat{R}_s)\,, \tag{56}$$

the integration constants A_2 and C_2 can be determined. One finds

$$\begin{aligned} A_2 = {} & \left\{\left[\left(\frac{\kappa\hat{G}\hat{J}}{\hat{R}_s^2}\right)^2\left(1+\frac{\Upsilon_s}{2}\right)^{-1} - h_2^{(P)}\right]\frac{1}{h_2^{(H)}(\hat{R}_s)}\frac{dh_2^{(H)}(\hat{R}_s)}{d\hat{r}} + \frac{dh_2^{(P)}(\hat{R}_s)}{d\hat{r}}\right. \\ & \left. - \left(\frac{\kappa\hat{G}\hat{J}}{\hat{R}_s^2}\right)^2\frac{1}{R_s}\left(1+\frac{\Upsilon_s}{2}\right)^{-1}\left[\frac{\Upsilon_s/2}{1+\Upsilon_s/2}-4\right]\right\} \\ & \times \left\{\frac{dQ_2^2(2/\Upsilon_s-1)}{d\hat{r}} - \frac{Q_2^2(2/\Upsilon_s-1)}{h_2^{(H)}(\hat{R}_s)}\frac{dh_2^{(H)}(\hat{R}_s)}{d\hat{r}}\right\}^{-1}, \end{aligned} \tag{57}$$

and

$$\begin{aligned} C_2 = {} & \left[\left(\frac{\kappa\hat{G}\hat{J}}{\hat{R}_s^2}\right)^2\left(1+\frac{\Upsilon_s}{2}\right)^{-1} + A_2\,Q_2^2(2/\Upsilon_s-1) - h_2^{(P)}(\hat{R}_s)\right] \\ & \times \left[h_2^{(H)}(\hat{R}_s)\right]^{-1}\,. \end{aligned} \tag{58}$$

The quadrupole mass and pressure perturbation functions, $\hat{m}_2$ and p_2, respectively, can be calculated once h_2 is known. The expression for $\hat{m}_2$ is

$$\hat{m}_2 = \hat{r}\,(1-\Upsilon)\left[-h_2 - \frac{\hat{r}^3}{3}\left(\frac{dj^2}{d\hat{r}}\right)\hat{\bar{\omega}}^2 + \frac{\hat{r}^4 j^2}{6}\left(\frac{d\hat{\bar{\omega}}}{d\hat{r}}\right)^2\right]. \tag{59}$$

The pressure perturbation function satisfies

$$p_2 = -h_2 - \frac{1}{3}(\hat{r}\,\hat{\bar{\omega}})^2\,e^{-2\Phi}\,. \tag{60}$$

Eq. (60) completes the Hartle hierarchy of rotating stellar structure equations. From the functions p_0, p_2, v_2, h_2 and the integration constant A_2 the properties of the

rotationally deformed star can be calculated. We begin with the spherical stretching, denoted by ξ_0, due to rotation. This quantity follows from the monopole function p_0 in the form

$$\hat{\xi}_0 \;=\; -\,p_0\,(\hat{\epsilon}+\hat{P})\,\left(\frac{d\hat{P}}{d\hat{r}}\right)^{-1}\;. \tag{61}$$

Knowledge of the quadrupole stretching function, ξ_2, given by

$$\hat{\xi}_2 \;=\; -\,p_2\,(\hat{\epsilon}+\hat{P})\,\left(\frac{d\hat{P}}{d\hat{r}}\right)^{-1}\;, \tag{62}$$

is necessary to determine the displacement of the star's surface of constant given density that lies on radius $\hat{r}$ in the non-rotating configuration. An invariant parametrization of a surface of constant density is given by (θ^* denotes the polar angle) [8]

$$\hat{r}^*(\theta^*) \;=\; \hat{r} \;+\; \hat{\xi}_0(\hat{r}) \;+\; \left\{\hat{\xi}_2(\hat{r}) \;+\; \hat{r}\,[v_2(\hat{r}) - h_2(\hat{r})]\right\}\; P_2(\cos\theta^*)\;. \tag{63}$$

The star's eccentricity, defined according to Hartle, is

$$e^{\rm HT} \;=\; \sqrt{\left(\frac{\hat{R}_{\rm eq}}{\hat{R}_{\rm p}}\right)^2 \;-\; 1} \;=\; \sqrt{-\,3\,[v_2(\hat{r}) - h_2(\hat{r}) + \frac{\hat{\xi}_2(\hat{r})}{\hat{r}}]}\;\Bigg|_{\hat{r}=\hat{R}_s}\;. \tag{64}$$

In this work we make also use of the definition given by Friedman, Ipser, and Parker [3]:

$$e^{\rm FIP} \;=\; \sqrt{1 \;-\; \left(\frac{\hat{R}_{\rm p}}{\hat{R}_{\rm eq}}\right)^2}\;. \tag{65}$$

The integration constant A_2 of Eq. (57) is related to the mass quadrupole moment of the rotating star by

$$\hat{\Pi} \;=\; \frac{8}{5}\,A_2\,\left(\frac{\Upsilon_s}{2}\right)^2 \;+\; \kappa\,\hat{G}\left(\frac{\hat{J}}{\hat{R}_s}\right)^2\;. \tag{66}$$

In summary the following set of equations is to be solved to determine the properties of a rotating star configuation:

1. Eqs. (8) - (10): Mass $\hat{M}$ and radius $\hat{R}_s$ of the spherical (non-rotating) star; furthermore pressure $\hat{P}(\hat{r})$, energy density $\hat{\epsilon}(\hat{r})$, and metric function $\Phi(\hat{r})$ for $0 \le \hat{r} \le \hat{R}_s$;

2. Eq. (26): Angular velocity $\hat{\bar{\omega}}$;

3. Eqs. (32) and (33): Monopole disturbation functions $\hat{m}_0$, p_0; Eqs. (38) and (39): M onopole disturbation function h_0;

4. Eqs. (40) and (41): Quadrupole disturbation functions v_2, h_2; Eqs. (59) and (60): Quadrupole disturbation functions $\hat{m}_2$, p_2.

2.3 Maximum rotation of relativistic stars

No simple stability criteria are known for rotating star configurations in general relativity. An absolute upper limit on neutron star rotation is however set by the Kepler frequency $\Omega_{\rm K}$, beyond which instability sets in because of mass shedding at the star's equator. For the metric functions of Eqs. (22) and (23), the Kepler frequency is given as the solution Ω of [3]

$$\Omega = \left[e^{\nu(\omega)-\psi(\Omega)} \; V(\Omega) + \omega(\Omega) \right]_{\rm eq} , \tag{67}$$

$$V(\Omega) \equiv \left[\frac{\omega(\Omega)'}{2\,\psi(\Omega)'} \, e^{\psi(\Omega)-\nu(\Omega)} + \sqrt{\frac{\nu(\Omega)'}{\psi(\Omega)'} + \left(\frac{\omega(\Omega)'}{2\,\psi(\Omega)'} \, e^{\psi(\Omega)-\nu(\Omega)} \right)^2} \right]_{\rm eq} . \tag{68}$$

The subscipt "eq" refers to evaluation of Eqs. (67) and (68) at the star's quator. The quantity V denotes the orbital velocity measured by an observer with zero angular momentum in the ϕ-direction. Primes denote derivatives with respect to the radial coordinate. If one neglects the distortion functions in the metric of Eq. (20) and sets $\bar{\omega} \equiv \Omega$ (i.e. the star's fluid moves with the constant frequency Ω), then the orbital velocity $V_{\rm eq}$ of Eq. (68) takes on the form

$$V_{\rm eq} = \sqrt{\frac{\Upsilon_{\rm eq}}{2}} \, \frac{1}{\sqrt{1-\Upsilon_{\rm eq}}} \tag{69}$$

$$\longrightarrow \quad \hat{R}_{\rm eq} \, \hat{\Omega}_c \qquad \text{for} \quad \Upsilon_{\rm eq} \ll 1 , \tag{70}$$

with $\hat{\Omega}_c$ given by Eq. (21). As indicated here, the result of classical Newtonian mechanics for the velocity of a particle in a circular orbit is recovered from Eq. (69) by neglecting the curvature of space-time geometry, i.e. $\Upsilon_{\rm eq} \ll 1$. From Eq. (67) then follows $\Omega_{\rm K} \rightarrow \Omega_c$ (note that $e^{\psi} \rightarrow \hat{r}$ for $\theta = \pi/2$ and $v_2 \ll 1$, $h_2 \ll 1$). An approximate solution of Eq. (67) in the case of a rotating neutron star of maximum possible mass (referred to as *limiting-mass* model) can be obtained from the empirically established expression of Friedman, Ipser, and Parker [34] (see also

Refs. [35, 36]) via

$$\Omega_{\rm K}^{\rm FIP} \;=\; 24\,\sqrt{[M_s/M_\odot]/[R_s/{\rm km}]^3}\cdot 10^4\ {\rm s}^{-1} \;=\; \frac{2}{3}\,\Omega_c \quad \text{cf. (Eq. (21))}\,. \tag{71}$$

This formula has been established from the exact numerical solution of Einstein's field equations. Equation (71) attains its importance because only knowledge of mass and radius of the non-rotating limiting-mass star is necessary. An analysis of Eq. (71) has been performed in two recent papers [5, 6], which motivates this dependence quantitatively. Ray and Datta [33, 37] have applied

$$\Omega_{\rm K}^{\rm RD} = 19\,\sqrt{[M_s/M_\odot]/[R_s/{\rm km}]^3}\cdot 10^4\ {\rm s}^{-1} \tag{72}$$

for the limiting rotational frequency. This expression has its origin in the onset of a secular instability of uniformly rotating, homogeneous Maclaurin spheroids [38].

2.4 Red- and blueshift, injection energy, stability parameter

Further important neutron star properties are listed in this Section. The frequency shift of light emitted at the star's equator in backward (B) or forward (F) direction is given, in terms of the metric functions of Eqs. (22) and (23), by [3]

$$z_{\rm B/F} \;=\; e^{-\nu}\,\left(1\pm\omega\,e^{\psi-\nu}\right)^{-1}\,\left(\frac{1\pm V}{1\mp V}\right)^{1/2} \;-\; 1\,. \tag{73}$$

The redshift of photons emitted at the star's pole follows from

$$z_{\rm p} \;=\; e^{-\nu} \;-\; 1\,. \tag{74}$$

The so-called injection enegy is defined in terms of $z_{\rm p}$ of Eq. (74) or the metric function of Eq. (22) in the following way:

$$\beta \equiv e^{2\nu}\big|_{\rm pole} \;=\; \frac{1}{(z_{\rm p}\,+\,1)^2}\,. \tag{75}$$

We conclude this Section by defining the stability parameter, t,

$$t \;\equiv\; \frac{\hat{T}}{|\,\hat{W}\,|}\,, \tag{76}$$

$$\hat{T} \;\equiv\; \frac{1}{2}\,\kappa\,\hat{J}\,\hat{\Omega}\,, \tag{77}$$

$$\hat{W} \;\equiv\; \hat{M}_P + \hat{T} - \hat{M}\,, \tag{78}$$

which is the ratio of the star's rotational energy, T, to gravitational energy, W. It is of importance for the investigation of the stability of rotating neutron stars [39, 40].

3 Determination of the neutron star matter equation of state

3.1 Physics of high-density neutron star matter

Up to now we have not specified the equation of state of neutron star matter. It is the basic input quantity for solving the hierarchies of both the stellar structure equations of non-rotating as well as rotating neutron stars.

From neutron star matter calculations it is known that such matter possesses a rather complex composition [41, 25, 21, 9, 10]. By imposing the constraint of electrical charge neutrality and solving the complicated many-body problem for the relativistic Hartree approximation [9, 10], it has been found that at nuclear densities $\varrho \approx \varrho_0$ such matter consists almost purely of neutrons with a small admixture of electrons. For increasing values of ϱ, high-momentum electrons β-decay into protons and electrons or muons. The μ^- threshold occurs at $\varrho \approx 0.12$ fm^{-3}, just below normal nuclear matter density. The π^- threshold, which indicates the onset on pion condensation, is reached at $\varrho \approx 0.18$ fm^{-3}, just above nuclear matter density [9]. Finally, hyperon population sets in at $\varrho \approx 0.32$ fm^{-3}. The contributing hyperon species calculated for the Hartree treatment are the Λ particle, and all charged states of Σ and Ξ. A quantitatively similar behavior has been obtained for the Hartree-Fock treatment [10], but with the exception that the Δ^- state is now populated too at already relatively low nuclear densities (i.e. $\varrho \approx 0.35$ fm^{-3}). This is in contrast to the Hartree treatment, where it is absent [9, 10]. Both the Hartree and Hartree-Fock treatment have in common that the parameters of the theory (meson masses and coupling strengths) must be adjusted to the bulk nuclear matter properties to achive saturation. The use of one-boson-exchange potential parameters deduced from the analysis of the free two-nucleon problem leads to unsatisfactory results as regards the saturation of nuclear matter. For that reason one has to go beyond the Hartree and Hartree-Fock method and treat the nuclear matter problem in the so-called ladder (denoted by Λ) approximation scheme [18, 11]. Within this framework one includes two-particle correlations in matter in terms of an effective scattering (T) matrix (cf. Refs. [42, 43] for the non-relativistic Λ method). A diagrammatic representation of T is shown in Fig. 1. The T-matrix sums repeated two-particle scattering processes in matter up to infinite order, and hence is given as the solution of an (Bethe-Goldstone type) integral equation whose Born term is given by the nucleon-nucleon interaction

Table 2: Equations of state of this work

Model	Equation of state (Interactions)	Mass density range † [g/cm^3]	Composition
	Harrison-Wheeler	$7.8 < \epsilon < 10^{11}$	Crystalline; light metals, electron gas
	Negele-Vautherin	$10^{11} < \epsilon < 10^{13}$	Crystalline; heavy metals, relativistic electron gas
$\Lambda^{00}_{\rm Bonn}$	Relativistic Λ^{00} approximation (T-matrix); based on the Bonn meson-exchange potential $(\sigma, \omega, \pi, \varrho, \eta, \delta)$	$10^{13} < \epsilon < 5 \cdot 10^{14}$	Neutrons
$\Lambda^{00}_{\rm HEA}$	Same; based on the HEA meson-exchange potential $(\sigma, \omega, \pi, \varrho, \eta, \delta, \phi)$	$10^{13} < \epsilon < 5 \cdot 10^{14}$	Neutrons
HV	Relativistic Hartree approximation $(\sigma, \omega, \varrho)$‡	$10^{13} < \epsilon < 9 \cdot 10^{15}$	p, n, Λ, $\Sigma^{\pm,0}$, $\Xi^{0,-}$; e^-, μ^-
HFV	Relativistic Hartree-Fock approximation $(\sigma, \omega, \pi, \varrho)$	$10^{13} < \epsilon < 9 \cdot 10^{15}$	p, n, Λ, $\Sigma^{\pm,0}$, $\Xi^{0,-}$, Δ^-; e^-, μ^-

†) The conversion of ϵ from MeV/fm^3 to g/cm^3 can be accomplished by multiplying the former quantity with $1.783 \cdot 10^{12}$.

‡ The symbol "V" takes reference to the notation introduced in earlier works [10, 27].

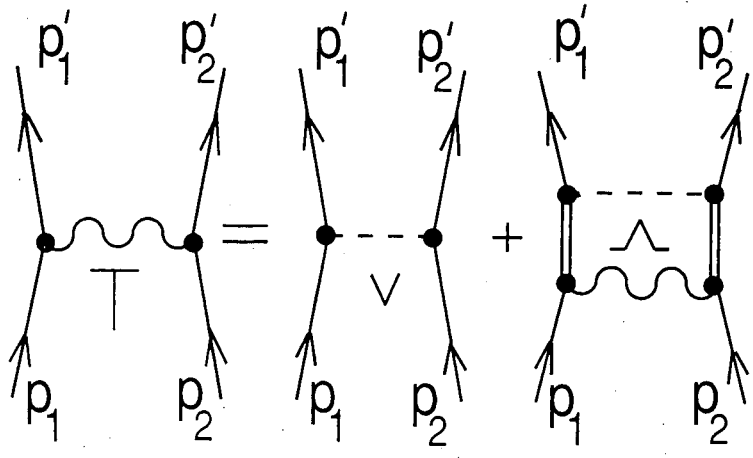

Figure 1: Diagrammatic representation of the integral equation of the scattering T-matrix (wavy lines) in nuclear matter. The second term sums repeated two-particle scattering processes (ladder summation) which are connected with the free two-nucleon interaction v (dashed lines). The baryon propagation in the intermediate scattering states is described by the propagator function Λ. The analytic form of the T-matrix is given in Eq. (124).

in free space, denoted by v in Fig. 1. These are chosen in our investigation to be the Bonn and HEA potentials. The parameters of the Λ method are those of the Born term. These are however determined by the relativistic nucleon-nucleon scattering problem in free space and the properties of the deuteron. Therefore, in other words, the Λ method contains *no free parameters*. However, the price one has to pay for this is that it is much more complicated than the Hartree or Hartree-Fock method. At present it cannot be applied for for the determination of the high-density neutron star matter equation of state for several reasons. Open questions encountered are, [44, 11, 4]:

1. Correlations other than those taken into account in the Λ approach may become important in the high-density regime, i.e. for $\varrho > (2\text{-}3)\varrho_0$ (many-body forces, modification of the boson-exchange description);

2. Lack of knowledge of baryon-baryon and baryon-meson coupling strengths;

3. Non-renormalizability of the Λ method.

In a reasonable first step, however, one may incorporate two-particle effects into the equation of state at *intermediate* nuclear densities [4], i.e. for $0.1\ \varrho_0 < \varrho < 2\varrho_0$

($20< \epsilon/(\mathrm{MeV/fm^3}) < 300$). For this density range neutron star matter consists to a good approximation only of neutrons, and hence the Λ method is applicable. Matter beyond $\varrho > 2\varrho_0$ may then be treated in the framework of the Hartree or Hartree-Fock approximation.

For our investigations we have calculated the equation of state in the framework of relativistic, finite-density Green's functions. These are coupled by the Martin-Schwinger hierarchy [18]. A systematic truncation procedure of the latter leads to the Hartree, Hartree-Fock, and Λ approximation. The former two make the many-baryon/lepton matter problem tractable [18, 11]. Our concern in what follows is (i) to demonstate how these approximations are related with each other in the language of Green's functions, and (ii) how the equation of state of neutron star matter can be obtained which accounts for the above mentioned effects (two-particle correlations, baryon/lepton population).

3.2 Lagrangian density

We start from the following Lagrangian governing the dynamics of many-baryon/lepton neutron star matter [9, 10]:

$$\begin{aligned} \mathcal{L}(x) &= \sum_{B=p,n,\Sigma^{\pm,0},\Lambda,\Xi^{0,-},\Delta^{++,+,0,-}} \mathcal{L}_B^0(x) \\ &+ \sum_{M=\sigma,\omega,\pi,\varrho,\eta,\delta,\phi} \left\{ \mathcal{L}_M^0(x) + \sum_{B=p,n,\ldots,\Delta^{++,+,0,-}} \mathcal{L}_{B,M}^{\mathrm{Int}}(x) \right\} \\ &+ \sum_{\lambda=e^-,\mu^-} \mathcal{L}_\lambda(x) \,. \end{aligned} \tag{79}$$

The summation index B runs over all baryon species which become populated in the star matter once their thresholds are reached [45]. The summation extends over hyperons as well as the $\Delta_1 232$ state [45, 10, 46, 47, 48, 49]. The nuclear forces are mediated by that collection of scalar, vector, and isovector-mesons which is used for the construction of relativistic one-boson-exchange potentials [13, 12]. The equations of motion resulting from the Lagrangian of Eq. (79) for the various baryon and meson field operators are to be solved subject to the boundary conditions of infinite charge neutral neutron star matter [9, 10]. For this purpose we apply the Green's function method.

Table 3: Masses, electric charges (q_B) and quantum numbers (spin (J_B), isospin (I_B), strangeness (S_B), hypercharge (Y_B), third component of isospin (I_{3B})) of the baryons included in the determination of the equation of state of neutron star matter.

Baryon (B)	m_B [MeV]	J_B	I_B	S_B	Y_B	I_{3B}	q_B
n	939.6	$\frac{1}{2}$	$\frac{1}{2}$	0	1	$-\frac{1}{2}$	0
p	938.3	$\frac{1}{2}$	$\frac{1}{2}$	0	1	$\frac{1}{2}$	1
Σ^+	1189	$\frac{1}{2}$	1	-1	0	1	1
Σ^0	1193	$\frac{1}{2}$	1	-1	0	0	0
Σ^-	1197	$\frac{1}{2}$	1	-1	0	-1	-1
Λ	1116	$\frac{1}{2}$	0	-1	0	0	0
Ξ^0	1315	$\frac{1}{2}$	$\frac{1}{2}$	-2	-1	$\frac{1}{2}$	0
Ξ^-	1321	$\frac{1}{2}$	$\frac{1}{2}$	-2	-1	$-\frac{1}{2}$	-1
Δ^{++}	1232	$\frac{3}{2}$	$\frac{3}{2}$	0	1	$\frac{3}{2}$	2
Δ^+	1232	$\frac{3}{2}$	$\frac{3}{2}$	0	1	$\frac{1}{2}$	1
Δ^0	1232	$\frac{3}{2}$	$\frac{3}{2}$	0	1	$-\frac{1}{2}$	0
Δ^-	1232	$\frac{3}{2}$	$\frac{3}{2}$	0	1	$-\frac{3}{2}$	-1

Table 4: Mesons of the Bonn and HEA meson-exchange models for the nucleon-nucleon interaction. The symbols J^{π}_{M} and T_M refer to spin (J_M), parity (π), and isospin (T_M) of meson M.

Meson (M)	J^{π}_{M}	T_M	coupling
σ	0^+	0	scalar
ω	1^-	0	vector
π	0^-	1	pseudo-vector
ϱ	1^-	1	vector
η	0^-	0	pseudo-vector
δ	0^+	1	scalar
ϕ	1^-	0	vector

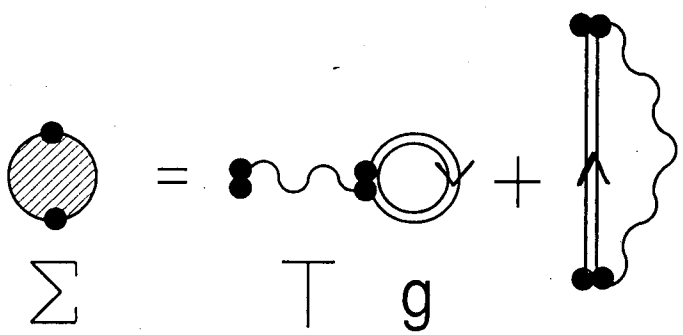

Figure 2: Diagrammatic equation of the baryon self-energy Σ. The first term corresponds to the direct, and the second to the exchange contribution. The analytic definition is given in Eq. (96). Explicit mathematical expressions for Σ calculated for the Λ and Hartree-Fock methods are given in Eqs. (308) - (310) and (150), (151), (278) - (282), respectively.

Table 5: Masses, spin quantum numbers and electric charges of the leptons included in the determination of the equation of state of neutron star matter.

Lepton (λ)	m_λ [MeV]	J_λ	q_λ
e^-	0.511	$\frac{1}{2}$	-1
μ^-	106	$\frac{1}{2}$	-1

3.3 Relativistic Green's function approach

The general definition of the 2n-point Green's function is given by the ground-state expectation value of the time-ordered product of baryon field operators, ψ_B, in the form [18, 11, 50, 51]

$$\begin{aligned} & g_n^{B_1,...,B_{n'}}(1,...,n;1',...,n') \\ & = i^n \; < \Phi_0 \mid \hat{T}\left(\psi_{B_1}(1)...\psi_{B_n}(n)\,\bar{\psi}_{B_{n'}}(n')...\bar{\psi}_{B_{1'}}(1')\right) \mid \Phi_0 > \; . \end{aligned} \tag{80}$$

The quantity $|\Phi_0>$ denotes the ground-state of infinite matter, and the integers $1 \equiv (x_1^0, \boldsymbol{x}_1; \zeta_1)$, ... , $n \equiv (x_n^0, \boldsymbol{x}_n; \zeta_n)$ stand for the space-time coordinates (denoted by $x_1 = (x_1^0, \boldsymbol{x}_1)$, ... , $x_n = (x_n^0, \boldsymbol{x}_n)$) as well as spin-isospin quantum numbers (ζ_1, ... , ζ_n) of baryons B_1 ... B_n. The quantity $\hat{T}$ stands for the time-ordering operator (see below). Of special interest is the so-called two-point Green's function, $g_1^B(1,1')$, since its knowledge is *sufficient* for the calculation of the properties of the many-body system. This will be shown below. It is convenient to decompose the two-point function in the following way (cf. Appendix C):

$$g_1^{BB'}(x,\zeta;x',\zeta') \equiv g_{\zeta\zeta'}^{BB'}(x,x') \equiv g_{\zeta\zeta'}^{BB'}(x-x') \tag{81}$$

$$= i \; < \hat{T}(\psi_B(x,\zeta)\,\bar{\psi}_{B'}(x',\zeta')) \; > \tag{82}$$

$$= \Theta(x_0 - x_0')\, g_>^{BB'}(x,\zeta;x',\zeta') + \Theta(x_0' - x_0)\, g_<^{BB'}(x,\zeta;x',\zeta') \; . \tag{83}$$

The definition of the time-ordering operator is given in Eq. (83), where we have introduced the auxiliary Green's functions $g_<$ and $g_>$ which are useful in the treatment. These are given by

$$g_>^{BB'}(x,\zeta;x',\zeta') \equiv i \; < \psi_B(x,\zeta)\,\bar{\psi}_{B'}(x',\zeta') > \, , \tag{84}$$

$$g_<^{BB'}(x,\zeta;x',\zeta') \equiv -i \; < \bar{\psi}_{B'}(x',\zeta')\,\psi_B(x,\zeta) > \; . \tag{85}$$

The Martin-Schwinger hierarchy couples the functions g_n of Eq. (80) to all orders of n with each other [18, 11]. The two-point Green's function $g_1^B(1,1')$ is coupled to the four-point Green's function, $g_2^{B'B}$, via a two-body "potential" term, $v^{BB'}$, which contains the nucleon-meson vertices. Introducing the shorthand notation $\int_{1,B} \equiv \sum_B \int d^4 x_1$ one gets

$$\begin{aligned} g_1^B(1,1') &= g_1^{0\,B}(1,1') \\ &\quad + i \int_{1'',2,3,4;B'} g_1^{0\,B}(1,1'') < 1''\,2 \mid v^{BB'} \mid 3\,4 > g_2^{B'B}(3\,4, 2^+\,1') \,. \end{aligned} \tag{86}$$

Here $g_1^{0\,B}$ denotes the free two-point baryon propagator which obeys ($p^\mu = i\partial^\mu$)

$$g_1^{0\,B}(x-x')^{-1}_{\zeta\zeta'} = (-\gamma^\mu\, p_{x\,\mu} + m_B)_{\zeta\zeta'}\; \delta^4(x-x') \,. \tag{87}$$

The matrix elements of $v^{BB'}$ are given by

$$\begin{aligned} < 1\,2 \mid v^{BB'} \mid 3\,4 > = \sum_{M=\sigma,\omega,\pi,\varrho,\eta,\delta,\phi} & \delta^4(x_1 - x_3)\, \delta^4(x_2 - x_4) \\ & \times \; \Gamma^{M;B}_{\zeta_1\zeta_3}\; \Gamma^{M;B'}_{\zeta_2\zeta_4}\; \Delta^0_M(x_1,x_2) \,. \end{aligned} \tag{88}$$

The function Δ^0_M in Eq. (88) denotes the single-particle propagator of free meson fields of type M, defined as

$$\Delta^0_M(x_1,x_2) = i\, < \Phi_0 \mid T\,[\,M(x_1)\, M(x_2)\,] \mid \Phi_0 > \,, \tag{89}$$

with ($r = 1,2,3$ refers to isospin)

$$M(x_1)\, M(x_2) = \begin{cases} \chi(x_1)\, \chi(x_2) & \text{if} \quad \chi = \sigma \,, \\ \chi_{r_1}(x_1)\, \chi_{r_2}(x_2) & \text{if} \quad \chi = \pi, \eta, \delta \,, \\ \chi^\mu(x_1)\, \chi^\nu(x_2) & \text{if} \quad \chi = \omega, \phi \,, \\ \chi^\mu_{r_1}(x_1)\, \chi^\nu_{r_2}(x_2) & \text{if} \quad \chi = \varrho \,. \end{cases} \tag{90}$$

Table 4 summarizes the different types of mesons which are included in the Bonn and HEA meson-exchange model of the nucleon-nucleon force, and therefore are of interest in this work. Explicit expressions for the Δ^0_M propagators of Eq. (89) are given in Appendix C.2.

For the purpose of brevity we have suppressed both Dirac indices as well as isospin quantum numbers in Eqs. (89) and (90). The scalar, pseudo-vector, and vector meson-baryon vertices $\Gamma^{M;B}$ of Eq. (88) are given by respectively

$$\Gamma^{\sigma,\delta;B}_{\zeta_1\zeta_3} = i\; g_{\sigma,\delta;B}\; \delta_{\zeta_1\zeta_3} \qquad \text{(scalar)} \,, \tag{91}$$

$$\Gamma^{\pi,\eta;B}_{\zeta_1\zeta_3} \;=\; -i\,\frac{f_{\pi B}}{m_\pi}\;(i\,\gamma_5\,\gamma_\mu\,\partial_1^\mu)_{\zeta_1\zeta_3} \qquad (\text{pseudo}-\text{vector})\,, \tag{92}$$

$$[\,\Gamma^{\omega,\varrho,\phi;B}_{\mu}\,]_{\zeta_1\zeta_3} \;=\; \Big(g_{\omega,\varrho,\phi;B}\;\gamma_\mu + \frac{i}{2}\,\frac{f_{\omega,\varrho,\phi;B}}{2\,m_{\omega,\varrho,\phi}}\;\partial_1^\xi\,[\gamma_\xi,\gamma_\mu]\Big)_{\zeta_1\zeta_3} \quad (\text{vector})\,. \tag{93}$$

(94)

By introducing the so-called reducible vertex T (effective scattering matrix in matter) in the form (cf. Ref. [11])

$$\int_{3,4;B'} < 1\,2 \mid v^{BB'} \mid 3\,4 > \qquad g_2^{B'B}(3\,4,1'\,2') \;= \tag{95}$$
$$\int_{3,4;B'} < 1\,2 \mid T^{BB'} \mid 3\,4 > \;\; g_1^{B'}(3,1')\,g_1^{B}(4,2')\,,$$

and the mass operator (self-energy) Σ, (see Fig. 2)

$$\Sigma^B(1,2) \;=\; -i\int_{3,4;B'} < 1\,3 \mid T^{BB'} \mid 4\,2 > \;\; g_1^{B'}(4,3^+)\,, \tag{96}$$

the $v\cdot g_2$-term of Eq. (86) can be replaced in favor of $\Sigma\cdot g_1$. One arrives at Dyson's equation,

$$g_1^B(1,1') \;=\; g_1^{0\,B}(1,1') \;-\; \int_{3,4} g_1^{0\,B}(1,3)\;\;\Sigma^B(3,4)\;\;g_1^B(4,1')\,, \tag{97}$$

which is graphically illustrated in Fig. 3. For later use we give the momentum-space representation of Dyson's equations ($p\equiv(p^0,\boldsymbol{p})$),

$$\Big(\gamma^\mu\,p_\mu \;-\; m_B \;-\; \Sigma^B(p)\Big)_{\zeta_1\zeta_3}\;g_1^B(p)_{\zeta_3\zeta_2} \;=\; -\,\delta_{\zeta_1\zeta_2}\,. \tag{98}$$

Equation (97) (or equivalently Eq. (98)) determines the two-point propagator g_1^B. Dyson's equation imposes self-consistency on the determination of g^B. From Eq. (96) one sees that the mass operator, which can can be viewed as the effective single-particle potential of a baryon in matter, is obtained from the effective two-baryon interaction in matter, i.e. the T-matrix, via integration. The latter obeys an integral equation whose Born term is given in Eq. (88). The restriction to the Born term leads to the *Hartree-Fock approximation* [50, 51, 10]. We will turn back to this point in Sect. 3.5. Before, however, we introduce the spectral representation of the two-point function. It is sufficient for the calculation of the properties (e.g. energy density, nuclear density, equation of state) of the system.

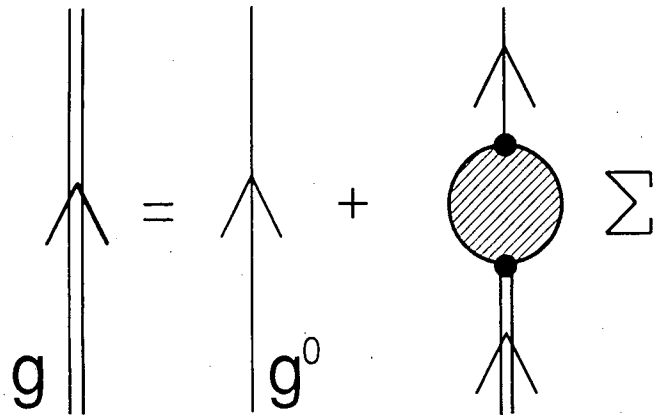

Figure 3: Graphical representation of Dyson's equation for the self-consistent baryon propagator g (Green's two-point function). The quantity g^0 denotes the free propagator which does not couple to the nuclear medium (described by Σ). The analytic form is given in Eq. (97).

3.4 Spectral representation

If one applies (anti) periodic time bondary conditions on the expectation value of Eq. (81), the following useful momentum-space representations of $g^B_{\zeta\zeta'}(x_1 - x_1')$ can be derived [10, 50, 52] (for the purpose of simplicity we drop the subcript "1" from g^B_1):

$$g^B_{\zeta\zeta'}(p) = \frac{i}{2\pi}\int_{-\infty}^{+\infty} d\omega \Big[\frac{g^B_>(\omega,\boldsymbol{p})_{\zeta\zeta'}}{p^0-\omega-\mu^B+i\eta} - \frac{g^B_<(\omega,\boldsymbol{p})_{\zeta\zeta'}}{p^0-\omega-\mu^B-i\eta}\Big] \tag{99}$$

$$= -\int_{-\infty}^{+\infty} d\omega \Big[\frac{1-\Theta(\mu^B-p^0)}{p^0-\omega-\mu^B+i\eta} + \frac{\Theta(\mu^B-p^0)}{p^0-\omega-\mu^B-i\eta}\Big]\, \Xi^B_{\zeta\zeta'}(\omega,\boldsymbol{p}) \tag{100}$$

$$= \int_{-\infty}^{+\infty} d\omega \frac{a^B_{\zeta\zeta'}(\omega,\boldsymbol{p})}{\omega-(p^0-\mu^B)\,(1+i\eta)}\,. \tag{101}$$

A derivation of the above equations (for finite temperatures) is performed in Appendix C.1. There we also derive an explicit expression for g^B in the Hartree approximation and give a physical interpretation. The quantity μ^B in Eqs. (99) - (101) denotes the chemical potential of baryons of type B. The spectral function Ξ^B of Eq. (101) is given by the cut of the analytically continued g_1-propagator, denoted by $\tilde{g}$, along the

real energy axis. The latter obeys

$$\tilde{g}^B_{\zeta\zeta'}(z,\boldsymbol{p}) \;=\; \int\limits_{-\infty}^{+\infty} d\omega\; \frac{\Xi^B_{\zeta\zeta'}(\omega,\boldsymbol{p})}{\omega - z}\;, \tag{102}$$

and therefore

$$\Xi^B_{\zeta\zeta'}(\omega,\boldsymbol{p}) \;=\; \frac{\tilde{g}^B_{\zeta\zeta'}(\omega+i\eta,\boldsymbol{p}) \;-\; \tilde{g}^B_{\zeta\zeta'}(\omega-i\eta,\boldsymbol{p})}{2\pi\, i}\;. \tag{103}$$

For each baryon of type B, the corresponding Green's function $\tilde{g}^B$ of Eq. (102) solves the analytically continued Dyson equation following from Eq. (98) ($\hat{\boldsymbol{p}} \equiv \boldsymbol{p}/|\boldsymbol{p}|$):

$$\Big[[m_B + \tilde{\Sigma}^B_S(z,\boldsymbol{p})] + [\mid \boldsymbol{p} \mid + \tilde{\Sigma}^B_V(z,\boldsymbol{p})]\,\boldsymbol{\gamma}\cdot\hat{\boldsymbol{p}} + [\tilde{\Sigma}^B_0(z,\boldsymbol{p}) + (z+\mu^B)]\,\gamma^0\Big]\;\tilde{g}^B(z,\boldsymbol{p}) = 1\,. \tag{104}$$

In Eq. (104), Σ^B has been decomposed into a scalar, vector, and time-like part according to

$$\Sigma^B_{\zeta\zeta'} \;=\; \Sigma^B_S\;(1)_{\zeta\zeta'} \;+\; \Sigma^B_V\;(\boldsymbol{\gamma}\cdot\hat{\boldsymbol{p}})_{\zeta\zeta'} \;+\; \Sigma^B_0\;\gamma^0_{\zeta\zeta'}\,. \tag{105}$$

Note that the unity matrix of Eq. (105) consists of a Dirac and an isospin part. It therefore has the explicit form

$$(1)_{\zeta\zeta'} \equiv \left(1^{\rm Dirac} \otimes 1^{\rm Iso}\right)_{\zeta\zeta'} \;=\; \delta_{\alpha\alpha'}\,\delta_{ii'} \tag{106}$$

when the spin (α,α') and isospin (i,i') indices comprised to ζ,ζ', i.e. $\zeta = (\alpha,i)$ and $\zeta' = (\alpha',i')$, are substituted.

Inversion of Eq. (104) yields [10, 53]

$$\tilde{g}^B(z,\boldsymbol{p}) \;=\; \frac{[m_B + \tilde{\Sigma}^B_S(z,\boldsymbol{p})] - [\mid \boldsymbol{p} \mid + \tilde{\Sigma}^B_V(z,\boldsymbol{p})]\,\boldsymbol{\gamma}\cdot\hat{\boldsymbol{p}} - [\tilde{\Sigma}^B_0(z,\boldsymbol{p}) - (z+\mu^B)]\,\gamma^0}{[m_B + \tilde{\Sigma}^B_S(z,\boldsymbol{p})]^2 + [\mid \boldsymbol{p} \mid + \tilde{\Sigma}^B_V(z,\boldsymbol{p})]^2 - [\tilde{\Sigma}^B_0(z,\boldsymbol{p}) - (z+\mu^B)]^2}\;. \tag{107}$$

The "physical" baryon propagators g^B and baryon self-energies Σ^B are connected to $\tilde{g}^B$ and $\tilde{\Sigma}^B$, respectively, by the following boundary values ($j = S,V,0$):

$$g^B_{\zeta\zeta'}(p) \;=\; \tilde{g}^B_{\zeta\zeta'}((p^0-\mu^B)(1+i\eta),\boldsymbol{p})\;, \tag{108}$$

$$\Sigma^B_{j\,\zeta\zeta'}(p) \;=\; \tilde{\Sigma}^B_{j\,\zeta\zeta'}((p^0-\mu^B)(1+i\eta),\boldsymbol{p})\;. \tag{109}$$

From Eq. (109) one obtains

$$\mathrm{Im}\;\tilde{\Sigma}^B_{j\,\zeta\zeta'}(\omega-\mu^B \pm i\,\eta,\boldsymbol{p}) \;=\; \mp\,\mathrm{sgn}(\mu^B-\omega)\;\Gamma^B_{j\,\zeta\zeta'}(\omega,\boldsymbol{p})\;, \tag{110}$$

where $\tilde{\Sigma}_j^B$ has been decomposed into the real and imaginary part,

$$\tilde{\Sigma}_j^B(\omega - \mu^B \pm i\,\eta, \boldsymbol{p}) \;=\; \mathrm{Re}\,\tilde{\Sigma}_j^B(\omega - \mu^B \pm i\,\eta, \boldsymbol{p}) \;+\; i\,\mathrm{Im}\,\tilde{\Sigma}_j^B(\omega - \mu^B \pm i\,\eta, \boldsymbol{p})\,,$$

with

$$\mathrm{Im}\,\tilde{\Sigma}_j^B(\omega - \mu^B \pm i\,\eta, \boldsymbol{p}) \;=\; \pm\,\mathrm{sgn}(\omega - \mu^{\mathrm{B}})\;\Gamma_{\mathrm{j}}^{\mathrm{B}}(\omega, \boldsymbol{p})\,. \tag{111}$$

One obtains for the latter functions [50, 53]

$$\begin{aligned}\Gamma^B(\omega,\boldsymbol{p}) \;\equiv\; & 2\,\Big(\Gamma_S^B(\omega,\boldsymbol{p})\,[m_B + \mathrm{Re}\,\Sigma_S^B(\omega,\boldsymbol{p})] \;+\; \Gamma_V^B(\omega,\boldsymbol{p})\,[|\boldsymbol{p}| + \mathrm{Re}\,\Sigma_V^B(\omega,\boldsymbol{p})] \\ & - \Gamma_0^B(\omega,\boldsymbol{p})\,[\mathrm{Re}\,\Sigma_0^B(\omega,\boldsymbol{p}) - \omega]\Big)\,.\end{aligned} \tag{112}$$

In the case of the Hartree-Fock and Λ^{00} approximations, which are of interest in this work, the imaginary part of Σ^B vanishes [11], and therefore $\Gamma^B(\omega,\boldsymbol{p}) \to 0$. By this the structure of the spectral function takes on a much simpler form (see [53] for the general case $\Gamma^B \neq 0$). As in the non-relativistic treatment [42], Eqs. (107) - (112) lead to a spectral function of *single-particle* structure,

$$\begin{aligned}\Xi^B(\omega,\boldsymbol{p}) \;=\; & \delta[D^B(\omega+\mu^B,\boldsymbol{p})]\;\mathrm{sgn}[-\omega\,\hat{\Gamma}^B(\omega+\mu^B)] \\ & \times\Big\{[m_B \;+\; \mathrm{Re}\,\Sigma_S^B(\omega,\boldsymbol{p})] \;-\; [|\boldsymbol{p}| \;+\; \mathrm{Re}\,\Sigma_V^B(\omega,\boldsymbol{p})]\;\boldsymbol{\gamma}\cdot\hat{\boldsymbol{p}} \\ & - [\mathrm{Re}\,\Sigma_0^B(\omega,\boldsymbol{p}) \;-\; \omega]\;\gamma^0\Big\}\,,\end{aligned} \tag{113}$$

with the definition

$$D^B(\omega,\boldsymbol{p}) = [m_B \;+\; \mathrm{Re}\,\Sigma_S^B(\omega,\boldsymbol{p})]^2 \;+\; [|\boldsymbol{p}| \;+\; \mathrm{Re}\,\Sigma_V^B(\omega,\boldsymbol{p})]^2 \;-\; [\mathrm{Re}\,\Sigma_0^B(\omega,\boldsymbol{p}) \;-\; \omega]^2\,. \tag{114}$$

In what follows, Σ_j^B denotes the pure real self-energy functions. Equation (113) can be decomposed into a baryon and an anti-baryon part. By this one arrives for the spectral functions of baryons (B, upper sign) and anti-baryons ($\bar{B}$, lower sign) at [11, 50, 51, 10]

$$\Xi_{\zeta\zeta'}^B(\omega,\boldsymbol{p}) = \delta[\omega + \mu^B - \omega^B(\boldsymbol{p})]\;\;\Xi_{\zeta\zeta'}^B(\boldsymbol{p}) \;+\; \delta[\omega + \mu^{\bar{B}} - \omega^{\bar{B}}(\boldsymbol{p})]\;\;\Xi_{\zeta\zeta'}^{\bar{B}}(\boldsymbol{p}) \tag{115}$$

with

$$\Xi_{\zeta\zeta'}^{B,\bar{B}}(\boldsymbol{p}) \;=\; \pm\frac{[m_B + \Sigma_S^B]\;1_{\zeta\zeta'} \;-\; [\,|\,\boldsymbol{p}\,|\,+\Sigma_V^B]\;(\boldsymbol{\gamma}\cdot\hat{\boldsymbol{p}})_{\zeta\zeta'} \;+\; [\omega^{B,\bar{B}}(\boldsymbol{p}) - \Sigma_0^B]\;\gamma_{\zeta\zeta'}^0}{\left|\frac{\partial D^B(\omega,\boldsymbol{p})}{\partial\omega}\right|_{\omega=\omega^{B,\bar{B}}(|\boldsymbol{p}|)}}$$

$$\equiv \Xi_S^{B,\bar{B}}\, 1_{\zeta\zeta'} + \Xi_V^{B,\bar{B}}\, (\boldsymbol{\gamma}\cdot\hat{\boldsymbol{p}})_{\zeta\zeta'} + \Xi_0^{B,\bar{B}}\, \gamma^0_{\zeta\zeta'}\,, \tag{117}$$

$$\frac{\partial D^B(\omega,\boldsymbol{p})}{\partial\omega} = 2\Big\{[m_B + \Sigma_S^B(\omega,\boldsymbol{p})]\,\frac{\partial\Sigma_S^B}{\partial\omega} + [\mid \boldsymbol{p} \mid + \Sigma_V^B(\omega,\boldsymbol{p})]\,\frac{\partial\Sigma_V^B}{\partial\omega} + [\Sigma_0^B(\omega,\boldsymbol{p}) - \omega]\,\Big[1 - \frac{\partial\Sigma_0^B}{\partial\omega}\Big]\Big\}\,. \tag{118}$$

The latter relation follows immediately form Eq. (114). The baryon, anti-baryon energy-momentum relation in matter is given by the zeroes of Eq. (114),

$$\omega^{B,\bar{B}}(\boldsymbol{p}) = \Sigma_0^B(\omega^{B,\bar{B}}) + I_{3B}\,\Sigma_{03}^B(\omega^{B,\bar{B}}(\boldsymbol{p}),\boldsymbol{p}) \pm \sqrt{[m_B + \Sigma_S^B(\omega^{B,\bar{B}}(\boldsymbol{p}),\boldsymbol{p})]^2 + [\mid \boldsymbol{p} \mid + \Sigma_V^B(\omega^{B,\bar{B}}(\boldsymbol{p}),\boldsymbol{p})]^2} \tag{119}$$

$$\equiv \Sigma_0^B + I_{3B}\,\Sigma_{03}^B \pm \epsilon^{B,\bar{B}}(\boldsymbol{p})\,. \tag{120}$$

The chemical potentials of baryons (anti-baryons) having Fermi momenta $p_{F;B}$ ($p_{F;\bar{B}}$) are obtained from

$$\mu^{B,\bar{B}} = \omega^{B,\bar{B}}(p_{F;B,\bar{B}})\,. \tag{121}$$

3.5 Approximation schemes

3.5.1 Ladder (Λ) approximation

The Fermi and Dirac sea contributions to the direct term of Σ are graphically depicted in Fig. 4. There the double-lines represent the full propagators g^B, single-lines the free ones $g^{0,B}$. Nuclear matter can be viewed of as a finite-density backround systemt in which baryon B moves (upper graph of Fig. 4). The knowledge of Σ is necessary to determine g^B. This self-consistency is mathematically imposed by Dyson's equation.

The momentum-space representation of the baryon self-energy of Eq. (96) has the form (using the notation $\int_{q^4} \equiv \int d^4q/(2\pi)^4$)

$$\Sigma^{\Lambda,B}_{\zeta_1\zeta_1'}(p) = i\sum_{B'}\sum_{\zeta_2\zeta_2'}\int_{q^4} e^{i\eta q_0}\Big[\Big\langle\zeta_1\,\zeta_2\,\frac{p-q}{2}\Big|\,T^{BB'}(p+q)\,\Big|\frac{p-q}{2}\,\zeta_1'\,\zeta_2'\Big\rangle - \Big\langle\zeta_1\,\zeta_2\,\frac{p-q}{2}\Big|\,T^{BB'}(p+q)\,\Big|\frac{q-p}{2}\,\zeta_2'\,\zeta_1'\Big\rangle\Big]\, g^{B'}_{\zeta_2'\zeta_2}(q) \tag{122}$$

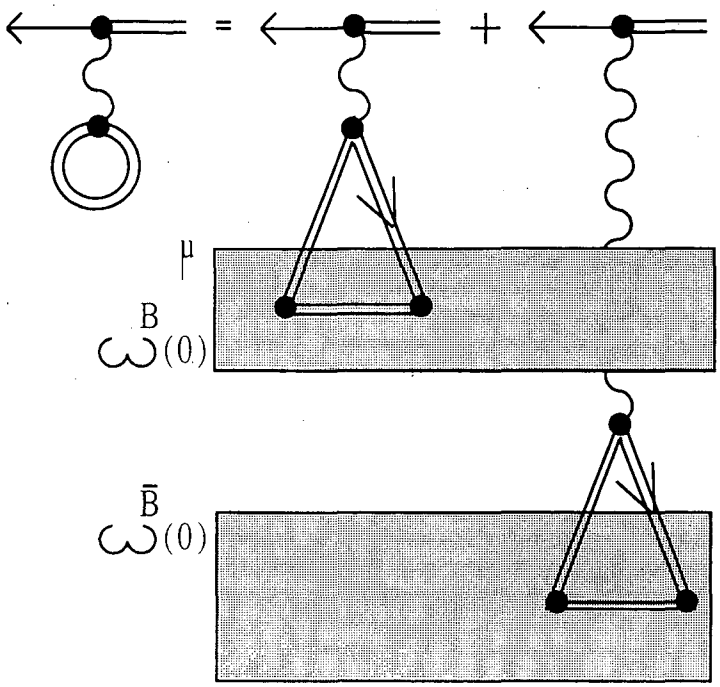

Figure 4: Graphical representation of the self-energy contributions arising from both the Fermi sea, i.e. nuclear matter consisting of filled single-baryon states of energies $\omega^B(0) \leq \omega^B(p) \leq \mu$ (upper graph), as well as Dirac sea (states $-\infty < \omega^{\bar{B}}(p) \leq \omega^{\bar{B}}(0)$, lower graph). The former (latter) lead to so-called medium (vacuum) polarization terms. The no-sea approximation, which in applied in this work, neglects the vacuum polarization contributions (see text).

(cf. Ref. [11]). By inserting the spectral decomposition of g^B of Eq. (101) into Eq. (122), and performing the contour integration in the q^0-plane, one arrives at both (finite) Fermi sea contributions to Σ but also divergent terms arising from the Dirac sea [54, 25, 14]. The latter are referred to as vacuum polarization graphs. As discussed in several articles [18, 55, 14, 15, 16, 17], one may neglect such contributions for the calculation of many-body properties (so-called no-sea approximation). A critical discussion of the influence of vacuum renormalization of relativitic nuclear field theory for both nuclar as well as neutron matter has been performed in Ref. [56]. It was found that these have negligible influence on the equation of state up to densities of at least ten times normal nuclear matter density, provided the coupling constants are tightly constrained by the saturation properties of nuclar matter.

By denoting the zero-temperature Fermi-Dirac distribution function as $\Theta^B(|\boldsymbol{q}|) \equiv$

$\Theta(p_{F,B} - |\boldsymbol{q}|)$, one obtains from Eq. (122)

$$\Sigma^{\Lambda,B}_{\zeta_1\zeta_1'}(p) = \sum_{B'}\sum_{\zeta_2\zeta_2'}\int_{\boldsymbol{q}^3} \Big[\langle\zeta_1\,\zeta_2\,\frac{p-q}{2}|\,T^{BB'}_{p+q}\,|\frac{p-q}{2}\,\zeta_1'\,\zeta_2'\rangle - \langle\zeta_1\,\zeta_2\,\frac{p-q}{2}|\,T^{BB'}_{p+q}\,|\frac{q-p}{2}\,\zeta_2'\,\zeta_1'\rangle\Big]_{q_0=\omega^{B'}(|\boldsymbol{q}|)} \times\ \Xi^{B'}_{\zeta_2'\zeta_2}(\boldsymbol{q}|)\ \Theta^{B'}(\boldsymbol{q})\,. \tag{123}$$

The matrix elements of the T-matrix in Eqs. (122) and (123) satisfy the following ladder-type integral equation which reads, written in terms of center of mass and relative four-momentum coordinates of particles 1 and 2, $P \equiv (P^0, \boldsymbol{p}) = p_1 + p_2$ and $p \equiv (p^0, \boldsymbol{p}) = (p_1 - p_2)/2$, respectively [16, 17, 11]:

$$T^{BB'}_P(p,p')_{\zeta_1\zeta_2;\zeta_1'\zeta_2'} = v^{BB'}(p-p')_{\zeta_1\zeta_2;\zeta_1'\zeta_2'} \tag{124}$$

$$+\sum_{B''}\sum_{\zeta_3\zeta_4;\zeta_5\zeta_6}\int_{q^4} v^{BB''}_{\zeta_1\zeta_2;\zeta_3\zeta_4}(p-q)\,\Lambda^{ij,B''}_{\zeta_3\zeta_4;\zeta_5\zeta_6}(\frac{P}{2}+q,\frac{P}{2}-q)\,T^{B''B'}_P(q,p')_{\zeta_5\zeta_6;\zeta_1'\zeta_2'}\,.$$

The Born term $v^{BB'}$ of Eq. (124) is given, in coordiante-space, by Eq. (88). Three different approximation schemes are distinguished by the choice of the intermediate Λ propagator. They are given in coordinate space by (we recall that $1 \equiv (x_1;\zeta_1)$, etc.)

$$\Lambda^{ij,B}(1\,2,3\,4) = \begin{cases} i\,g_1^{0\,B}(1,3)\,g_1^{0\,B}(2,4^+) & \text{if}\quad ij = 00\ , \\ \frac{i}{2}\,[g_1^B(1,3)\,g_1^{0\,B}(2,4^+) + g_1^{0\,B}(1,3)\,g_1^B(2,4^+)] & \text{if}\quad ij = 10\ , \\ i\,g_1^B(1,3)\,g_1^B(2,4^+) & \text{if}\quad ij = 11\ . \end{cases}$$

We will restrict ourselves in this work to the Λ^{00} treatment. The application of the Λ^{10} and Λ^{11} approximations is more complicated. To date the former method has been applied for nuclear matter calculations [11], and the latter was solved for its non-relativistic limit [57, 58, 59, 43].

In the Λ^{00} treatment both baryons propagate freely in the intermediate *particle* states (we recall that $g^{0\,B}$ denotes the propagator of free baryons, for which $\Sigma \equiv 0$). Intermediate *anti-particle* states do not occur in the integral equations for the T-matrix. These states are excluded from the construction of the Bonn and HEA meson-exchange potentials. For that reason all intermediate anti-nucleon contributions must be dropped (see above), and the vertices are to be regularized. We will come back to this topic in Sect. 5.1 when discussing the parameters of the Λ method. We stress

that the initial and final scattering states, occuring in the T-matrix elements, contain both particle as well as anti-particle states. Hence the determination of a complete set of spinors and anti-spinors is necessary. This is discussed below (see also Appendix H for the representation of the T-matrix in this self-consistent basis).

The Fourier transformed Λ^{00} propagator function is given by

$$\Lambda^{00,B}_{\zeta_1\zeta_2;\zeta_3\zeta_4}(p_1,p_2) \;=\; i\, e^{i\eta p_2^0}\; g_1^{0\,B}(p_1)_{\zeta_1\zeta_3}\; g^{0\,B}(p_2)_{\zeta_2\zeta_4}\;. \tag{125}$$

From Eq. (125) one deduces, using the spectral representation of Eq. (115) and the definitions $p_\pm \equiv (p_\pm^0, \boldsymbol{p}_\pm)$, with $p_\pm^0 \equiv P^0/2 \pm q^0$, $\boldsymbol{p}_\pm \equiv \boldsymbol{p}/2 \pm \boldsymbol{q}$, the following form:

$$\begin{aligned}\Lambda^{00,B}_{P^0}(p_+,p_-)_{\zeta_1\zeta_2;\zeta_3\zeta_4} \;&=\; 2\pi\,\delta\Big(q^0 \,-\, \omega^{0\,B}(|\boldsymbol{p}_+|) \,+\, \frac{P^0}{2}\Big) \\ &\quad\times \frac{\Xi^{0\,B}_{\zeta_1\zeta_3}(|\boldsymbol{p}_+|)\;\; \Xi^{0\,B}_{\zeta_2\zeta_4}(|\boldsymbol{p}_-|)}{P^0 \,-\, \omega^{0\,B}(|\boldsymbol{p}_+|) \,-\, \omega^{0\,B}(|\boldsymbol{p}_-|) \,+\, i\eta}\;.\end{aligned} \tag{126}$$

In Eq. (126), $\Xi^{0\,B}$ and $\omega^{0\,B}$ denote the spectral functions and single-particle energies of free baryons, which follow from Eqs. (115) - (120) by setting $\Sigma^B \equiv 0$.

In principle, the integral equation for the T-matrix of Eq. (124) has 256 elements with respect to the spin indices. Hence one is interested in a basis which decouples the integral equations for these elements and makes the one-particle propagators Λ^{ij} of Eqs. (125 - (126 diagonal. This can be achieved by introducing a self-consistent basis of nucleon and anti-nucleon spinors [60], $\Phi_l(p)$ and $\Theta_l(p)$, respectively ($l = \pm 1/2$ denote the helicity eigenvalues). The anti-spinors are given by $\Theta_l(p) = \gamma_5\,\Phi_l(p)$, with negative energy and reversed momentum and helicity. The former are the solutions of ($p \equiv p^0 = (\omega^N(\boldsymbol{p}), \boldsymbol{p})$)

$$\Big(\,[p_0 - \Sigma_0^N(p)]\,\gamma^0 \;-\; \boldsymbol{\gamma}\cdot\hat{\boldsymbol{p}}\;\; p^*(p) \;-\; m_N^*(p)\,\Big)\,\Phi_l(p) \;=\; 0\;, \tag{127}$$

i.e. (cf. Erkelenz [61]),

$$\Phi_l(p) \;=\; \sqrt{\frac{\epsilon(p)}{2\,m_N^*(p)}}\;\begin{pmatrix} 1 \\ \\ \frac{2\,l\,p^*(p)}{\epsilon(p)} \end{pmatrix} \otimes\; |\,l\,>\,, \tag{128}$$

with the definitions

$$m_N^*(p) \;=\; m_N + \Sigma_S^N(p)\;, \tag{129}$$

$$p^*(p) \;=\; |\boldsymbol{p}\,| + \Sigma_V^N(p)\;, \tag{130}$$

$$W(p) \;=\; \sqrt{[m_N^*(p)]^2 + [p^*(p)]^2}\;, \tag{131}$$

$$\epsilon(p) \;=\; W(p) \;+\; m_N^*(p)\;, \tag{132}$$

and

$$|l> = \hat{D}(\hat{\boldsymbol{p}}) \cdot \chi_l \,, \qquad \chi_+ = \begin{pmatrix} 1 \\ 0 \end{pmatrix} \,, \qquad \chi_- = \begin{pmatrix} 0 \\ 1 \end{pmatrix} \,. \tag{133}$$

The quantity $\hat{D}(\hat{\boldsymbol{p}})$ in Eq. (133) denotes the rotation operator [62, 63].

The spinors and anti-spinors obey the following orthogonality and completeness relations [11, 62]:

$$\bar{\Phi}_l(p)\, \Phi_{l'}(p) = \delta_{ll'} \,, \tag{134}$$

$$\bar{\Theta}_l(p)\, \Theta_{l'}(p) = -\,\delta_{ll'} \,, \tag{135}$$

$$\bar{\Theta}_l(p)\, \Phi_{l'}(p) = \bar{\Phi}_l(p)\, \Theta_{l'}(p) = 0 \,, \tag{136}$$

$$\sum_l \left[\bar{\Phi}_l(p;\zeta)\, \Phi_l(p;\zeta') - \bar{\Theta}_l(p;\zeta)\, \Theta_l(p;\zeta')\right] = \delta_{\zeta\zeta'} \,. \tag{137}$$

By means of Eqs. (134) - (137) the matrix elements of the spectral functions Ξ^N and self-energies Σ^N in the self-consistent particle-antiparticle basis can be determined [60, 11]. One obtains for the former

$$< \Phi_l(\omega^N(|\boldsymbol{p}|),\boldsymbol{p})|\, \Xi^N(\boldsymbol{p})\, |\Phi_{l'}(\omega^N(|\boldsymbol{p}|),\boldsymbol{p}) > = \delta_{ll'}\, n^N(|\boldsymbol{p}|) \,, \tag{138}$$

$$< \Theta_l(\omega^{\bar{N}}(|\boldsymbol{p}|),\boldsymbol{p})|\, \Xi^{\bar{N}}(\boldsymbol{p})\, |\Theta_{l'}(\omega^{\bar{N}}(|\boldsymbol{p}|),\boldsymbol{p}) > = \delta_{ll'}\, n^{\bar{N}}(|\boldsymbol{p}|) \,, \tag{139}$$

with

$$n^{\bar{N},N}(|\boldsymbol{p}|) = \left[m^* \left| W - \left(m^* \frac{\partial \Sigma_S}{\partial \omega} + p^* \frac{\partial \Sigma_V}{\partial \omega} + W \frac{\partial \Sigma_0}{\partial \omega} \right) \right|^{-1} \right]_{p^0 = \omega^{\bar{N},N}(|\boldsymbol{p}|)} \,. \tag{140}$$

The latter function plays the role of a momentum dirstribution function of the single-particle states (occupation probability, $n \leq 1$)

All matrix elements of Ξ^N with respect to anti-nucleon spinors give no contributions if retardation effects in their calculation are neglected [11] (retardation is taken into account everywhere else in the treatment). Thereby the goal of decoupling the T-matrix equation with respect to nucleon and anti-nucleon components can be achieved. More details are given in Appendix H.

The matrix elements of the self-energy follow from Eqs. (123) and (138) - (140), and take the form

$$\Sigma^{\Phi\Phi}(p) \equiv < \Phi_l(p)|\, \Sigma(p)\, |\Phi_l(p) >$$

$$= \frac{1}{2}\int_{\boldsymbol{q}^3}\Big(<\Phi_l(p),\Phi_{l'}(p')|\,T\,|\Phi_l(p),\Phi_{l'}(p')> \qquad (141)$$
$$- \quad <\Phi_l(p),\Phi_{l'}(p')|\,T\,|\Phi_{l'}(p'),\Phi_l(p)>\Big)\,n^N(|\boldsymbol{q}|)\,\Theta^N(|\boldsymbol{q}|)\,,$$

$$\Sigma^{\Theta\Theta}(p) \equiv <\Theta_l(p)|\,\Sigma(p)\,|\Theta_l(p)>$$
$$= \frac{1}{2}\int_{\boldsymbol{q}^3}\Big(<\Theta_l(p),\Phi_{l'}(p')|\,T\,|\Theta_l(p),\Phi_{l'}(p')> \qquad (142)$$
$$- \quad <\Theta_l(p),\Phi_{l'}(p')|\,T\,|\Phi_{l'}(p'),\Theta_l(p)>\Big)\,n^N(|\boldsymbol{q}|)\,\Theta^N(|\boldsymbol{q}|)\,,$$

$$\Sigma^{\Theta\Phi}(p) \equiv <\Theta_{\frac{1}{2}}(p)|\,\Sigma(p)\,|\Phi_{\frac{1}{2}}(p)>$$
$$= \frac{1}{2}\int_{\boldsymbol{q}^3}\Big(<\Theta_{\frac{1}{2}}(p),\Phi_{l'}(p')|\,T\,|\Phi_{\frac{1}{2}}(p),\Phi_{l'}(p')> \qquad (143)$$
$$- \quad <\Theta_{\frac{1}{2}}(p),\Phi_{l'}(p')|\,T\,|\Phi_{l'}(p'),\Phi_{\frac{1}{2}}(p)>\Big)\,n^N(|\boldsymbol{q}|)\,\Theta^N(|\boldsymbol{q}|)\,.$$

One sees from Eqs. (141) - (143) that for the calculation of these matrix elements *both the nucleon-nucleon scattering amplitudes as well as the mixed nucleon-antinucleon amplitudes must be calculated.* This renders the numerical treatment rather complicated. The T-matrix equations occuring in the above expressions are listed in Appendix H.

3.5.2 Hartree-Fock approximation

The Hartree-Fock approximation is obtained by treating only the Born term of the T-matrix of Eq. (124), i.e. $T^{BB'} = v^{BB'}$, with the matrix elements of $v^{BB'}$ given by Eq. (88). The anti-symmetrized Hartree-Fock T-matrix has the form

$$<1\,2\,|\,T^{\mathrm{HF},BB'}\,|\,3\,4> = <1\,2\,|\,v^{BB'}\,|\,3\,4> - <1\,2\,|\,v^{BB'}\,|\,4\,3>\,, \qquad (144)$$

where the first respectively second term refers to the direct (i.e. Hartree) and exchange (Fock) contribution. A graphical illustration of T^{HF} is given in Fig. 5, which is to be compared with the full integral equation of Fig. 1. This leads for the baryon self-energy of Eq. (96) to the following Hartree ($\Sigma^{\mathrm{H},B}$) and Fock ($\Sigma^{\mathrm{F},B}$) terms

$$\Sigma^{\mathrm{H},B}(1,1') = i\sum_{B'} <1\,2\,|\,v^{BB'}\,|\,1'\,3>\; g_1^{B'}(3,2^+)\,, \qquad (145)$$

$$\Sigma^{\mathrm{F},B}(1,1') = i\sum_{B'} <1\,2\,|\,v^{BB'}\,|\,3\,1'>\; g_1^{B'}(3,2^+)\,, \qquad (146)$$

which give the total contribution:

$$\Sigma^{\mathrm{HF},B}(1,1') \equiv \Sigma^{\mathrm{H},B}(1,1') + \Sigma^{\mathrm{F},B}(1,1')\,. \qquad (147)$$

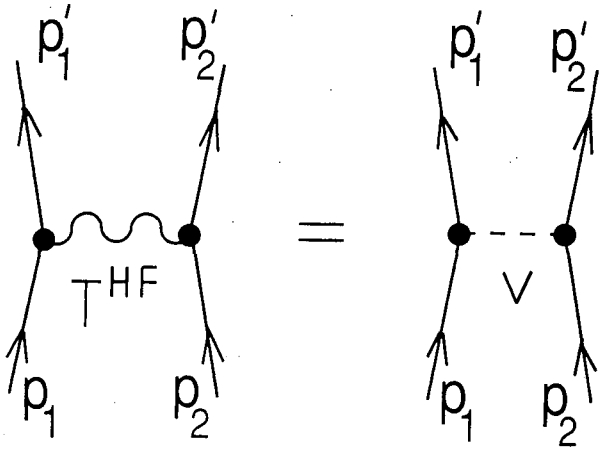

Figure 5: Graphical representation of the Hartree-Fock T-matrix, $T^{\rm HF}$. This approximation scheme is obtained via restriction to the Born term of the T-matrix of Eq. (124). The analytic form of $T^{\rm HF}$ is given in Eq. (144).

As an example we scetch in the following the calculation of the self-energy of the σ-meson. More details can be found in Refs. [10, 50, 51]. After a lenghty calculation one obtains for the Hartree term of $\Sigma^{{\rm HF},B}$

$$\Sigma^{{\rm H},B}_{\zeta_1\zeta_1'}(p)\Big|_\sigma = -i\,\delta_{\zeta_1\zeta_1'}\,\Delta^0(0)\,g_{\sigma B}\sum_{B'} g_{\sigma B'}\int_{q^4} e^{i\eta q^0}\;\delta_{\zeta_2\zeta_3}\,g^{B'}_{\zeta_3\zeta_2}(q)\,. \tag{148}$$

The meson propagator Δ^0 is given in Appendix C.2. The Fock term reads

$$\Sigma^{{\rm F},B}_{\zeta_1\zeta_1'}(p)\Big|_\sigma = i\,g^2_{\sigma B}\int_{q^4} e^{i\eta q^0}\,\Delta^0(p-q)\Big(1\otimes g^B(q)\otimes 1\Big)_{\zeta_1\zeta_1'}\,. \tag{149}$$

Via substituting g^B, from Eq. (101), in Eqs. (148) and (149), and subsequent contour integations, one obtains for the Hartree self-energy

$$\Sigma^{{\rm H},B}_{\zeta_1\zeta_1'}\Big|_\sigma = -2\,\delta_{\zeta_1\zeta_1'}\left(\frac{g_{\sigma B}}{m_\sigma}\right)^2\sum_{B'}(2\,J_{B'}+1)\left(\frac{g_{\sigma B'}}{g_{\sigma B}}\right)\int_{\boldsymbol{q}^3}\Xi^{B'}_S(\boldsymbol{q})\,\Theta^{B'}(\boldsymbol{q})\,, \tag{150}$$

and for the Fock self-energy

$$\begin{aligned}\Sigma^{{\rm F},B}_{\zeta_1\zeta_1'}(p)\Big|_\sigma = \quad & g^2_{\sigma B}\int_{\boldsymbol{q}^3}\Big\{\delta_{\zeta_1\zeta_1'}\,\Xi^B_S(\omega^B(\boldsymbol{q}),\boldsymbol{q}) \;+\; (\boldsymbol{\gamma}\cdot\hat{\boldsymbol{p}})_{\zeta_1\zeta_1'}\,\hat{\boldsymbol{p}}\cdot\hat{\boldsymbol{q}}\;\Xi^B_V(\omega^B(\boldsymbol{q}),\boldsymbol{q}) \\ & + \gamma^0_{\zeta_1\zeta_1'}\,\Xi^B_0(\omega^B(\boldsymbol{q}),\boldsymbol{q})\Big\}\Delta^0(p^0-\omega^B(\boldsymbol{q}),\boldsymbol{p}-\boldsymbol{q})\;\Theta^B(|\boldsymbol{q}|)\,.\end{aligned} \tag{151}$$

The self-energies arising from ω, π, and ϱ-mesons are summarized in Appendix E.

The quantity $2J_B + 1$ in Eq. (150) denotes the spin degeneracy factor of baryons of type B (see Table 3). An important feature of Eqs. (150) and (151) is that the determination of the spectral functions Ξ_i^B (with $i = S, V, 0$) is *sufficient* for their calculation. An explicit calculation of the propagator functions g^B is neither here nor for the determination of the equation of state of the system (see Sect. 3.6) necessary.

3.5.3 Hartree approximation ($\sigma - \omega$ model)

The Hartree self-energies of σ and ω-mesons, given by respectively Eq. (150) and (278), serve to apply the spectral function formalism to the reproduction of Walecka's $\sigma-\omega$ mean-field results [64, 65, 14]. The spectral function of Eq. (116) and the energy-momentum relation of Eq. (119) take, in the Hartree limit, for which $\Sigma_V^{\mathrm{H},B} \equiv 0$ (cf. [50, 51, 10]), the form:

$$m_B^* \equiv m_B + \Sigma_S^{\mathrm{H},B} , \tag{152}$$

$$\Xi_S^{\mathrm{H},B}(\boldsymbol{q}) = \frac{m_B^*}{2\,\epsilon^{\mathrm{H},B}(\boldsymbol{q})} , \qquad \Xi_V^{\mathrm{H},B}(\boldsymbol{q}) = \frac{-\,|\boldsymbol{q}|}{2\,\epsilon^{\mathrm{H},B}(\boldsymbol{q})} , \qquad \Xi_0^{\mathrm{H},B}(\boldsymbol{q}) = \frac{1}{2} , \tag{153}$$

with

$$\epsilon^{\mathrm{H},B} = \sqrt{[m_B^*]^2 + \boldsymbol{q}^2} = \frac{1}{2}\left|\frac{\partial D^B}{\partial \omega}\right|_{\omega^B(\boldsymbol{q})} . \tag{154}$$

By substituting Eqs. (152) - (154) into Eq. (150), one arrives for the nucleon self-energies (only scalar and time-like terms contribute) at the well-known expressions

$$\begin{aligned} \Sigma_S^{\mathrm{H},N} = & \left(\frac{g_{\sigma N}}{m_\sigma}\right)^2 \sum_B \left(\frac{g_{\sigma B}}{g_{\sigma N}}\right) \frac{2J_B+1}{4\,\pi^2}\, m_B^* \\ & \times \left(p_{F,B}\,\epsilon_F^B - [m_B^*]^2 \ln\left|\frac{p_{F,B} + \epsilon_F^B}{m_B^*}\right| \right) \\ & + \left(\frac{g_{\sigma N}}{m_\sigma}\right)^2 \left(\bar{b}_N\, m_N \left[\Sigma_S^N\right]^2 - \bar{c}_N \left[\Sigma_S^N\right]^3 \right) , \end{aligned} \tag{155}$$

$$\Sigma_0^{\mathrm{H},N} = \left(\frac{g_{\omega N}}{m_\omega}\right)^2 \sum_B \left(\frac{g_{\omega B}}{g_{\omega N}}\right) \frac{2J_B+1}{6\,\pi^2}\, p_{F,B}^3 . \tag{156}$$

A characteristic feature of this approach is that the Hartree self-energy depends only on nuclear density, ϱ ($\propto p_F^3$), and hence neither on energy ($p^0 = \omega^B(\boldsymbol{p})$) nor momentum (compare Eqs. (148) and (150)). This is in contrast to the Hartree-Fock approach where one gets for the exchange terms $\Sigma^{\mathrm{F},B} = \Sigma^{\mathrm{F},B}(p^0 = \omega^B(\boldsymbol{p}), \boldsymbol{p})$.

The second term in Eq. (155) occurs if cubic and quartic self-interactions of the σ-field are taken into account in the Lagrangian of Eq. (79). An explicit expression for $\mathcal{L}$ is given in Eq. (223) of Appendix B. The resulting self-energy, denoted by $\Sigma^{(\sigma^4)}$, has the form (for more details, see Refs. [10, 50, 51]):

$$\Sigma^{(\sigma^4)}_{\zeta_1\zeta_1'}(p) \;=\; \delta_{\zeta_1\zeta_1'} \left(\frac{g_{\sigma N}}{m_\sigma}\right)^2 \left[m_N\, \bar{b}_N \left(\Sigma_S^{\mathrm{H},N}\right)^2 - \bar{c}_N \left(\Sigma_S^{\mathrm{H},N}\right)^3\right] . \qquad (157)$$

Cubic and quartic terms are known to be important for the linear $\sigma - \omega$ nuclear field theory to obtain an effective nucleon mass in matter, m_N^*, and a compression modulus, K, which are compatible with experimental values [66]. However, it has recently been noticed by Zimanyi and Moszkowski [67] that if the scalar field is coupled to the derivative of the nucleon field, these two nuclear properties are automatically in fairly reasonable accord with present knowledge of their values. Neutron star matter equations of state within this framework have been determined by Glendenning, Weber, and Moszkowsi [68].

3.6 Equation of state

3.6.1 Λ approximation

The energy density of the system, described by the Lagrangian of Eq. (79), can be split into the following three different contributions [16, 11]:

$$\epsilon \;\equiv\; \frac{1}{\Omega}\int_\Omega d^3\boldsymbol{x} \,<\Phi_0\,|\mathcal{H}_{\mathrm{Bary}}(x) \,+\, \mathcal{H}_{\mathrm{Mes}}(x) \,+\, \mathcal{H}_{\mathrm{Int}}(x)\,|\Phi_0> \qquad (158)$$

$$\equiv\; \epsilon^0_{\mathrm{Bary}} \;+\; [\,\epsilon^0_{\mathrm{Mes}} \,+\, \epsilon_{\mathrm{Int}}\,] . \qquad (159)$$

The first term in Eqs. (158) and (159) is the energy density of free baryons in the medium. The remaining two terms refer to the free meson term and the interaction term of Eq. (79). These are to be expressed in terms of Green's functions. We discuss this in the following for the free baryonic part of Eq. (158). The Hamiltonian density of free baryons is given by

$$\mathcal{H}^0_{\mathrm{Bary}}(x) \;=\; \sum_B \bar{\psi}_B(x)\,(\gamma^\mu\, p_\mu \,+\, m_B)\,\psi_B(x) . \qquad (160)$$

The ground-state expectation value $<\Phi_0|\bar{\psi}_B\,\psi_B|\Phi_0>$ can be replaced by the two-point Green's function which results from Eq. (80) by setting $n = 1$. Fourier transformation then leads to (cf. Ref. [50, 51])

$$\epsilon^0_{\mathrm{Bary}} \;=\; -\lim_{x'\to x^+} \sum_B \partial_0 \int_{q^4} e^{-i\,q\,(x-x')}\;\gamma^0_{\zeta\zeta'}\, g^B_{\zeta'\zeta}(q) \qquad (161)$$

$$= \; 2 \sum_B (2J_B+1) \int_{\boldsymbol{q}^3} \left[m_B \, \Xi_S^B(\boldsymbol{q}) \; - \; |\boldsymbol{q}| \, \Xi_V^B(\boldsymbol{q}) \right] \; \Theta^B(|\boldsymbol{q}|) \, . \qquad (162)$$

Eq. (162) follows by making use of Eqs. (101) and (116). The treatment of the interaction term is more complicated. It can be combined with the free-meson term to give

$$\epsilon^0_{\rm Mes} + \epsilon_{\rm Int} = -\frac{1}{2\,\Omega} \sum_{BB'} \int_\Omega d^3\boldsymbol{x} \qquad < \zeta_1\zeta_2 \; x_1 x_2 | v^{BB'} | x_3 x_4 \; \zeta_3\zeta_4 > \qquad (163)$$
$$\times \; g_2^{B'B}(x_3 x_4, x_1^+ x_2^+)_{\zeta_3\zeta_4,\zeta_1\zeta_2} \, .$$

Eqs. (95) and (96) can be used to replace the right hand side of Eq. (163) by $i\,\Sigma\cdot g_1$. Afterwards one can proceed in the same way as described above (to arrive at Eq. (162)). The final result is [50, 51]

$$\epsilon^0_{\rm Mes} + \epsilon_{\rm Int} = \sum_B (2J_B+1) \int_{\boldsymbol{q}^3} \quad \left[\Sigma_S^B(\omega^B(\boldsymbol{q}),\boldsymbol{q}) \, \Xi_S^B(\boldsymbol{q}) - \Sigma_V^B(\omega^B(\boldsymbol{q}),\boldsymbol{q}) \, \Xi_V^B(\boldsymbol{q}) \right.$$
$$\left. + \, \Sigma_0^B(\omega^B(\boldsymbol{q}),\boldsymbol{q}) \, \Xi_0^B(\boldsymbol{q}) \right] \, \Theta^B(|\boldsymbol{q}|) \, . \qquad (164)$$

The density of baryons of type B is obtained as follows [11, 50, 51, 10]:

$$\varrho^B \equiv \frac{N^B}{\Omega} = \frac{1}{\Omega} \int_\Omega d^3\boldsymbol{x} \; < \Phi_0 | \psi_B^\dagger(x) \, \psi_B(x) | \Phi_0 > \Big|_{x^0=0} \qquad (165)$$
$$= i \lim_{x' \to x^+} \gamma^0_{\zeta\zeta'} \, g^B_{\zeta'\zeta}(x,x') \qquad (166)$$
$$= i \, \gamma^0_{\zeta\zeta'} \int_{q^4} e^{i\eta q^0} \, g^B_{\zeta'\zeta}(q) \qquad (167)$$
$$= 2 \, (2J_B+1) \int_{\boldsymbol{q}^3} \Xi_0^B(\boldsymbol{q}) \, \Theta^B(|\boldsymbol{q}|) \, . \qquad (168)$$

The total number density, ϱ, is obtained from

$$\varrho \equiv \sum_B \varrho^B \, . \qquad (169)$$

From the energy density and density of baryons, the energy per baryon, E/A, follows as

$$\frac{\epsilon^{\rm Int}(\varrho)}{\varrho} = \frac{\epsilon(\varrho)}{\varrho} - m_N \, , \qquad \text{where} \qquad \epsilon^{\rm Int}(\varrho) \equiv \frac{E(\varrho)}{A} \, . \qquad (170)$$

The energy $\epsilon^{\rm Int}$ is referred to as internal energy. It plays a role in the calculation of the total baryon mass of a neutron star (cf. Eqs. (209) - (210)). Finally, the pressure of the system follows from the thermodynamic relation

$$P = \varrho^2 \, \frac{\partial}{\partial \varrho} \, \frac{E}{A}(\varrho) \, . \qquad (171)$$

Another important quantity, besides the nuclear density, is the scalar baryon density, $\bar{\varrho}^B$. It can be obtained in a similar fashion as ϱ:

$$\begin{aligned}
\bar{\varrho}^B &= \frac{1}{\Omega}\int_\Omega d^3\,\boldsymbol{x}\; <\Phi_0|\bar{\psi}_B(x)\,\psi_B(x)|\Phi_0>\Big|_{x^0=0} && (172)\\
&= i\lim_{x'\to x^+}\delta_{\zeta\zeta'}\,g^B_{\zeta'\zeta}(x,x') && (173)\\
&= i\,\delta_{\zeta\zeta'}\int_{q^4} e^{i\eta q^0}\,g^B_{\zeta'\zeta}(q) && (174)\\
&= 2\,(2J_B+1)\int_{\boldsymbol{q}^3}\Xi^B_S(\boldsymbol{q})\,\Theta^B(|\boldsymbol{q}|)\,. && (175)
\end{aligned}$$

The total scalar density, $\bar{\varrho}$, is defined by

$$\bar{\varrho}\equiv\sum_B\,\bar{\varrho}^B\,. \tag{176}$$

3.6.2 Hartree-Fock equation of state

From the energy density expressions of Eqs. (162) and (164) derived for the Λ method, the following Hartree ($\epsilon^{\rm H}$) and Fock ($\epsilon^{\rm F}$) energy densities of neutron star matter in generalized β equilibrium can be obtained [10]. The Hartree expression has the form

$$\begin{aligned}
\epsilon^H &= \frac{1}{2}\sum_B\Big[\Sigma_0^{{\rm H},B}+I_{3B}\,\Sigma_{03}^{{\rm H},B}\Big]\,\varrho^{{\rm H},B}-\frac{1}{2}\sum_B\Big[\Sigma_S^{{\rm H},B}\;\bar{\varrho}^{{\rm H},B}\Big]\\
&+ \frac{1}{2\pi^2}\sum_B(2J_B+1)\int_0^{p_{F,B}}dq\,q^2\sqrt{[m_B+\Sigma_S^{{\rm H},B}]^2+q^2}\\
&- \frac{1}{2}\Big[-\frac{1}{3}\,\bar{b}_N\,m_N\Big(\Sigma_S^{{\rm H},N}\Big)^3+\frac{1}{2}\,\bar{c}_N\,\Big(\Sigma_S^{{\rm H},N}\Big)^4\Big] \qquad (177)\\
&+ \frac{1}{2\pi^2}\sum_{\lambda=e,\mu}(2J_\lambda+1)\int_0^{p_{F,B}}dq\,q^2\,\sqrt{m_\lambda^2+q^2}\;.
\end{aligned}$$

This result agrees with the energy density obtained from Walecka's mean-field theory, derived in Ref. [45]. More details are given in Appendix —reftensor:app, where the calculation of the energy-momentum tensor in the framwork of relativistic Green's functions is demonstrated for the $\sigma-\omega$ model. The Fock term gives

$$\begin{aligned}
\epsilon^F &= \sum_B(2J_B+1)\int_{\boldsymbol{q}^3}\Big[\Sigma_S^{{\rm F},B}(\boldsymbol{q})\,\Xi_S^{{\rm H},B}(\boldsymbol{q})-\Sigma_V^{{\rm F},B}(\boldsymbol{q})\,\Xi_V^{{\rm H},B}(\boldsymbol{q})\\
&\quad+\Sigma_0^{{\rm F},B}(\boldsymbol{q})\,\Xi_0^{{\rm H},B}(\boldsymbol{q})\Big]\,\Theta^B(|\boldsymbol{q}|)\,. \qquad (178)
\end{aligned}$$

The pressure terms are given by

$$
\begin{aligned}
P^H &= \frac{1}{2}\sum_B \left[\Sigma_0^{\mathrm{H},B} + I_{3B}\,\Sigma_{03}^{\mathrm{H},B}\right]\,\varrho^{\mathrm{H},B} + \frac{1}{2}\sum_B\left[\Sigma_S^{\mathrm{H},B}\;\bar{\varrho}^{\mathrm{H},B}\right] \\
&+ \frac{1}{6\pi^2}\sum_B (2J_B+1)\int_0^{p_{F,B}} dq\,\frac{q^4}{\sqrt{[m_B+\Sigma_S^{\mathrm{H},B}]^2\,+\,q^2}} \\
&+ \frac{1}{2}\left[-\frac{1}{3}\,\bar{b}_N\,m_N\left(\Sigma_S^{\mathrm{H},N}\right)^3 + \frac{1}{2}\,\bar{c}_N\left(\Sigma_S^{\mathrm{H},N}\right)^4\right] \qquad (179) \\
&+ \frac{1}{6\pi^2}\sum_{\lambda=e,\mu}(2J_\lambda+1)\int_0^{p_{F,B}} dq\,\frac{q^4}{\sqrt{m_\lambda^2+q^2}}\,, \\
P^F &= \epsilon^F\,. \qquad (180)
\end{aligned}
$$

The inclusion of cubic and quartic self-interactions (Eq. (223)) as well as leptons (Eq. (224)) in the Lagrangian of Eq. (79) leads to additional terms in the energy density. The former give [50, 51, 10]

$$
\epsilon^{(\sigma^4)}(\Sigma^{\mathrm{H},N}) = \frac{1}{2}\left[\frac{1}{3}\,\bar{b}_N\,m_N\left[\Sigma^{\mathrm{H},N}\right]^3 - \frac{1}{2}\,\bar{c}_N\left[\Sigma^{\mathrm{H},N}\right]^4\right]. \qquad (181)
$$

The calculation of energy density and pressure of free leptons serves for an easy demonstration of the Green's function technique. We start from the energy-momentum tensor of Eq. (286). One obtains for the expectation value $<\Phi_0|\,\mathcal{T}^{\mathrm{Lep}}\,|\Phi_0>$ [10]

$$
\begin{aligned}
<\Phi_0|\,\mathcal{T}^{\mathrm{Lep}}_{\mu\nu}(x)\,|\Phi_0> &= -\lim_{x'\to x^+}\sum_{\lambda=e,\mu}\partial_\nu\,Tr\left(\gamma_\mu\,G^\lambda(x,x')\right) \qquad (182) \\
&= -\lim_{x'\to x^+}\partial_\nu\sum_{\lambda=e,\mu}\int\frac{d^4q}{(2\pi)^4}e^{-i\,q(x-x')}\,Tr\left(\gamma_\mu\,G^\lambda(q)\right). \qquad (183)
\end{aligned}
$$

(Compare with the determination of $<\mathcal{T}>$ in the case of baryons performed in Appendix F.) In analogy to Eq. (101), the momentum-space representation of the lepton propagator, denoted by G^λ, reads (α and α' refer to spin quantum numbers)

$$
G^\lambda_{\alpha\alpha'}(p) = \int_{-\infty}^{+\infty} d\omega\,\frac{\Gamma^\lambda_{\alpha\alpha'}(\omega,\boldsymbol{p})}{\omega-(p^0-\mu^\lambda)\,(1+i\eta)}\,. \qquad (184)
$$

The free leptonic spectral functions are (compare with Eqs. (115) - (118))

$$
\Gamma^\lambda_i(\omega,\boldsymbol{p}) = \delta\left(\omega+\mu^\lambda\,-\,\omega^\lambda(\boldsymbol{p})\right)\;\Gamma^\lambda_i(\boldsymbol{p})\,,\qquad i=S,V,0\,, \qquad (185)
$$

with

$$\omega^\lambda(\boldsymbol{p}) = \sqrt{m_\lambda^2 + \boldsymbol{p}^2} \tag{186}$$

$$\Gamma_S^\lambda(\boldsymbol{p}) = \frac{m_\lambda}{2\sqrt{m_\lambda^2 + \boldsymbol{p}^2}}, \tag{187}$$

$$\Gamma_V^\lambda(\boldsymbol{p}) = -\frac{|\boldsymbol{p}|}{2\sqrt{m_\lambda^2 + \boldsymbol{p}^2}}, \tag{188}$$

$$\Gamma_0^\lambda(\boldsymbol{p}) = \frac{1}{2}. \tag{189}$$

The calculation of the lepton density, denoted by ϱ^λ, can be performed analogously to Eqs. (165) - (168). By denoting the leptonic distribution function with $\Theta^\lambda(\boldsymbol{q}) \equiv \Theta(p_{F,\lambda} - |\boldsymbol{q}|)$, one gets

$$\varrho^\lambda = i \lim_{x' \to x^+} \gamma^0_{\zeta\zeta'} G^\lambda_{\zeta'\zeta}(x, x') \tag{190}$$

$$= i \int_{q^4} e^{i\eta q^0} \gamma^0_{\zeta\zeta'} G^\lambda_{\zeta'\zeta}(q) \tag{191}$$

$$= 2(2J_\lambda + 1) \int_{\mathrm{q}^3} \Gamma_0^\lambda(\boldsymbol{q})\, \Theta^\lambda(\boldsymbol{q}) \tag{192}$$

$$= \frac{2J_\lambda + 1}{2} \frac{p_{F,\lambda}^3}{3\pi^2}. \tag{193}$$

The total number density of leptons, ϱ^{Lep}, is given by

$$\varrho^{\mathrm{Lep}} \equiv \sum_\lambda \varrho^\lambda. \tag{194}$$

The energy density and pressure contributions result from Eq. (183) as

$$\epsilon^0_{\mathrm{Lep}} \equiv < \mathcal{T}^{\mathrm{Lep}}_{00}(x) > = \frac{1}{\pi^2} \sum_{\lambda=e,\mu} (2J_\lambda + 1) \int_0^{p_{F,\lambda}} dq\, q^2 \sqrt{m_\lambda^2 + q^2}, \tag{195}$$

and

$$P^0_{\mathrm{Lep}} \equiv \frac{1}{3} \sum_i < \mathcal{T}^{\mathrm{Lep}}_{ii}(x) > = \frac{1}{6\pi^2} \sum_{\lambda=e,\mu} (2J_\lambda + 1) \int_0^{p_{F,\lambda}} dq \frac{q^4}{\sqrt{m_\lambda^2 + q^2}}. \tag{196}$$

In the above equations, $2J_\lambda + 1$ refers to the spin degeneracy factor of leptons of type λ (see Table 5), and $p_{F,\lambda}$ denotes their Fermi momenta.

4 Summary of the self-consistent matter equations

In the following we list the equations which must be solved self-consistently to obtain the HV, HFV, $\Lambda^{00}_{\mathrm{Bonn}}$ + HV, and $\Lambda^{00}_{\mathrm{HEA}}$ + HFV equations of state. For the Hartree and Hartree-Fock treatment these equations are given by [45, 10]:

1. Eqs. (116) - (119): Spectral functions $\Xi^{B,\bar{B}}$ and energy-momentum relations $\omega^{B,\bar{B}}$. We note that at zero temperature, the anti-baryons do not contribute. The energy-momentum relations determine the Fermi momenta $p_{F,B}$ of the baryons via the relation $\mu^B = \omega^B(p_{F,B})$ for

$$B = p\ ,\ \ n\ ,\ \ \Sigma^{\pm,0}\ ,\ \ \Lambda\ ,\ \ \Xi^{0,-}\ ,\ \ \Delta^{++,+,0,-}\ , \tag{197}$$

i.e.,

$$p_{F,p}\ ,\ \ p_{F,n}\ ,\ \ p_{F,\Sigma^{\pm,0}}\ ,\ \ p_{F,\Lambda}\ ,\ \ p_{F,\Xi^{0,-}}\ ,\ \ p_{F,\Delta^{++,+,0,-}}\ . \tag{198}$$

This constitutes a maximum number of $b = 13$ unknowns (see Table 3). The actual number of populated baryon states depends on the density ϱ of the system, given by Eq. (169).

2. Chemical equilibrium is imposed through the chemical potentials and involves two independent potentials, μ^n and μ^e, corresponding to baryon and electric charge conservation [45]. For baryon B the chemical potential is (q_B denotes the electric charge of the baryon)

$$\mu^B \ = \ \mu^n \ - \ q_B\, \mu^e\ . \tag{199}$$

Hence knowledge of μ^n and μ^e is sufficient for the determination of all μ^B (two unknowns). For the leptons (Table 5) the chemical potentials are

$$\mu^\mu \ = \ \mu^e\ . \tag{200}$$

The energy-momentum relations of Eq. (186) determine the Fermi momenta of the leptons (two unknowns):

$$p_{F,e} \qquad p_{F,\mu}\ ; \tag{201}$$

3. Eq. (147): Baryon self-energies Σ^B,

$$\Sigma^{\mathrm{H},B}\Big|_{\sigma,\omega,\varrho}\ , \qquad \Sigma^{\mathrm{F},B}\Big|_{\sigma,\omega,\pi,\varrho}\ , \tag{202}$$

which constitutes seven unknown functions;

4. The constraint of zero total electric charge of neutron star matter, $\varrho^{\mathrm{el}}_{\mathrm{tot}} = \varrho^{\mathrm{el}}_{\mathrm{Bary}} + \varrho^{\mathrm{el}}_{\mathrm{Lep}} \equiv 0$, leads to

$$\sum_B q_B\,(2J_B+1)\,\frac{p^3_{F,B}}{6\pi^2} \ - \ \Big[\sum_{\lambda=e,\mu}\frac{p^3_{F,\lambda}}{3\pi^2} + \varrho_\pi\,\Theta(\mu^\pi - m_\pi)\Big] \ = \ 0\ . \tag{203}$$

To arrive at this relation, Eqs. (169) and (194) have been used. It has been demonstrated [45] that the only meson that can condense in neutron stars is the π^-, other than those that are driven by finite baryon source currents in the normal state (e.g. the σ and ω-mesons). The impact of pion condensation on charge neutrality is taken into account by the last term of Eq. (203). In this work however we shall not treat the complicated problem of pion condensation [69, 70, 71, 72, 73] as far as the equations of state HV, HFV, Bonn, and HEA are concerned.

In summary, the number of unknowns encountered in the Hartree and Hartree-Fock treatment equals respectively $(7 + b)$ and $(11 + b)$;

5. Eqs. (162), (164), and (181): Baryonic energy densities $\epsilon^0_{\rm Bary}$, $\epsilon^0_{\rm Mes} + \epsilon_{\rm Int}$, and $\epsilon^{(\sigma^4)}$;

6. Eqs. (195) and (196): Leptonic equation of state $P^0_{\rm Lep}(\epsilon)$.

The equations of the Λ^{00} method have been solved in the low nuclear density regime where neutron star matter consists to a good approximation of only neutrons [9, 10]. Restriction to neutrons implies in the equations of the previous sections $B = n$. The following set of equations must be solved self-consistently (cf. [11]),

1. Eq. (124): Integral equations of the T-matrix. The Bonn and HEA meson-exchange potentials serve as an input;

2. Eq. (123): Neutron self-energies Σ^n;

3. Eqs. (116) - (119): Spectral functions Ξ^n;

4. Eq. (162) and (164): Equation of state.

5 Parameters of the many-body theories

5.1 HEA and Bonn meson-exchange models

The HEA and Bonn meson-exchange models for the nucleon-nucleon interaction allow for so-called parameter-free nuclear matter calculations since their parameters are determined by the relativistic two-nucleon scattering problem and the properties of the deuteron, and *not* to by the bulk properties of infinite nuclear matter or finite

nuclei (effective coupling constants). Therefore the above models are referred to as *realistic* potentials. Their applicability for nuclear matter calculations however makes it necessary to go beyond the Hartree and Hartree-Fock approach, because they do not saturate nuclar matter [11] (see Sect. 5.2 for the determination of the parameters of the Hartree-Fock method). To achive saturation, a self-consistent determination of the effective two-particle interaction in matter (i.e. the T-matrix) must be performed. In other words the applicability of the above potentials is restricted to the Λ^{ij} methods of Sect. 3.5.1, of which we treat the Λ^{00} version in this work.

Since the above meson-exchange potentials are constructed by restricting the intermediate propagators to positive energy states only, one uses a *regularized* interaction with form factors $F_M(q)$. These are summarized for the Bonn and HEA potentials in Table 7. The regularization scheme implies the following replacements for the meson coupling strengths [61, 14, 12, 74]

$$g_M \longrightarrow F_M(p - p')\, g_M \,, \tag{204}$$

where M refers to the different meson types, given in Table 4. This can be incorporated via replacing the meson propagators by

$$\Delta^0(q) \longrightarrow F_M^2(q)\, \Delta^0(q) \tag{205}$$

in Eqs. (148) - (151) and (272) - (282). The parameters of the Bonn and HEA potentials, i.e. meson masses, coupling constants, and cut-off masses, are listed in Tables 6 and 7.

5.2 Effective coupling constants of the Hartree-Fock method

The coupling constants of the scalar-vector-isovector Lagrangian of Eq. (211) are not determined by the nucleon-nucleon interaction in free space, but must be adjusted to the bulk properties of nuclear matter at saturation. These are binding energy, effective mass, compression modulus, and symmetry energy. At first sight it seems as if $\mathcal{L}(x)$ would contain a large number of unknowns. If one assumes the prescription of universal coupling, which is the case here, there remain in principle the following unknown parameters (the baryons are given their physical masses [75]): four mesons masses $(m_\sigma, m_\omega, m_\pi, m_\varrho)$ and seven coupling constants $(g_{\sigma N}, g_{\omega N}, f_{\pi N}, g_{\varrho N}, f_{\varrho N}; \bar{b}_N, \bar{c}_N)$. The meson masses usually are taken to be equal to their physical values, except for the hypothetical σ-meson, which is introduced to simulate the correlated 2π exchange.

Table 6: The coupling strengths and masses used for the Hartree (HV) and Hartree-Fock (HFV) calculations (effective Lagrangian of Eq. (211)). The parameters of the Bonn and HEA meson-exchange potentials served as an input for solving the relativistic Λ^{00} equations.

Quantity	HV	HFV	Bonn	HEA
m_N [MeV]	939	938.9	938.926	938.9
m_σ [MeV]	550	550	550[†]	500
m_ω [MeV]	783	783	782.6	782.8
m_π [MeV]	-	138	138.03	138.5
m_ϱ [MeV]	770	770	769	763
m_η [MeV]	-	-	548.8	548.5
m_δ [MeV]	-	-	983	960
m_ϕ [MeV]	-	-	-	1020
$g^2_{\sigma N}/4\pi$	6.16	7.10	8.2797	4.63
$g^2_{\omega N}/4\pi$	6.71	6.80	20	14
$g^2_{\pi N}/4\pi$	-	-	14.6	13.00
$f^2_{\pi N}/4\pi$	-	0.08	-	-
$g^2_{\varrho N}/4\pi$	7.51	0.55	0.81	1.5
$f_{\varrho N}/g_{\varrho N}$	-	6.6	6.1	3.5
$g^2_{\eta N}/4\pi$	-	-	5	6.0
$g^2_{\delta N}/4\pi$	-	-	1.1075	4.74
$g^2_{\phi N}/4\pi$	-	-	-	7.0
$10^3\ \bar{b}_N$	4.14	-	-	-
$10^3\ \bar{c}_N$	7.16	-	-	-
Ref.	[45]	[77]	[12]	[13]

[†] The parameters for the σ-meson apply only for the isospin $T = 1$ potential. For T=0, one has: $m_\sigma = 720$ MeV, $g^2_\sigma/4\pi$=16.9822.

For it one takes a tentative value of about 550 MeV. The ϱ-meson vector coupling constant $g_{\varrho N}$ can be deduced from the description of the nucleon-nucleon interaction, and the ratio of the tensor to the vector coupling strength, i.e. $f_{\varrho N}/g_{\varrho N}$, can be obtained from the vector-dominance model [76] which leads to $f_{\varrho N}/g_{\varrho N} \approx 3.7$. Hence, there remain two (four, if σ^4 self-interactions are taken into account) undetermined coupling strengths in the theory: $g_{\sigma N}, g_{\omega N}, \bar{b}_N, \bar{c}_N$. These are adjusted to the above mentioned ground-state properties of nuclear matter. A parameter set adjusted in this way, which allows for Hartree-Fock calculations based of the scalar-vector-isovector Lagrangian, but without σ^4-terms, has been given by Bouyssy et al. [77]. We have adopted this set, which is denoted HFV according to an earlier inves-

Table 7: Cut-off masses $\Lambda_M(p,p')$ ($M = \sigma,\omega,\pi,\varrho,\eta,\delta,\phi$) of the Bonn and HEA meson-exchange potentials. The form factors $F_M(p,p')$ † are defined below.

Quantity	σ	ω	π	ϱ	η	δ	ϕ
				Bonn			
Λ_M [GeV]	2.0	1.5	1.3	2.0	1.5	2.0	-
κ_M	1	1	1	2	1	1	-
				HEA			
Λ_M [GeV]	1.95	1.9	1.95	1.95	1.95	1.95	1.95
$\Lambda_M^{(v)}$ [GeV]		1.25		1.25			1.25

† The form factor of the Bonn potential is given by
$F_M(\boldsymbol{p}^2) = (\Lambda_M^2 - m_M^2)/(\Lambda_M^2 + \boldsymbol{p}^2)^{\kappa_M}$.
The form vactors of the HEA potential are:
$F_M(p,p') = \Lambda_M^2 \,/\, [\Lambda_M^2 - (p-p')^2]$ for $M = \sigma,\pi,\delta,\eta$,
$F_M(p,p') = [\Lambda_M^2 \,/\, [\Lambda_M^2 - (p-p')^2]]$
$\times \sqrt{[[\Lambda_M^{(v)}]^2 - m_M^2] \,/\, [[\Lambda_M^{(v)}]^2 - (p-p')^2]}$ for $M = \omega,\varrho,\phi$.

tigation [27]. Secondly we make use of a parameter set labeled HV which has been adjusted by Glendenning [45] for Hartree calculations. Therein σ, ω, and ϱ-mesons and σ^4 self-interactions are included. The parameter sets are summarized in Table 6.

6 Results and discussion

6.1 Neutron star matter equations of state

The physical features of the equations of this work are listed in Table 2. For energy densities $0.056 < \epsilon/(\mathrm{MeV/fm^3}) < 5.6$ (inner star surface region), the equations of state of Harrison-Wheeler [78] and Negele-Vautherin [79] have been used (cf. first two entries of Table 2). From relativistic Hartree [9, 10] and Hartree-Fock [10] neutron star matter calculations performed for the HV and HFV equations of state , it is known that the population of hyperon states sets in at energy densities $\epsilon^{\mathrm{HV}} \gtrsim 320$ MeV/fm^3 ($\varrho^{\mathrm{HV}} \gtrsim 0.32$ fm^{-3}) in the Hartree case, and $\epsilon^{\mathrm{HFV}} \gtrsim 240$ MeV/fm^3 ($\varrho^{\mathrm{HFV}} \gtrsim 0.22$ fm^{-3}) in the Hartree-Fock case. For the purpose of comparison, normal nuclear matter saturates at $\epsilon_0 \approx 140$ MeV/fm^3, which corresponds to $\varrho_0 \approx 0.15$ fm^{-3}. From both of these approximations it was found that matter consists of nearly 100% neutrons at ϵ_0 [9, 10]. This figure decreases to 85% for $\epsilon \lesssim 300$ MeV/fm^3. Beyond such energy densities the influence of hyperons and leptons on the equation of state of neutron star

Table 8: $\Lambda^{00}_{\rm Bonn}$ + HV neutron star matter equation of state.

ϵ [Mev/fm^3]	P [Mev/fm^3]	ϵ [Mev/fm^3]	P [Mev/fm^3]	ϵ [Mev/fm^3]	P [Mev/fm^3]
20.00	0.0334	240.00	16.8402	800.00	185.2495
30.00	0.0716	250.00	19.8478	850.00	207.0768
40.00	0.1252	260.00	22.3301	900.00	229.8470
50.00	0.1940	270.00	24.5069	950.00	253.2220
60.00	0.2543	280.00	26.3141	1000.00	277.0967
70.00	0.2881	290.00	27.8400	1100.00	326.2753
80.00	0.3168	300.00	29.2735	1200.00	377.8391
90.00	0.3726	320.00	31.8729	1300.00	431.9030
100.00	0.4867	340.00	34.9293	1400.00	488.3641
110.00	0.6732	360.00	38.5936	1500.00	547.0107
120.00	0.9309	380.00	43.0821	1600.00	607.6985
130.00	1.2422	400.00	47.6383	1700.00	670.0674
140.00	1.5604	420.00	52.6424	1800.00	734.2850
150.00	1.8597	440.00	58.0886	1900.00	799.9583
160.00	2.2221	460.00	63.8877	2000.00	867.2625
170.00	2.7560	480.00	70.0592	2100.00	935.7751
180.00	3.5382	500.00	76.2301	2200.00	1005.4905
190.00	4.6249	550.00	91.1712	2300.00	1076.5145
200.00	6.0850	600.00	106.3596	2400.00	1148.7158
210.00	8.0066	650.00	124.0257	2500.00	1221.8511
220.00	10.4791	700.00	143.6154	2600.00	1295.6761
230.00	13.5411	750.00	164.0439	2700.00	1369.9474

matter becomes important, leading to less pressure for a given value of ϵ (softening of the equation of state). The complete set of baryon states of Table 3 which become populated in the framwork of our Hartree and Hartree-Fock calculations are shown in the last two rows (labeled HV and HFV) of Table 2. These populations are obtained by means of solving the self-consistent matter equations summarized in Sect. 4.

The significant difference between the Hartree and Hartree-Fock populations has its origin in the rather different coupling parameters of both methods [10]. These are listed in the second and third column of Table 6. This is in particular the case for the vector coupling constant of the ϱ-meson, g_ϱ, which is for HV roughly fourteen times as large as for HFV. As a consequence, the Δ^- state is present in charge neutral many-baryon/lepton star matter treated in the HFV approximation, but none of its states becomes populated for HV [10]. As outlined above, at "intermediate" densities

Table 9: $\Lambda^{00}_{\rm HEA} + HFV$ neutron star matter equation of state.

ϵ [Mev/fm^3]	P [Mev/fm^3]	ϵ [Mev/fm^3]	P [Mev/fm^3]	ϵ [Mev/fm^3]	P [Mev/fm^3]
20.00	0.0339	240.00	13.7560	800.00	260.4816
30.00	0.0729	250.00	15.3049	850.00	294.1008
40.00	0.1256	260.00	16.7614	900.00	326.2991
50.00	0.1928	270.00	18.1674	950.00	359.8443
60.00	0.2571	280.00	19.3265	1000.00	395.9482
70.00	0.3038	290.00	20.3201	1100.00	471.4739
80.00	0.3422	300.00	21.2778	1200.00	545.1085
90.00	0.3889	320.00	23.2768	1300.00	621.1187
100.00	0.4722	340.00	25.9289	1400.00	698.6987
110.00	0.6267	360.00	28.9374	1500.00	777.6942
120.00	0.8547	380.00	32.8234	1600.00	857.9180
130.00	1.1177	400.00	37.8371	1700.00	939.2037
140.00	1.3756	420.00	43.9641	1800.00	1021.4135
150.00	1.6159	440.00	51.2438	1900.00	1104.4231
160.00	1.9403	460.00	59.1727	2000.00	1188.1268
170.00	2.5268	480.00	67.7602	2100.00	1272.4475
180.00	3.5641	500.00	76.9150	2200.00	1357.3187
190.00	5.0433	550.00	101.9551	2300.00	1442.6742
200.00	6.7660	600.00	130.1272	2400.00	1528.4540
210.00	8.5651	650.00	159.7626	2500.00	1614.6289
220.00	10.3642	700.00	191.9908	2600.00	1701.2031
230.00	12.1043	750.00	225.8395	2700.00	1788.1018

of $5.6 \lesssim \epsilon/(\mathrm{MeV/fm^3}) \lesssim 300$ (i.e. $0.02 \lesssim \varrho/\ \mathrm{fm}^{-3} \lesssim 0.3$) the neutrons dominate in charge neutral neutron star matter (neutron-rich regime). Therefore one can treat star matter for this density region to a good approximation as being pure of neutrons. This of course simplifies the treatment of the complicated many-body problem considerably. Of interest here is that the goal of incorporating dynamical two-particle (Brueckner-type) correlations in terms of the (relativistic) scattering T-matrix in matter can be accomplished in the pure-neutron domain. Otherwise unsolved theoretical as well as numerical problems are encountered. To mention several are three- and higher-body correlations, many-body forces, one-boson-exchange description of the nuclear forces, and the problem of solving a large set of coupled, nonlinear matter equations (cf. Sect. 4 and Appendix H).

The benefit of the ladder appoximation consists in the use of realistic one-boson-

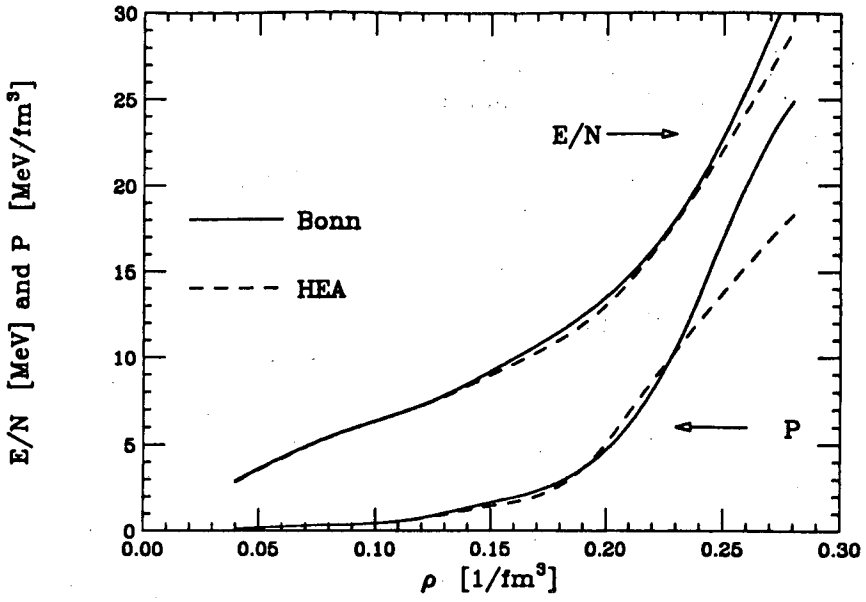

Figure 6: Energy per nucleon E/A and pressure P as a function of nuclear density ϱ calculated for neutron matter (neutrons only) in the Λ^{00} approximation. The underlying one-boson-exchange potentials are Bonn and HEA.

exchange potentials, which cannot be applied for neither the Hartree nor the Hartree-Fock method (no saturation of nuclear matter). We have calculated the T-matrix for the relativistic Λ^{00} approximation introduced in Sect. 3.5.1 by using the HEA and Bonn meson-exchange potentials of the nucleon-nucleon interaction as an input. The resulting equations of state, denoted by $\Lambda^{00}_{\rm HEA}$ and $\Lambda^{00}_{\rm Bonn}$, have been joined with those calculated in the framework of the relativistic Hartree (HV equation of state) and Hartree-Fock (HFV equation of state) method. Table 2 gives an survey of the equations of state obtained in this way [4]. The combined versions are denoted by $\Lambda^{00}_{\rm Bonn}$ + HV and $\Lambda^{00}_{\rm HEA}$ + HFV. In other words, we account for the influence of two-particle correlations in neutron matter by modifying two relativistic Hartree and Hartree-Fock equations of state, *calculated for charge neutral many-baryon/lepton matter*, only at densities which cover the *neutron-rich* star matter regime. The tabulated representation of the equations of state obtained in this way is given in Tables 8 ($\Lambda^{00}_{\rm Bonn}$ + HV) and 9 ($\Lambda^{00}_{\rm HEA}$ + HFV) for energy densities $20{\rm MeV/fm^3} \lesssim \epsilon \lesssim 2.7{\cdot}10^3{\rm MeV/fm^3}$. The density at which the equations of state have been joined is in both cases $\epsilon_{\rm comb} \approx 280$ MeV/fm^3.

Fig. 6 shows the energy per particle, E/A, and pressure, P, as a function of nuclear density ϱ calculated for pure neutron matter in the Λ^{00} approximation. Both

Table 10: Bulk nuclear matter properties (from top to bottom: binding energy, saturation density, compression modulus, effective mass) obtained for calculations performed for the Hartree (HV), Hartree-Fock (HFV), and Λ^{00} method. In the latter case the Bonn and HEA meson-exchange potentials served as an input.

Quantity	HV	HFV	Bonn	HEA
$\frac{E}{N}$ [MeV]	−15.98	−15.54	−11.9	−8.7
ϱ_0 [fm^{-3}]	0.145	0.159	0.134	0.132
K [MeV]	285	376	186	115
M^* ($\equiv m^*/m$)	0.77	0.62	0.79	0.82

E/A as well as P computed for $\Lambda^{00}_{\rm Bonn}$ and $\Lambda^{00}_{\rm HEA}$ are similar to each other up to $\varrho \approx 0.23$ fm^{-3}. Beyond this density the E/A and P curves of the HEA potential turn out to be smaller than those obtained for $\Lambda^{00}_{\rm Bonn}$. The bulk properties obtained for nuclear matter at saturation are summarized in Table 10. The Λ^{00} calculations with the parameters of the Bonn and HEA potential give to little binding energy, however saturate at the right saturation density. We recall that these potential are fitted to the two-nucleon data, which is in contrast to the parameters of the Hartree and Hartree-Fock approximations which are adjusted to the nuclear matter data. These are given for HV and HFV in the second and third column of Table 10. At nuclear matter saturation density ϱ_0, we obtain from neutron matter calculations performed for the $\Lambda^{00}_{\rm HEA}$ approximation (ne = neutron): $\varrho_0 = 0.132$ fm^{-3}, $[E/A]_{0,\rm ne}$=7.8 MeV, and $P_{\rm ne} = 0.98$ MeV/fm^3. The same values, but calculated for $\Lambda^{00}_{\rm Bonn}$, are: $\varrho_0 = 0.134$ fm^{-3}, $[E/A]_{0,\rm ne} = 8.1$ MeV, $P_{\rm ne} = 1.13$ MeV/fm^3, and $K_{\rm Bonn} = 186$ MeV. From $K_{\rm HEA} < K_{\rm Bonn}$ it follows that the $\Lambda^{00}_{\rm HEA}$ equation of state behaves softer, i.e. the dependence of E/A on density is weaker, at densities $\varrho \approx \varrho_0$ than the $\Lambda^{00}_{\rm Bonn}$ equation of state.

The relatively small values of the nuclear matter compression moduli at saturation calculated for the HEA and Bonn potentials are typical for approximation schemes which take two-particle correlations in matter into account [15, 16, 17, 11]. Inversely, such equations of state exhibit a rather stiff behavior at larger nuclear densities ($\varrho \gtrsim 1.5\,\varrho_0$) [4, 16, 17, 44]. A soft equation of state may be of importance in nuclear astrophysics, where a controversy is concerned with the softness of the equation of state as constrained by supernova calculations [80]: only softer equations of state seem to allow in supernova calculations for a sufficiently large enough energy release

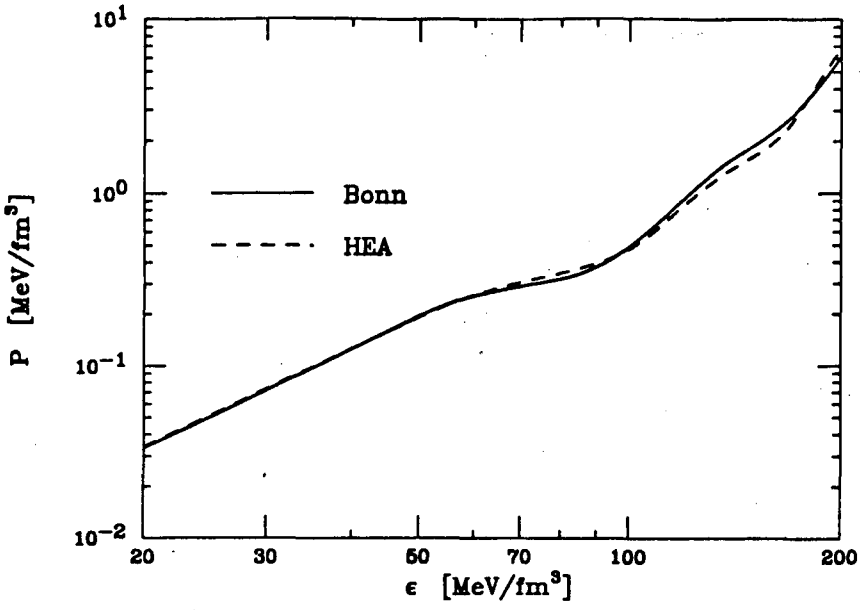

Figure 7: Neutron matter equations of state, i.e. pressure as a function of energy density ϵ (neutrons only), calculated for the Λ^{00} approximaion. The underlying one-boson-exchange potentials are Bonn and HEA.

necessary to catalyze the promt-bounce mechanisms. Equation of state derived from realistic Lagrangians, which are fitted to two-nucleon data, exhibit this softening at smaller nuclear densities as well as the rather stiff behavior in the large density region, necessary to obtain large enough neutron star masses and to withstand fast rotation [20, 36].

The effective nucleon mass M^* in matter, defined in Eq. (129) and Table 10, obtained from the HEA potential is larger than the one of the Bonn potential. It is known from mean-field investigations that M^* behaves inversely to the compression modulus [81, 27], and hence the larger M^* the softer behaves the equations of state. We find $M^*_{\rm HEA} = 0.82 > M^*_{\rm Bonn} = 0.79$ in the case of nuclear matter, and $M^*_{\rm HEA} = 0.91 > M^*_{\rm Bonn} = 0.88$ for neutron matter, indicating that the HEA equation of state behaves softer than the Bonn equations of state. This behavior can be seen from Fig. 6. It exhibits the somewhat weaker density dependence of both energy per particle and pressure obtained for the HEA potential in comparison with the Bonn interaction. The slopes of the E/A curves enter in the thermodynamic relation for the pressure, given in Eq. (171). The pressure as a function of energy density is graphically depicted in Fig. 7 for intermediate ϵ values. For $\epsilon \gtrsim 220$ MeV/fm^3, the $\Lambda^{00}_{\rm Bonn}$ and $\Lambda^{00}_{\rm HEA}$ equations of state begin to differ from each other to a larger extent.

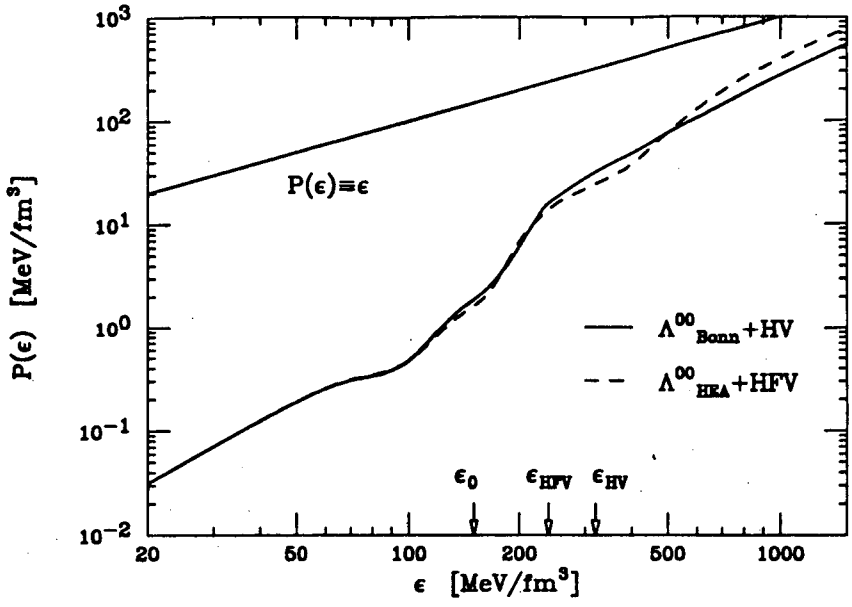

Figure 8: Neutron star matter equations of state $P(\epsilon)$ over a large range of energy densities, i.e. 20 MeV/fm^3 $< \epsilon <$ 2700 MeV/fm^3. The arrow pointing towards the ϵ-axis shows that ϵ value (280 MeV/fm^3) at which the $\Lambda^{00}_{\rm Bonn}$ and HV and the $\Lambda^{00}_{\rm HEA}$ and HFV equations of state have been combined with each other. The stiffest possible equation of state, $P(\epsilon) \equiv \epsilon$, is shown too. The numerical outcome is given in Tables 8 and 9, respectively.

According to the arguments given in Ref. [4], the pressure curves calculated from HEA, HFV, Bonn, and HV tend smoothly against each other in the following way: $P^{\Lambda^{00}_{\rm HEA}} \rightarrow P^{\rm HFV}$ and $P^{\Lambda^{00}_{\rm Bonn}} \rightarrow P^{\rm HV}$ for $\epsilon \approx 280 - 300$ MeV/fm^3. The joined equations of state, $\Lambda^{00}_{\rm Bonn}$+HV and $\Lambda^{00}_{\rm HEA}$+HFV, are displayed in Fig. 8 for energy densities up to $2.7{\cdot}10^3$ MeV/fm^3. Typical ϵ values reached in the treatment of massive neutron stars are for out four equations of state $\epsilon \lesssim 1400$ MeV/fm^3. One sees that both of these equations of state behave softer, i.e. less pressure values for a given ϵ value, than the stiffest possible equation of state, $P \equiv \epsilon$. At large energy densities, $P^{\Lambda^{00}_{\rm Bonn}+{\rm HV}}(\epsilon)$ and $P^{\Lambda^{00}_{\rm HEA}+{\rm HFV}}(\epsilon)$ tend smoothly against $P(\epsilon) \equiv \epsilon$ from below. The "causality" condition $dP/d\epsilon \leq 1$ is fulfilled by our equations of state, which is an important constraint on a realistic neutron matter equation of state. A consequence from this is that the speed of sound, c_S, is smaller than the velocity of light, c. This is shown in the next Fig. 9 where $c_S/c = \sqrt{dP/d\epsilon}$ is plotted as a function of energy density for $\Lambda^{00}_{\rm Bonn}$ + HV and $\Lambda^{00}_{\rm HEA}$ + HFV. The so called "microscopic stability" condition [19], $dP/d\epsilon \geq 0$, is satisfied by our models.

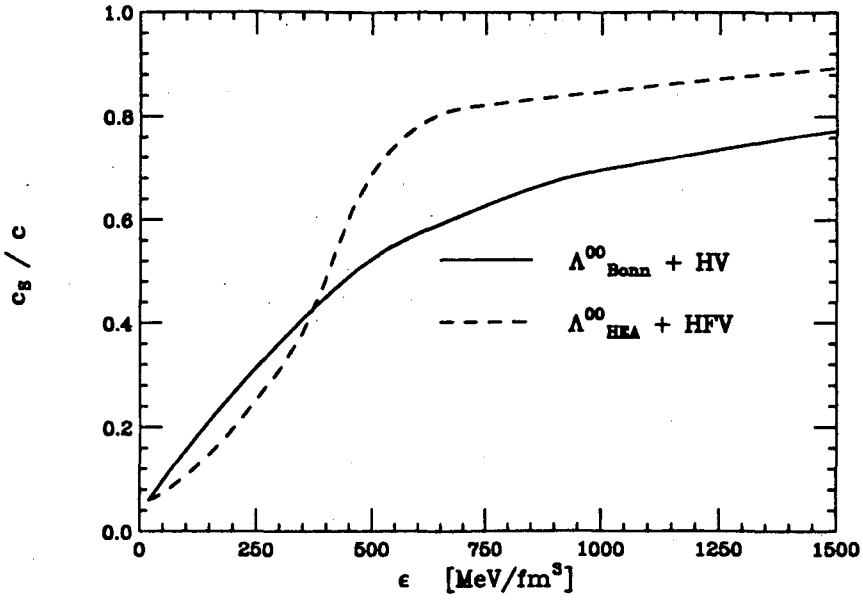

Figure 9: Velocity of sound c_S in units of the speed of light, c, as a function of energy density calculated from the combined equations of state $\Lambda^{00}_{\rm Bonn}$+HV and $\Lambda^{00}_{\rm HEA}$+HFV.

A special feature of the $\Lambda^{00}_{\rm Bonn}$ + HV and $\Lambda^{00}_{\rm HEA}$ + HFV equations of state is their intersection at $\epsilon_{\rm ints} \approx 500$ MeV/fm^3. For $\epsilon < \epsilon_{\rm ints}$ ($\epsilon > \epsilon_{\rm ints}$) the $\Lambda^{00}_{\rm Bonn}$ + HV ($\Lambda^{00}_{\rm HEA}$ + HFV) equation of state gives less (more) pressure for a given ϵ value than $\Lambda^{00}_{\rm HEA}$+HFV ($\Lambda^{00}_{\rm Bonn}$ + HV). The reason for the asymptotically stiffer behavior of HFV lies in the Fock term, which is not taken into account in HV. A similar qualitative behavior show the frequently used hyperonic matter equations of state of Pandharipande (model Pan(C)) [41] and Bethe and Johnson (model BJ(V)) [82], calculated in the non-relativistic variational technique of Pandharipande. The intersection point of Pan(C) and BJ(V) is $\epsilon^{\rm Pan(C),BJ(V)}_{\rm ints} \approx 10^3$ MeV/fm^3. For $\epsilon < \epsilon^{\rm Pan(C),BJ(V)}_{\rm ints}$ one has $P^{\rm Pan(C)}(\epsilon) < P^{\rm BJ(V)}(\epsilon)$ and $P^{\rm BJ(V)}(\epsilon) > P^{\rm Pan(C)}(\epsilon)$, otherwise. Such a functional dependence of P on ϵ has an important impact on the Kepler frequency in so far that asymptotically stiffer equations of state (HFV in our case) generally lead to larger rotation rates. However as mentioned above, the softness at intermediate densities is of importance too (and it is the functional dependence of pressure on density at all values beyond nuclear which finally determines the limiting frequency).

6.2 Models of rotating neutron stars

6.2.1 Bulk properties

Tables 12-14 contain the properties of stable neutron star configurations rotating at Kepler frequencies 4000, 6000, and 9000 s^{-1}. These star models are constructed from the four equations of state of this work, which may serve to demonstrate the influence of different many-body treatments on the properties of rotating neutron stars: The fist colums refer to results calculated for the relativistic Hartree equation of state HV (combined with the Harrison-Wheeler and Negele-Vautherin equations of state according to Table 2). The second, third and fourth columns refer to results calculated for $\Lambda^{00}_{\rm Bonn}$ + HV, HFV, and $\Lambda^{00}_{\rm HEA}$ + HFV, respectively.

The method of constructing neutron star models from Hartle's method that rotate at their respective Kepler frequencies has been outlined in Ref. [4]. It is based on the self-consistent construction of sequences of rotating star configurations from given neutron star matter equations of state. Self-consistency is encountered by supplementing Hartle's stellar structure equations (Sect. 2.2) by the general relativistic expression for the Kepler frequency $\Omega_{\rm K}$ of Eq. (67) (Sect. 2.3). When constructing star models, one starts from a given value of the star's central energy density, ϵ_c. That value of ϵ_c for which $M(\epsilon_c)$ reaches its maximum value defines the *limiting* mass model of the sequence (turning-point method [3, 4, 83, 84]); it rotates at its respective limiting Kepler frequency, $\Omega^{\rm lim}_{\rm K}$. Stars beyond the mass limit ($\epsilon_c > \epsilon_c^{\rm lim} \equiv \epsilon_c|_{M=M_{\rm lim}}$) are expected to be gravitationally unstable [83, 84]. The construction method is self-consistent because of the Kepler frequency $\Omega_{\rm K}$. This quantity depends on the metric functions $\nu(\Omega)$ and $\psi(\Omega)$ of Eqs. (22) and (23), respectively, which in turn are given in terms of the perturbation functions $h_0(\Omega)$, $h_2(\Omega)$, $v_2(\Omega)$. The latter are the solutions of the Hartle's equations of Sect. 2.2, which are to be solved for a *given* rotational frequency of the neutron star model, i.e. $\Omega = \Omega_{\rm K}$ in our case. The frequency $\Omega_{\rm K}$ however is not known but given in terms of the unknown perturbation functions $h_0(\Omega_{\rm K})$, $h_2(\Omega_{\rm K})$, and $v_2(\Omega_{\rm K})$. The only free parameter in the treatment, which can be chosen arbitrarily, is ϵ_c. The task therefore is to solve Hartle's equations simultaneously in combination with Eq. (67) (which determines $\Omega_{\rm K}$ for a given value of ϵ_c ($\leq \epsilon_c^{\rm lim}$)) iteratively till the input and output values of $\Omega_{\rm K}$ coincide. In this work we are interested in neutron star configurations that rotate at Kepler frequencies $\Omega_{\rm K}$ = 4000, 6000, 8000 s^{-1}, which are *smaller* than the maximum possible frequencies $\Omega^{\rm lim}_{\rm K}$ of the

Table 11: Angular velocities ω of the inertial frames at the center (c) and surface (s) of rotating neutron stars, as measured by a distant observer.

	Ω_K [s^{-1}]	HV	Λ^{00}_{Bonn} + HV	HFV	Λ^{00}_{HEA} + HFV
	4000	0.198	0.140	0.146	0.138
ω_c [s^{-1}]	6000	0.371	0.286	0.248	0.281
	9000	0.612	0.578	0.557	0.544
	4000	0.035	0.019	0.024	0.019
ω_s [s^{-1}]	6000	0.093	0.077	0.060	0.071
	9000	0.177	0.185	0.179	0.177

limiting mass models.

To be more specific, the first step consists in solving Hartle's equations for properly chosen values of ϵ_c and $\bar{\omega}_c \equiv \bar{\omega}(r=0)$, i.e. one solves Eq. (26) for the function $\bar{\omega}(r)$ by choosing a boundary value for $\bar{\omega}_c$ (see Sect. 2.2.1) and a not too large value for ϵ_c ($< \epsilon_c^{\rm lim}$). Equation (30) then determines the star's frequency $\Omega(\epsilon_c, \bar{\omega}_c(\Omega))$ for these values ϵ_c and $\bar{\omega}_c(\Omega)$, which in general will be different from $\Omega_K(\epsilon_c)$ obtained from Eq. (67). The function $\bar{\omega}(r;\Omega)$ therefore is to be rescaled with respect to the latter value $\Omega_K(\epsilon_c)$ as described at the end of Sect. 2.2.1. Once this has been performed, the monopole and quadrupole equations of Sects. 2.2.2 and 2.2.3 can be solved using the rescaled function $\bar{\omega}(r;\Omega)$ as an input. Their outcome then serves to re-calculate $\Omega_K(\epsilon_c, \bar{\omega}_c)$ from Eq. (67). This procedure is repeated till convergence with respect to input and output values of Ω_K is achieved (i.e. until both of these values coincide). The obtained solution $\Omega_K(\epsilon_c)$ ($\equiv \Omega_K(\epsilon_c, \bar{\omega}_c(\Omega_K))$) then is the Kepler frequency of a neutron star model of rotational mass $M(\epsilon_c, \Omega_K(\epsilon_c))$. According to above, we restrict ourselves in this investigation to nominal Kepler frequencies $\Omega_K(\epsilon_c)|_{\rm nom} = 4000$, 6000, and 9000 s^{-1}, i.e.

$$\Omega_K(\epsilon_c)|_{\text{Eq. (67)}} \;=\; \Omega_K(\epsilon_c)|_{\rm nom}\,. \tag{206}$$

In other words only neutron star models of masses $M < M_{\rm lim}$, which consequently rotate at $\Omega_K < \Omega_K^{\rm lim}$, are considered.

The first row of Table 12 shows those central energy densities which solve Eq. (171) for a nominal Kepler frequency of $\Omega_K = 4000$ s^{-1}. Tables 13 and 14 refer to nominal frequencies of 6000 s^{-1} and 9000 s^{-1}, respectively.

The density ϵ_c increases for increasing values of Ω_K since the centrifugal forces

Table 12: Properties of rotating neutron star models, calculated for an angular velocity Ω_K=4000 s^{-1}.

	HV	Λ^{00}_{Bonn} + HV	HFV	Λ^{00}_{HEA} + HFV
$\log \epsilon_c/(g \cdot cm^{-3})$	14.52	14.57	14.52	14.56
$M/M_\odot$	0.87	0.45	0.53	0.44
$\Delta M/M_s$	0.23	0.16	0.20	0.16
R_{eq} [km]	17.92	14.47	15.20	14.62
R_p [km]	12.64	10.52	10.77	10.47
$\log I/(g \cdot cm^2)$	44.896	44.370	44.514	44.356
t	0.074	0.059	0.070	0.058
β	0.80	0.87	0.85	0.88
V_{eq}	0.25	0.20	0.21	0.20
z_B	0.37	0.26	0.27	0.25
z_F	−0.15	−0.12	−0.12	−0.12
z_p	0.12	0.07	0.08	0.07
e^{FIP}	0.70	0.69	0.70	0.70
$\hat{\Pi}$	0.052	0.038	0.050	0.039

Table 13: Properties of rotating neutron star models, calculated for an angular velocity Ω_K=6000 s^{-1}.

	HV	Λ^{00}_{Bonn} + HV	HFV	Λ^{00}_{HEA} + HFV
$\log \epsilon_c/(g \cdot cm^{-3})$	14.80	14.67	14.78	14.76
$M/M_\odot$	1.67	1.23	1.29	1.15
$\Delta M/M_s$	0.22	0.24	0.24	0.23
R_{eq} [km]	16.86	15.24	15.46	14.93
R_p [km]	11.77	10.47	10.61	10.29
$\log I/(g \cdot cm^2)$	45.249	45.015	45.050	44.958
t	0.092	0.097	0.096	0.094
β	0.58	0.65	0.64	0.67
V_{eq}	0.38	0.33	0.34	0.33
z_B	0.76	0.59	0.61	0.56
z_F	−0.20	−0.17	−0.18	−0.17
z_p	0.31	0.24	0.25	0.22
e^{FIP}	0.70	0.71	0.71	0.71
$\hat{\Pi}$	0.060	0.075	0.073	0.072

Table 14: Properties of rotating neutron star models, calculated for an angular velocity Ω_K=9000 s^{-1}.

	HV	$\Lambda^{00}_{\rm Bonn}$ + HV	HFV	$\Lambda^{00}_{\rm HEA}$ + HFV
$\log \epsilon_c/(g \cdot cm^{-3})$	15.18	15.13	15.04	15.03
$M/M_\odot$	2.23	2.18	2.13	2.09
$\Delta M/M_s$	0.16	0.17	0.18	0.19
$R_{\rm eq}$ [km]	14.25	14.07	13.95	13.84
$R_{\rm p}$ [km]	10.25	9.93	9.84	9.72
$\log I/(g \cdot cm^2)$	45.353	45.344	45.319	45.298
t	0.098	0.107	0.107	0.108
β	0.36	0.35	0.36	0.37
$V_{\rm eq}$	0.52	0.51	0.50	0.50
$z_{\rm B}$	1.44	1.39	1.38	1.34
$z_{\rm F}$	−0.23	−0.23	−0.23	−0.23
$z_{\rm p}$	0.67	0.69	0.67	0.65
$e^{\rm FIP}$	0.69	0.71	0.71	0.71
$\hat{\Pi}$	0.043	0.054	0.054	0.056

acting on the star matter are to be counterbalanced by the attractive gravitational forces, which must be the larger the faster the neutron star rotates.

It has been shown in Ref. [4] that two-particle correlations influence the behavior of the equation of state of neutron matter at most for $20 < \epsilon/(\mathrm{MeV/fm^3}) < 300$. Hence, the properties of star models with central energy densities $\epsilon_c < 300$ MeV/fm^3 are most sensitive to these correlations since the behavior of the equation of state at the star's core region is known to determine essentially its properties [9]. This is the case for the rotating star models of Table 12, which are characterized by central densities of $\epsilon_c^{\rm HV} = 186$ MeV/fm^3, $\epsilon_c^{\Lambda^{00}_{\rm Bonn}+{\rm HV}} = 208$ MeV/fm^3, $\epsilon_c^{\rm HFV} = 186$ MeV/fm^3, and $\epsilon_c^{\Lambda^{00}_{\rm HEA}+{\rm HFV}} = 204$ MeV/fm^3. Neglection of correlation, which is the case for HV and HFV, leads to rotating star models of slightly smaller central energy densities. These are characterized by:

1. Larger gravitational masses, i.e. 23% increase for HV and 20% for HFV relative to the corresponding (same ϵ_c) spherical Oppenheimer-Volkoff values; the mass increase is 16% (for both the $\Lambda^{00}_{\rm Bonn}$ as well as $\Lambda^{00}_{\rm HEA}$ calculation) if correlations in the equation of state are taken into account;

2. The larger mass increase obtained for HV is accompanied by relatively large equatorial and polar radius values of $R_{\rm eq} = 17.9$ km and $R_{\rm p} = 12.6$ km, respec-

tively. These values are followed by HFV, i.e. R_{eq} =15.2 km and R_p = 10.8 km. As a consequence, all star quantities influenced by the equatorial or polar radius values are largest for the HV equation of state and second largest for HFV. To mention are

3. the moment of inertia, I, the rotational velocity at the star's equator, V_{eq}, the redshift in backward direction, z_B, the polar redshift, z_p, and the quadrupole moment, Π.

On the other hand, the star properties calculated for both Λ equations of state do not differ very much for the Kepler frequency of Ω_K=4000 s^{-1}. This is related to the similar energy dependence of pressure for both of these equations of state for $\epsilon < 210$ MeV/fm^3 (see Figs. 6-8). Larger ϵ_c values are reached for larger Kepler velocities. These are for Ω_K = 6000 s^{-1} (cf. Table 13) ϵ_c^{HV} = 354 MeV/fm^3, $\epsilon_c^{\Lambda^{00}_{Bonn}+HV}$ = 263 MeV/fm^3, ϵ_c^{HFV} = 338 MeV/fm^3, and $\epsilon^{\Lambda^{00}_{HEA}}+HFV_c$ = 323 MeV/fm^3. For that reason the differences of the rotating star properties obtained for HV and HFV in comparison with Λ^{00}_{Bonn} + HV and Λ^{00}_{HEA} + HFV are less extreme. In the case of the rotating star model of Table 14 (Ω_K = 9000 s^{-1}) these differences are even more reduced. The latter have central energy densities of ϵ_c^{HV} = 849 MeV/fm^3, $\epsilon_c^{\Lambda^{00}_{Bonn}+HV}$ = 757 MeV/fm^3, ϵ_c^{HFV} = 615 MeV/fm^3, and $\epsilon_c^{\Lambda^{00}_{HEA}+HFV}$ = 601 MeV/fm^3.

A remarkable result that follows from Tables 12-14 is that the value of the energy density of the rotating star configuration is rather sensitive against two-particle correlations in matter. For example, the Hartree outcome of Table 14 with and without correlations is characterized by a central energy density which is $\approx$ 11% smaller if correlations are taken into account. The reduction of ϵ_c in the case of the Hartree-Fock treatment with two-particle correlations (Λ^{00}_{HEA} + HFV equation of state) is $\approx$ 2%. Of course, a lower density in the cores of neutron stars favors the treatment of the many-body neutron star matter problem in terms of baryons and mesons instead of quarks and gluons. However a precise answer to this subject can only be given once the transition density from the hadronic phase to the quark-gluon regime is known. (See Ref. [68] for the discussion of the transition density in neutron star matter in the case of two (electric charge and baryon number) conserved quantities.)

Figures 10-15 show the total rotational star masses, the moments of inertia, the velocities reached at the equator, and the polar redshifts in backward and forward direction as well as at the star's pole, respectively, as a function of the Kepler frequency Ω_K. For Ω_K=4000, 6000, and 9000 s^{-1}, these values are given in Tables 12-14,

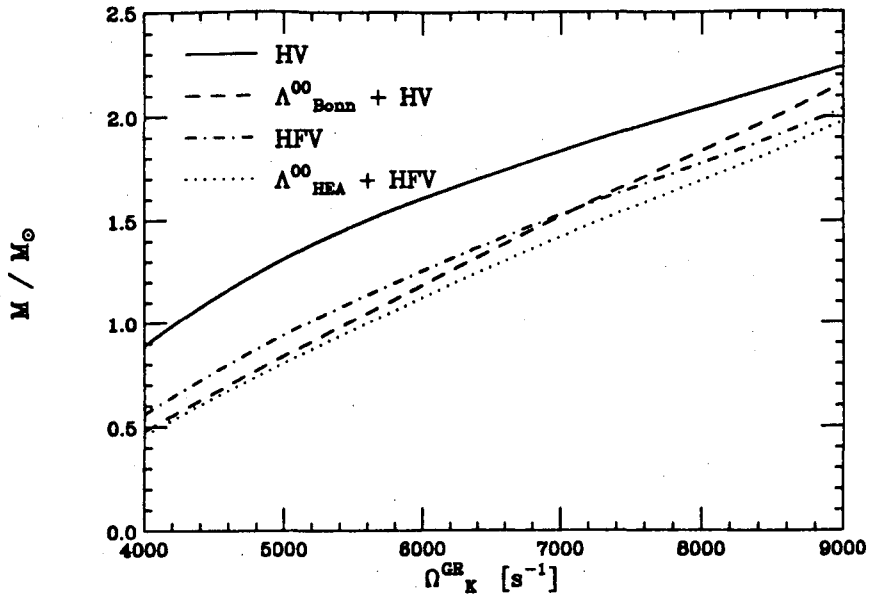

Figure 10: Gravitational neutron star masses M in units of the solar mass, $M_\odot$, as a function of Kepler frequency Ω_K for equations of state HV, $\Lambda^{00}_{\text{Bonn}}$ + HV, HFV, and $\Lambda^{00}_{\text{HEA}}$ + HFV.

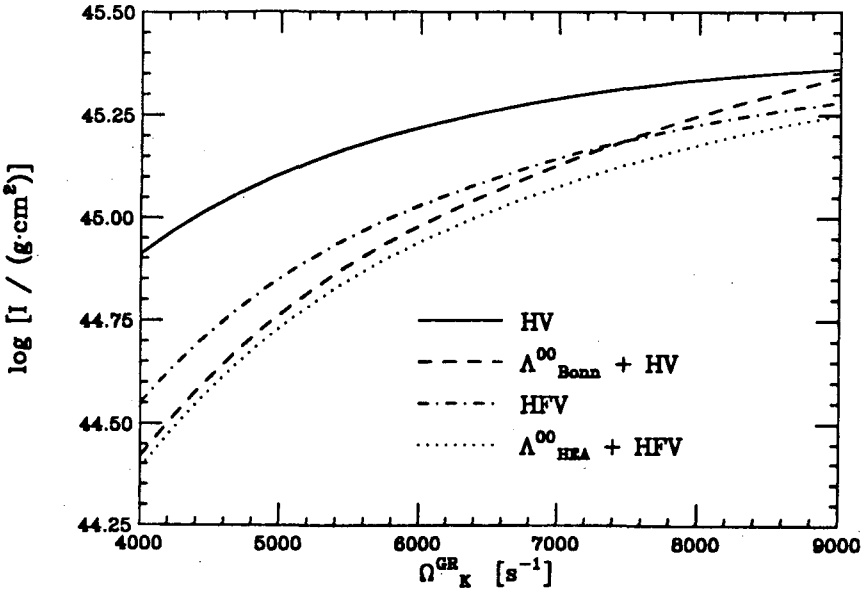

Figure 11: Moment of inertia I as a function of Kepler frequency for the equations of state of this work (cf. Table 2).

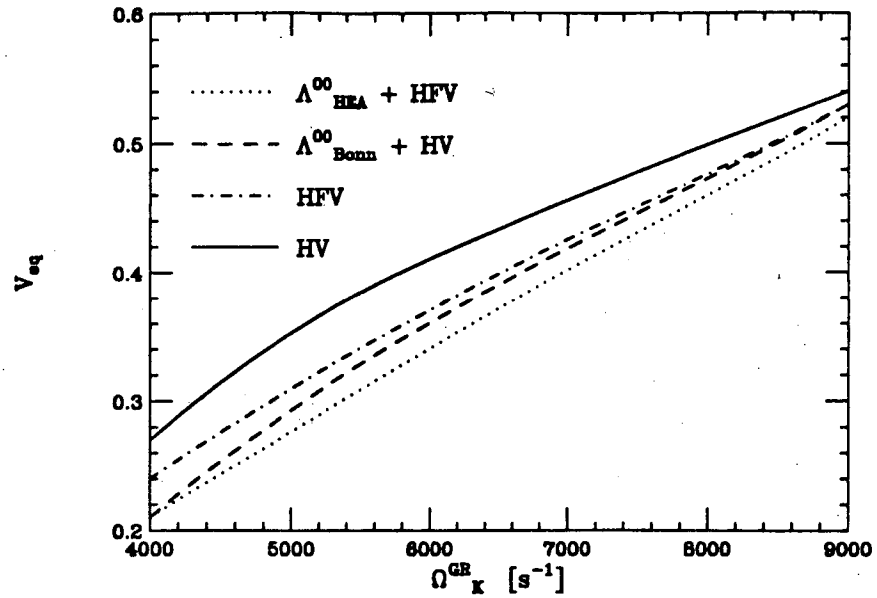

Figure 12: Velocity of a co-moving observer at the star's equator relative to a locally non-rotating observer as a function of Kepler frequency for the equations of state of this work.

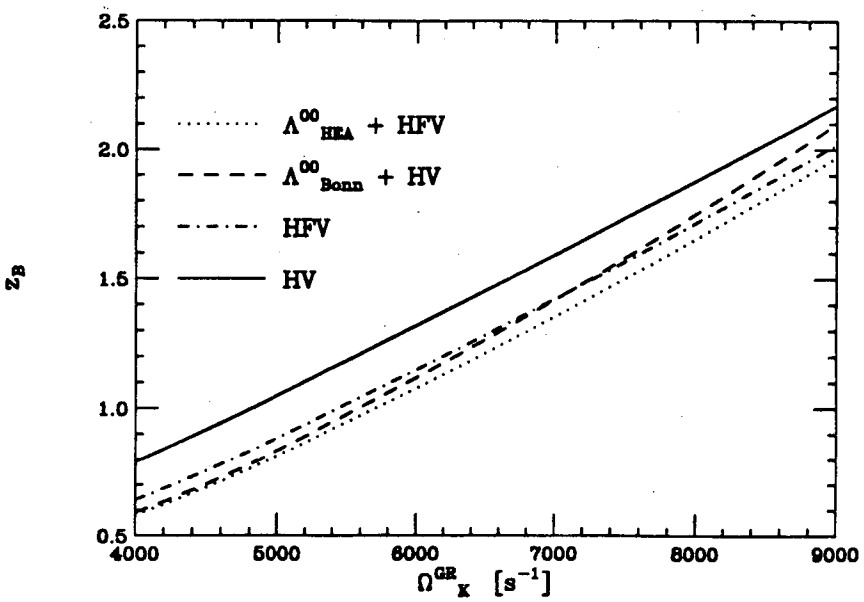

Figure 13: Equatorial redshift in backward direction for stars rotating at different Kepler frequencies calculated for the equations of state of this work.

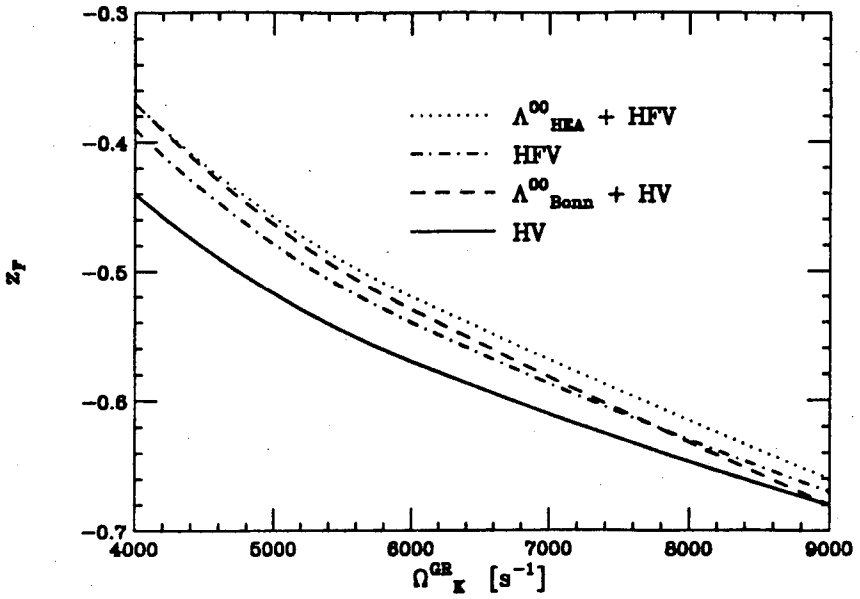

Figure 14: Same as Fig. 13, but calculated for the equatorial redshift in forward direction.

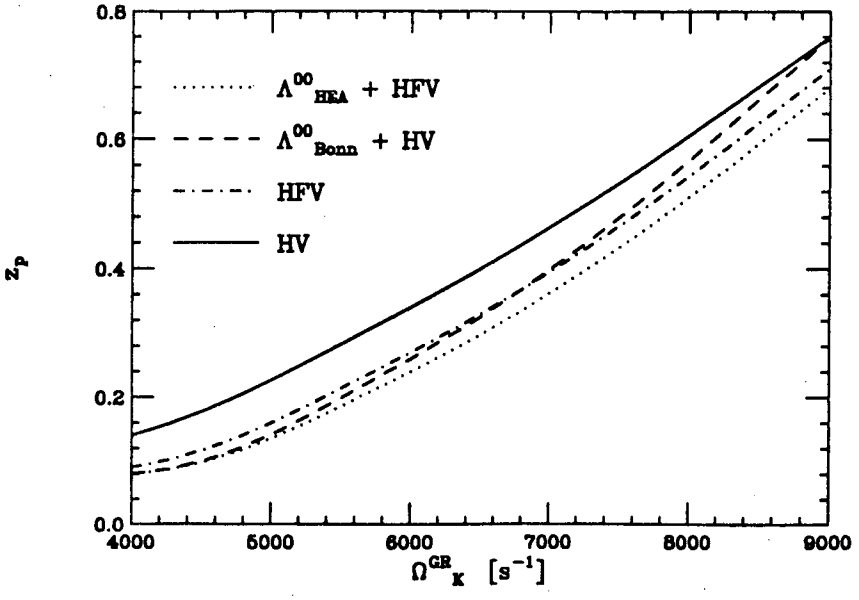

Figure 15: Same as Fig. 13, but calculated for the polar redshift in forward direction.

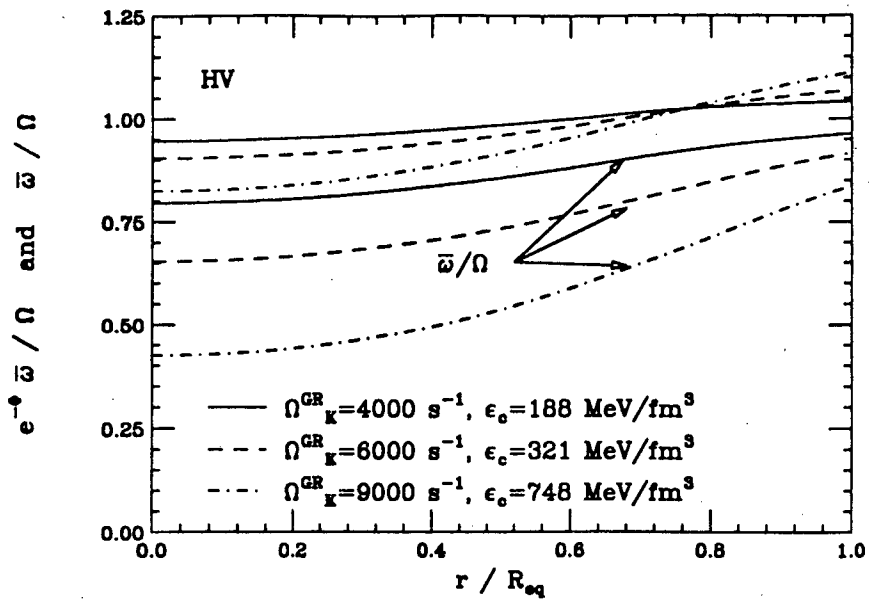

Figure 16: Dragging of inertial frames as a function of radius calculated for the HV equation of state for stars rotating at Ω_K= 4000, 6000, and 9000 s^{-1}. The symbol ϵ_c labels the corresponding central energy density values (in MeV/fm^3). The curves $\bar{\omega}/\Omega \equiv (\Omega-\omega)/\Omega$ are the fluid angular velocity at radius r relative to the local inertial frames there, as measured by a *distant* observer, divided by the angular velocity Ω of the fluid with respect to the *distant* stars. The remaining curves refer to the same angular velocity, but as measured by a (local) observer *in the fluid* at radius r (see Sect. 6.2.2).

respectively.

6.2.2 Dragging of inertial frames

The dragging of inertial frames expresses the proportionality of the angular velocity ω (see below) to the frequency Ω. The dragging of frames as a function of radial distance from the star's center is exhibited in Figs. 16-19.

The rotating star configurations are constructed from the HV, $\Lambda^{00}_{\rm Bonn}$ + HV, HFV, and $\Lambda^{00}_{\rm HEA}$ + HFV equations of state, respectively. The rotational frequencies in each of these Figures are 4000, 6000, and 9000 s^{-1}. In Fig. 20 we compare the influence of two-particle correlations (for the HFV equation of state) on the dragging of inertial frames for rotation at Ω_K=4000 and 6000 s^{-1}.

The relevant frequencies in these Figures, i.e. Ω, ω and $\bar{\omega} \equiv \Omega - \omega$, are [8, 9]:

1. the angular velocity of the star fluid relative to the distant stars,

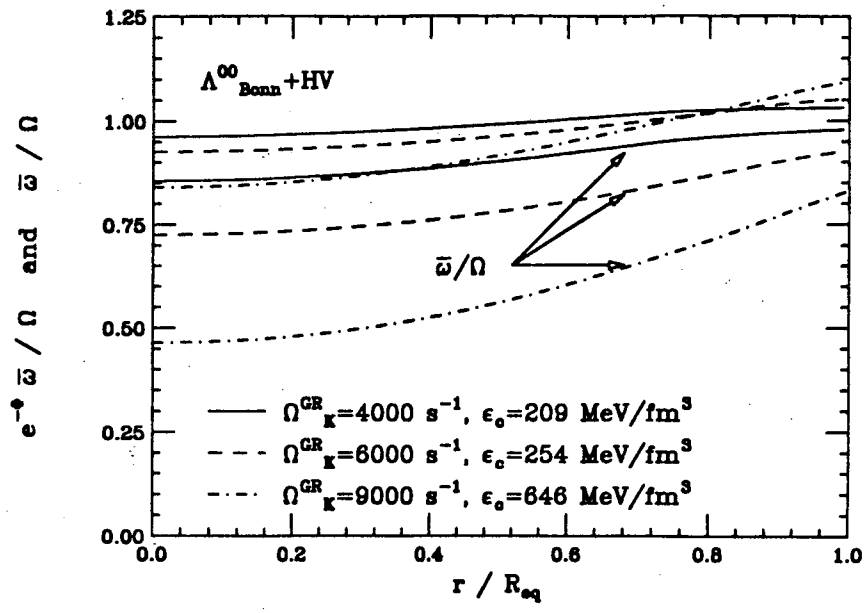

Figure 17: Same as Fig. 16, but calculated for the equation of state $\Lambda^{00}_{\rm Bonn}$ + HV.

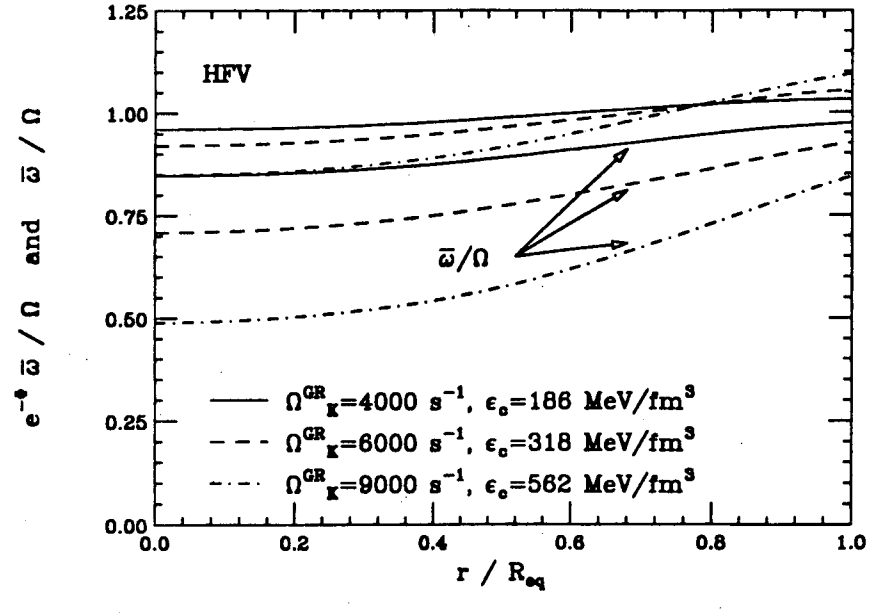

Figure 18: Same as Fig. 16, but calculated for the equation of state HFV.

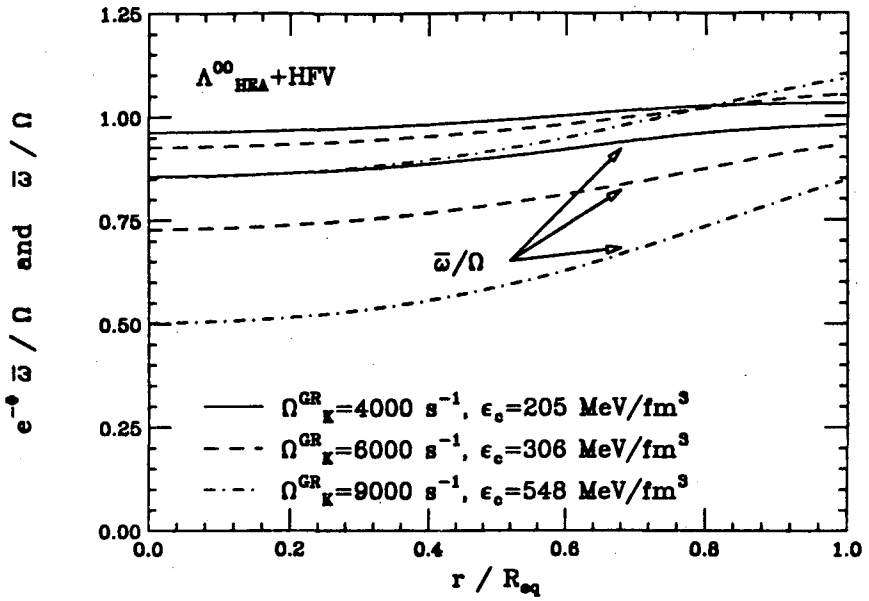

Figure 19: Same as Fig. 16, but calculated for the equation of state $\Lambda^{00}_{\rm HEA}$ + HFV.

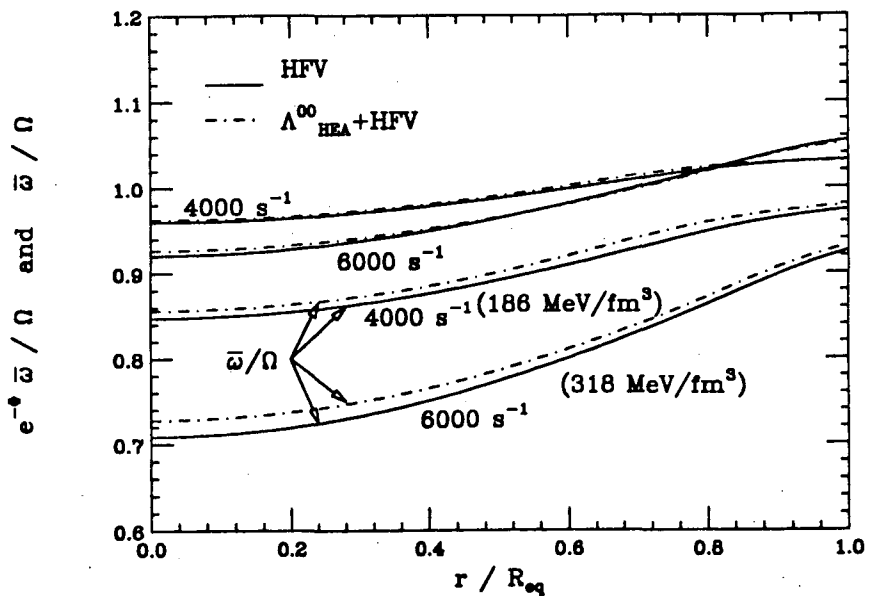

Figure 20: Influence of two-particle correlations on the dragging of inertial frames in the case of the HFV equation of state. The Kepler frequencies of the rotating star configurations shown are $\Omega_{\rm K}$=4000, 6000, and 9000 s^{-1}. The corresponding values of the central energy densities, ϵ_c, are given in units of MeV/fm^3.

2. the angular velocity of the inertial frames relative to the distant stars, and

3. the angular velocity of the fluid relative to the inertial frames,

respectively. As mentioned, these frequencies are measured by the *distant* observer. The angular velocities measured by a *local* observer are $e^{-\Phi}\Omega$, $e^{-\Phi}\omega$, and $e^{-\Phi}\bar{\omega}$ (time dilation factor $e^{-\Phi}$ included, see Eq. (22)). As pointed out by Hartle and Thorne [8], at any given radius, Ω, ω, and $\bar{\omega}$ are greater when measured by a *local* observer than when measured by an observer far away (who looks down into the star). This can clearly be seen from Figs. 16-20. According to a theorem of Hartle, the dragging of inertial frames with respect to a distant observer is always greater at the star's center, and it decreases in the outward direction. The smooth behavior of $\bar{\omega}/\Omega$ and $e^{-\Phi}\bar{\omega}/\Omega$ as a function of r is typical for a *stable* star configuration. Otherwise the dargging of frames would be sharply peaked at the core.

The actual amount of dragging depends on the value of the central energy density of the star: the larger ϵ_c the larger is the dragging of inertial frames. Figures 16-20 exhibit this very clearly. In Fig. 16 (HV equation of state) this is the case for ϵ_c=849 MeV/fm^3, which corresponds to the Kepler frequency of $\Omega_{\rm K}$=9000 s^{-1}. The dragging effect is smallest for $\Omega_{\rm K}$=4000 s^{-1}, for which ϵ_c=186 MeV/fm^3, and lies between these values for rotation at $\Omega_{\rm K}$=6000 s^{-1} (ϵ_c=354 MeV/fm^3). *Total* dragging values, calculated at the center (ω_c) and at the surface (ω_s) of the star models of Figs. 16-20 are listed in Table 11. They are $\omega_c \approx 54-61\%$ at the star's center and fall off to $\omega_s \approx 18\%$ at the surface in the case of the largest Kepler frequency ($\Omega_{\rm K}$=9000 s^{-1}). Values of $\omega_c \approx 14-20\%$ are reached for $\Omega_{\rm K} = 4000$ s^{-1}, which decrease to $\omega_s \approx 2-4\%$ at the surface. (Hartle and Thorne [8] find in their investigation values up to $\omega_c \approx 75\%$ and $\omega_s \approx 25\%$ for a neutron star of ϵ_c=1685 MeV/fm^3 rotating near the rotational shedding frequency of $\Omega \approx 16000$ s^{-1}. An important point is that the star's rotational frequency in this case is calculated from the *Newtonian* expression, given by Eq. (21), which neglects the important effect of dragging of local inertial frames. The lower bounds are roughly set by $\omega_c \approx 3\%$ and $\omega_s \approx 0.002\%$ for a neutron star rotating at $\Omega = 113$ s^{-1}.) Large ω_c and ω_s values stress the importance of relativity in the case of the treatment of neutron stars. This is contrary to the case of white dwarfs for which the dragging of inertial frames is negligible (i.e. $\omega_c \leq 0.3\%$ and $\omega_s \leq 0.01\%$) [8].

Of physical importance is the gravitational redshift of photons emitted from (rotating) neutron stars. From this the observer gets information about the rotating

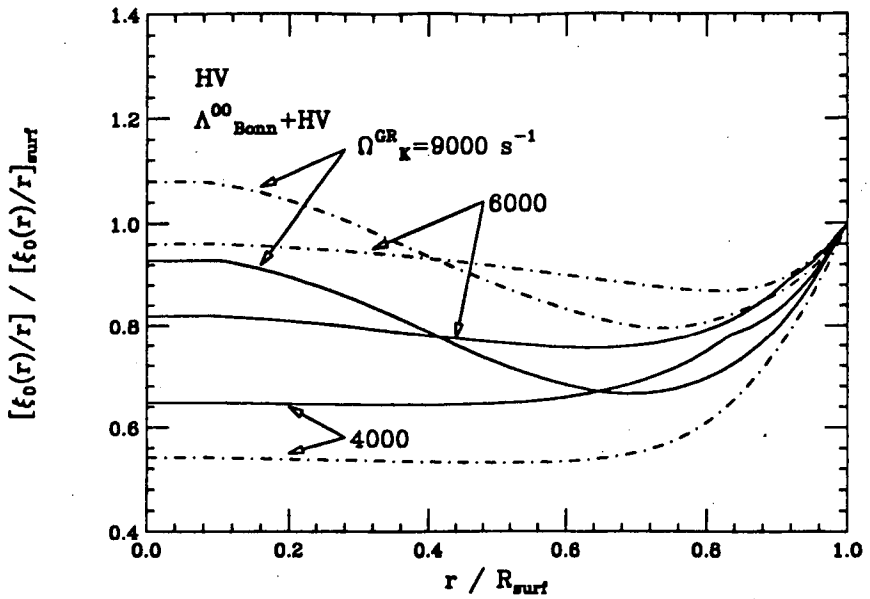

Figure 21: Influence of two-particle correlations on the spherical stretching ξ_0, relative to its surface value, plotted as a function of radius. Shown is the outcome for star configurations rotating at Ω_K=4000, 6000, and 9000 s^{-1}. The underlying equations of state are HV and Λ^{00}_{Bonn} + HV.

object. The redshift (cf. Eq. (74)) is associated with to the difference in the measurement of the angular velocity by a *local* observer and an observer far away [8]. The effect of redshift on the angular velocities can be seen in Figs. 16-20.

The influence of two-particle correlations on the dragging of the inertial frames is graphically depicted in Fig. 20 for the HFV equation of state. The dragging with respect to a local observer, $\bar{\omega}e^{-\Phi}/\Omega$, is less influenced by them than the dragging of inertial frames measured by a distant observer, $\bar{\omega}/\Omega$.

The spherical stretching $\xi_o(r)$ (Eq. (61)) of a star due to rotation as a function of radius inside the star is shown in the following two Figs. 21 and 22.

The Kepler frequencies are again 4000, 6000, and 9000 s^{-1}. The stretching function is much more influenced by two-particle correlations than the dragging of inertial frames.

Figs. 23 and 24 illustrate the eccentricity e^{HT} (defined according to Hartle and Thorne [8], Eq. (64)) of surfaces of constant density plotted as a function of radial distance. The intrinsic geometries of the surfaces in the Hartle method are spheroids (accurate to order Ω^2, the 3-surface in flat space is given by Eq. (63).) The eccentricity of these spheroids is related to the amount of quadrupole deformation of the star.

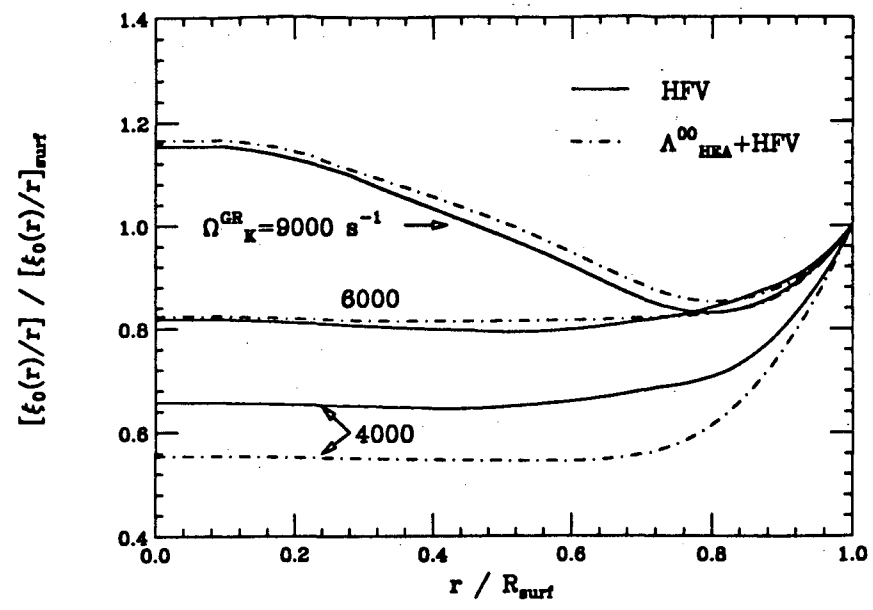

Figure 22: Same as Fig. 21, but calculated for equations of state HFV and $\Lambda^{00}_{\rm HEA}$ + HFV.

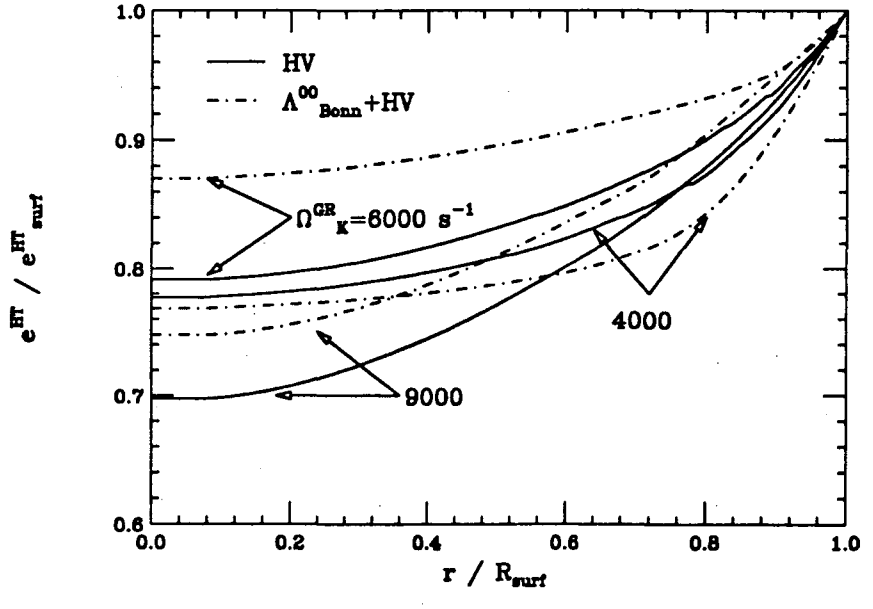

Figure 23: Influence of two-particle correlations on the eccentricity of surfaces of constant density at radius r. Plotted is the eccentricity $e^{\rm HT}$, as defined by Hartle and Thorne (Eq. (64)), relative to its surface value $e_s^{\rm HT}$. The results shown are calculated for the HV and $\Lambda^{00}_{\rm Bonn}$ + HV equations of state.

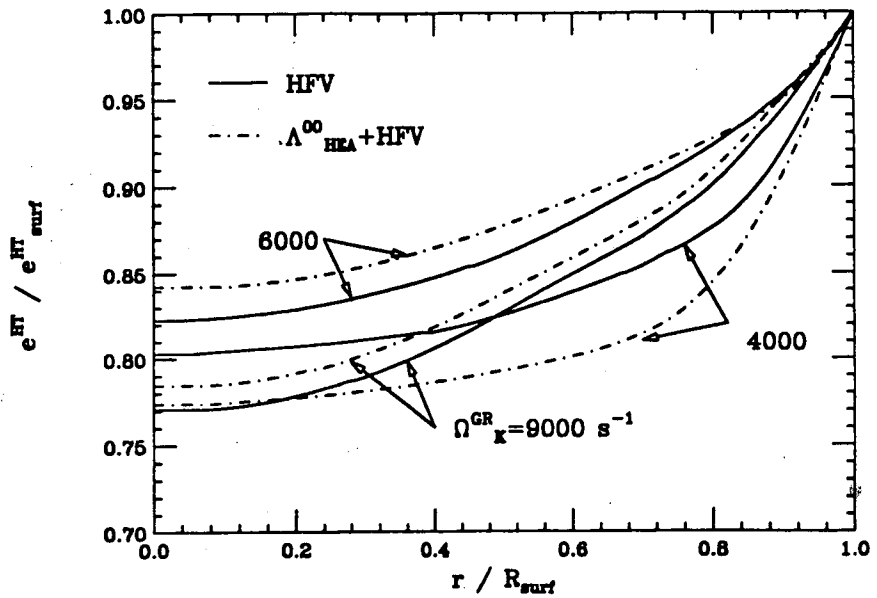

Figure 24: Same as Fig. 23, but calculated for the HFV and Λ^{00}_{HEA} + HFV equation of state.

According to Figs. 23 and 24, it is largest at the star's surface. However, e^{HT} does not monotonously increase with the Kepler frequency. This is only the case for the "slow" frequency models Ω_K =4000 and 6000 s^{-1} with ϵ_c values of 186 and 354 MeV/fm^3, respectively (Fig. 23). The eccentricity for rotation at Ω_K = 9000 s^{-1} is characterized by a significant reduction of e^{HT} in the star's core, caused by the larger central energy density of ϵ_c=849 MeV/fm^3 in this case. With increasing distance from the core the eccentricity increases rather rapidly since the core's strong gravitational attraction is the more counterbalanced by centrifugal forces the larger the radial distance from the center of the star is. A similar qualitative behavior was found for the Hartree-Fock equation of state with and without two-particle correlations, which can be seen in Fig. 24. The influence of correlations on e^{HT} is again largest in the core region. They change the magnitude of the eccentricity at the star's *surface* only to a less extent, as shown in Tables 12-14.

7 Summary

The rapidly increasing number of observed pulsars rotating at periods in the millisecond range has renewed great interest in the properties of rotating neutron stars. The study of these objects covers both Einstein's theory of general relativity as well as

nuclear many-body physics.

We have studied the properties of rotating neutron stars by solving Hartle's general relativistic stellar structure equations. The idea in this treatment is to develop a solution of Einstein's field equations that is based on perturbation of the line element from that of a static star. Our investigations performed elsewhere [5, 6] support the applicability of Hartle's method for the construction of models of rotating neutron star configurations up to rotational frequencies $\approx 1.2 \cdot 10^4$ s^{-1}. This correspnds to a period of $P \approx 0.5$ msec and is a fraction of the smalles yet observed periods (1.6 msec). The unknown quantity in solving stellar structure equations is the equation of state of neutron star matter. It is needed over a huge density range, ranging from zero at the star's edge to roughly ten times normal nuclear matter density reached in the cores of neutron stars.

The determination of the supernuclear equation of state of (electrically charge-neutral many-baryon/lepton) neutron star matter in the framework of the relativistic Green's function formalism was one of the topics of this work. Neutron star matter equations of state have been derived for the the Hartree, Hartee-Fock and the so-called ladder (Λ) approximations. The fundamental difference between these methods lies in the treatment of the nucleon-nucleon scattering problem in matter in the case of the Λ mehtod. This implies the self-consistent calculation of the scattering T-matrix in matter, for which two boson-exchange models for the nucleon-nucleon force served as an input (Bonn and HEA potentials). The Hartree and Hartree-Fock schemes emerge via restriction to the Born term of the T-matrix (the above potentials). The parameters of the latter two approximations must be adjusted to the bulk properties of nuclear matter (binding energy, effective mass, compression modulus, and symmetry energy at saturation) since the Bonn and HEA meson-exchange potentials with parameters adjusted to the two-nucleon data do not saturate nuclear matter.

In our investigation one Hartree parameter set (σ, ω, ϱ mesons plus cubic and quartic self-interactions of the σ field) and one Hartree-Fock parameter set ($\sigma, \omega, \pi, \varrho$-mesons) has been used for the calculation of the equation of state of charge neutral many-baryon/lepton neutron star matter. The influence of two-particle correlations on the equation of state is taken into account in the neutron-rich density regime ($\varrho \lesssim 0.3$ fm^{-3}; matter almost pure in neutrons) by self-consistently solving the equations of the Λ method for the Bonn and HEA potentials (including $\sigma, \omega, \pi, \varrho, \eta, \delta, \phi$-mesons) with restriction to only neutrons. The equations of state calculated in this way are

given in tabulated form in Tables 8 (Bonn) and 9 (HEA). Their characteristic features can be summarized as follows:

– inclusion of two-particle correlations,

– inclusion of charged hyperon- (Σ, Λ, Ξ) and baryon (Δ) states, which are in general β equilibrium,

– the microscopic stability condition $dP/d\epsilon \geq 0$ and

– the causality condition $dP/d\epsilon \leq 1$ at high densities are fulfilled.

Rotating star models have been constructed from these equations of state for a representative set of Kepler velocities (4000, 6000, 9000 s^{-1}). Our equations of state allow for a systematic investigation of the impact of two-particle correlations in matter as well as different many-body approximations (Hartree, Hartee-Fock, Λ scheme) on the properties of rotating neutron star configurations. By this the compatibility of the four different models of the nuclear equation of state with data on pulsar periods can be tested conveniently. This should help clarifying the central problem of the behavior of the nuclear equation of state at densities beyond normal nuclear matter density. We find that the minimum periods so far observed of $P = 1.6$ msec is the case of pulsar PSR 1937+21 and PSR 1957+20 can easily be accomodated by our equations of state.

The most sensitive dependence on correlations exhibit the low-mass star models of Table 12 ($0.44 < M/M_\odot < 0.87$) with central energy densities 186 MeV/fm^3 ($3.3 \cdot 10^{14}$ g/cm^3) $\leq \epsilon_c \leq$ 208 MeV/fm^3 ($3.7 \cdot 10^{14}$ g/cm^3). The calculated increase of gravitational mass due to rotation is $\approx 16\%$ (without correlations) and $\approx 23\%$ (with correlations) for star models rotating at $\Omega_K = 4000$ s^{-1}. Two-particle correlations influence the properties of rotating stars the less the larger ϵ_c is. For example, correlations reduce the gravitational masses of our most massive and hence most rapidly rotating models of Table 14 ($\Omega_K = 9000$ s^{-1}) by approximately 3%. The values of the central energy densities of these models is reduced by 11% ($\Lambda^{00}_{\text{Bonn}} + \text{HV}$). This is of great importance as concerns the question of what are the "fundamental" constituents (hadrons or quarks) in the cores of neutron stars.

The stability parameter t calculated for the rotating star models of Tables 12-14 has values of 0.07, 0.10, and 0.12, respectively. From this it follows that instability to

a bar mode (perturbation mode with angular dependence $e^{im\phi}$ for $m = 2$) appears unlikely.

A Total baryon mass of a neutron star

The total baryon number of a spherical neutron star is given by (see Table 1 for the definition of the dimensionless quantities, denoted by a hat)

$$A_s \;=\; 4\,\pi \int_0^{\hat{R}_S} d\hat{r}\;\hat{r}^2\;\frac{\hat{\varrho}(\hat{r})}{\sqrt{1-\Upsilon}}\;, \tag{207}$$

where $\hat{\varrho}$ is the number density of Eq. (169). The change in total baryon number due to rotation, ΔA, follows from ($\hat{m}_n$ is the neutron mass)

$$\hat{m}_n\,\Delta A \;=\; \hat{m}_0(\hat{R}_s) \;+\; 4\,\pi\,\kappa \int_0^{\hat{R}_s} d\hat{r}\;\hat{r}^2\;\mathcal{B}(\hat{r})\;, \tag{208}$$

where $\mathcal{B}$ is defined by

$$\begin{aligned}\mathcal{B}(\hat{r}) \;=\; & (\hat{\epsilon}+\hat{P})\,p_0\left\{\frac{\partial\hat{\epsilon}}{\partial\hat{P}}\left[\frac{1}{\sqrt{1-\Upsilon}}-1\right]-\frac{\partial\hat{\epsilon}^{\rm Int}}{\partial\hat{P}}\,\frac{1}{\sqrt{1-\Upsilon}}\right\}\\ & +\frac{(\hat{\epsilon}-\hat{\epsilon}^{\rm Int})}{\sqrt{1-\Upsilon}^{\,3}}\left[\frac{\hat{m}_n\hat{G}}{\hat{r}}+\frac{1}{3}\,(j\,\hat{r}\,\hat{\bar{\omega}})^2\right]\\ & -\frac{1}{4\pi}\,\frac{1}{\kappa\,\hat{G}\,\hat{r}^2}\left[\frac{1}{12}\left(j\,\hat{r}^2\,\frac{d\hat{\bar{\omega}}}{d\hat{r}}\right)^2-\frac{1}{3}\,\frac{dj^2}{d\hat{r}}\,\hat{r}^3\,\hat{\bar{\omega}}^2\right]\;.\end{aligned} \tag{209}$$

The quantities $\hat{m}_0$ and p_0 are the monopole distribution functions of respectively mass and pressure of Sect. 2.2.2. The functions j and $\hat{\bar{\omega}}$ are defined in Eqs. (26) and (27). Finally $\hat{P}=\hat{P}(\hat{\epsilon})$ is the equation of state. The internal energy occuring in Eq. (209), $\hat{\epsilon}^{\rm Int}$, is given in terms of the energy density, $\hat{\epsilon}$, and number density, $\hat{\varrho}$:

$$\hat{\epsilon}^{\rm Int} \;=\; \hat{\epsilon} \;-\; \frac{\hat{m}_n\,\hat{\varrho}}{\kappa}\;. \tag{210}$$

B Lagrangian of the scalar-vector-isovector theory of nuclear field theory

The Lagrangian of the so-called scalar-vector-isovector theory, in which baryons B interact via the exchange of iso-scalar (σ, ω) and iso-vector (π, ϱ) mesons, is introduced below. Since we are interested in neutron star matter in generalized β equilibrium, it has been supplemented by a leptonic part and has the form

$$\mathcal{L}(x) = \sum_B \mathcal{L}_B^0 + \sum_{M=\sigma,\omega,\pi,\varrho} \Big\{ \mathcal{L}_M^0(x) + \mathcal{L}_{BM}(x) \Big\} + \mathcal{L}^{(\sigma^4)}(x) + \mathcal{L}_{\rm Lep}^0(x) \,. \tag{211}$$

The free baryon and meson fields in Eq. (211) are given by

$$\mathcal{L}_B^0(x) = \bar\psi_B(x) \left(i\,\gamma^\mu \partial_\mu - m_B \right) \psi_B \,, \tag{212}$$

$$\mathcal{L}_\sigma^0(x) = \frac{1}{2} \Big(\partial^\mu \sigma(x)\, \partial_\mu \sigma(x) - m_\sigma^2\, \sigma^2(x) \Big) \,, \tag{213}$$

$$\mathcal{L}_\omega^0(x) = -\frac{1}{4} F^{\mu\nu}(x)\, F_{\mu\nu}(x) + \frac{1}{2}\, m_\omega^2\, \omega^\nu(x)\, \omega_\nu(x) \,, \tag{214}$$

$$\mathcal{L}_\pi^0(x) = \frac{1}{2} \Big(\partial^\mu \boldsymbol{\pi}(x) \cdot \partial_\mu \boldsymbol{\pi}(x) - m_\pi^2\, \boldsymbol{\pi}(x) \cdot \boldsymbol{\pi}(x) \Big) \,, \tag{215}$$

$$\mathcal{L}_\varrho^0(x) = -\frac{1}{4} \boldsymbol{G}^{\mu\nu}(x) \cdot \boldsymbol{G}_{\mu\nu}(x) + \frac{1}{2}\, m_\varrho^2\, \boldsymbol{\varrho}^\mu(x) \cdot \boldsymbol{\varrho}_\mu(x) \,. \tag{216}$$

The interaction Lagrangians are

$$\mathcal{L}_{B\sigma}(x) = \sum_B g_{\sigma B}\, \bar\psi_B(x)\, \sigma(x)\, \psi_B(x) \,, \tag{217}$$

$$\begin{aligned} \mathcal{L}_{B\omega}(x) = & -\sum_B g_{\omega B}\, \bar\psi_B(x)\, \gamma^\mu \omega_\mu(x)\, \psi_B(x) \\ & -\sum_B \frac{f_{\omega B}}{4\, m_B}\, \bar\psi_B(x)\, \sigma^{\mu\nu}\, F_{\mu\nu}(x)\, \psi_B(x) \,, \end{aligned} \tag{218}$$

$$\mathcal{L}_{B\pi}(x) = -\sum_B \frac{f_{\pi B}}{m_\pi}\, \bar\psi_B(x)\, \gamma^5 \gamma^\mu\, (\partial_\mu \boldsymbol{\tau} \cdot \boldsymbol{\pi}(x))\, \psi_B(x) \,, \tag{219}$$

$$\begin{aligned} \mathcal{L}_{B\varrho}(x) = & -\sum_B g_{\varrho B}\, \bar\psi_B(x)\, \gamma^\mu \boldsymbol{\tau} \cdot \boldsymbol{\varrho}_\mu(x)\, \psi_B(x) \\ & -\sum_B \frac{f_{\varrho B}}{4\, m_B}\, \bar\psi_B(x)\, \sigma^{\mu\nu}\, \boldsymbol{\tau} \cdot \boldsymbol{G}_{\mu\nu}(x)\, \psi_B(x) \,. \end{aligned} \tag{220}$$

The field tensors $F_{\mu\nu}$ and $\boldsymbol{G}_{\mu\nu}$ of Eqs. (214), (216), (218), and (220) are defined by

$$F_{\mu\nu}(x) = \partial_\mu \omega_\nu(x) - \partial_\nu \omega_\mu(x) \,, \quad \boldsymbol{G}_{\mu\nu}(x) = \partial_\mu \boldsymbol{\varrho}_\nu(x) - \partial_\nu \boldsymbol{\varrho}_\mu(x) \,. \tag{221}$$

The quantity $\sigma^{\mu\nu}$ occurring in Eqs. (218) and (220) is defined by (for the γ matrices we use the notation of Ref. [62])

$$\sigma^{\mu\nu} = \frac{i}{2} \left[\gamma^\mu, \gamma^\nu \right] \,. \tag{222}$$

Self-interactions of the scalar σ-meson field are described by

$$\mathcal{L}^{(\sigma^4)}(x) \;=\; -\frac{1}{3}\, m_N\, \bar{b}_N\, \left[g_{\sigma N}\, \sigma(x)\right]^3 \;-\; \frac{1}{4}\, \bar{c}_N\, \left[g_{\sigma N}\, \sigma(x)\right]^4 \;. \tag{223}$$

Finally the Lagrangian of free leptons is

$$\mathcal{L}^0_{Lept}(x) \;=\; \sum_{\lambda = e^-\, \mu^-} \bar{\Psi}_\lambda(x) \left(i\, \gamma^\mu \partial_\mu \;-\; m_\lambda \right) \Psi_\lambda(x) \;. \tag{224}$$

C Baryon and meson propagators

A central role in the treatment of many-particle systems play the fermion two-point Green's functions $g^B(p)$. In the following we derive their finite-temperature spectral decomposition. The zero-temperature results (Eqs. (99) - (101) and (184) for baryons and leptons, respectively) were of essential importance in Sect. 3 for the determination of the equation of state. The meson propagators are given in Sect. C.2.

C.1 Spectral decomposition of the baryon two-point functions

We start from the finite-temperature definition of the two-point function (the quantity $\beta = 1/k_{\rm B}T$, $k_{\rm B}$ denotes Boltzman's constant),

$$g^{BB'}(x,\zeta;x',\zeta') \;=\; i\,\frac{Tr\left(e^{-\beta H}\,T(\psi_B(x,\zeta)\,\bar{\psi}_{B'}(x',\zeta'))\right)}{Tr\,e^{-\beta H}}\,, \tag{225}$$

defined as the quantum mechanical average of time-ordered baryon field operators over a canonical ensemble [50, 51, 27, 52, 85]. The functions $g_<$ and $g_>$ of Eqs. (84) and (85) are given by ($< \ldots >_\beta$ refers to the finite-temperature definition)

$$\begin{aligned} g_>^{BB'}(x,\zeta;x',\zeta') &\equiv i\,<\psi_B(x,\zeta)\,\bar{\psi}_{B'}(x',\zeta')>_\beta \\ &= i\,\frac{Tr\,(e^{-\beta H}\,\psi_B(x,\zeta)\,\bar{\psi}_{B'}(x',\zeta'))}{Tr\,e^{-\beta H}}\,, \end{aligned} \tag{226}$$

$$\begin{aligned} g_<^{BB'}(x,\zeta;x',\zeta') &\equiv -i\,<\bar{\psi}_{B'}(x',\zeta')\,\psi_B(x,\zeta)>_\beta \\ &= -i\,\frac{Tr\,(e^{-\beta H}\,\bar{\psi}_{B'}(x',\zeta')\,\psi_B(x,\zeta))}{Tr\,e^{-\beta H}}\,. \end{aligned} \tag{227}$$

In the next step we turn to the time-development operator e^{-iHx_0}. It bears a strong formal similarity to the weighting factor $e^{-\beta H}$ occuring in the grand-canonical average of Eqs. (225) and (226) - (227). By means of (1) considering the time variables x_0, x_0' of $g^B(x,x')$ to being restricted to $0 \le ix_0,\, ix_0' \le \beta$ and (2) extending the definition of the time-ordering operator to mean ix_0, ix_0'-ordering when times are imaginary, then the Green's functions are again well defined in the intervall $ix_0,\, ix_0' \in [0,\beta]$ [52, 85]. The following relations for imaginary times in the intervall $[0,-i\beta]$ can be veryfied by making use of the cyclic property of the trace:

$$g^B(x,\zeta;x',\zeta')\Big|_{x_0=0} \;=\; g_<^B(x,\zeta;x',\zeta')\Big|_{x_0=0}\,, \tag{228}$$

$$g^B(x,\zeta;x',\zeta')\Big|_{x_0=-i\beta} = g^B_>(x,\zeta;x',\zeta')\Big|_{x_0=-i\beta} , \tag{229}$$

$$g^B_<(x,\zeta;x',\zeta')\Big|_{x_0=0} = -\, g^B_>(x,\zeta;x',\zeta')\Big|_{x_0=-i\beta} , \tag{230}$$

$$g^B(x,\zeta;x',\zeta')\Big|_{x_0=0} = -\, g^B(x,\zeta;x',\zeta')\Big|_{x_0=-i\beta} . \tag{231}$$

Equation (231) follows from Eqs. (228) - (231). It expresses the anti-periodic boundary condition of fermion propagators. The anti-periodicity can be incorporated in the representation of $g^B(x,x')$ by Fourier series and integrals. Defining the frequency $\omega_n \equiv \frac{2n+1}{-i\beta}\,\pi$ ($n = 0, \pm 1, ...$), one gets [52, 86, 87, 88]:

$$g^B(x,\zeta;x',\zeta') = \frac{1}{(-i\beta)^2}\sum_{n,n'} e^{-i\omega_n x_0 + i\omega_{n'} x'_0} \times \int_{\boldsymbol{p}^3}\int_{\boldsymbol{p}'^3} e^{i\boldsymbol{p}\cdot\boldsymbol{x} - i\boldsymbol{p}'\boldsymbol{x}'}\, g^B(\omega_n,\boldsymbol{p},\zeta;\omega_{n'},\boldsymbol{p}',\zeta') . \tag{232}$$

From the inverse transformation formula

$$g^B(\omega_n,\boldsymbol{p},\zeta;\omega_{n'},\boldsymbol{p}',\zeta') = \int_0^{-i\beta} dx_0 \int_0^{-i\beta} dx'_0\, e^{i\omega_n x_0 - i\omega_{n'} x'_0} \times \int d^3\boldsymbol{x} \int d^3\boldsymbol{x}'\, e^{-i\boldsymbol{p}\cdot\boldsymbol{x} + i\boldsymbol{p}'\cdot\boldsymbol{x}'}\, g^B_{\zeta\zeta'}(x-x') , \tag{233}$$

and the fact that for infinite matter the propagator functions depend only on their relative coordinates, the energy-momentum representation g^B can be written as ($\delta(x_0) = \frac{1}{-i\beta}\sum_n e^{-i\omega_n x_0}$, $\delta_{nn'} = \frac{1}{-i\beta}\int_0^{-i\beta} dx_0\, e^{ix_0(\omega_n - \omega_{n'})}$):

$$g^B(\omega_n,\boldsymbol{p},\zeta;\omega_{n'},\boldsymbol{p},\zeta') = (-i\beta)\,(2\pi)^3\,\delta_{nn'}\,\delta^3(\boldsymbol{p}-\boldsymbol{p}')\,g^B_{\zeta\zeta'}(\omega_n,\boldsymbol{p}) . \tag{234}$$

The free baryon propagator g^{0B} satisfies, according to Eq. (87) ($p = (p^0,\boldsymbol{p}) \equiv (\omega_n,\boldsymbol{p})$):

$$\left(\gamma^\mu p_\mu - m_B\right)_{\zeta\zeta''} g^{0B}_{\zeta''\zeta'}(p) = -\,\delta_{\zeta\zeta'} . \tag{235}$$

It should be noted that $(\gamma^\mu p_\mu - m_B) \neq 0$ in Eq. (235), so that there is no ambiguity in the division process [52]. In the next step the real time formalism is applied to represent the propagator $g^B(x-x')$ by Fourier integrals. We use the definitions:

$$g(p) = \int d^4x\, e^{ipx}\, g(x) , \qquad g(x) = \int_{p^4} e^{-ipx}\, g(p) , \tag{236}$$

$$\delta^4(p) = \int \frac{d^4x}{(2\pi)^4}\, e^{ipx} , \qquad \delta^4(x) = \int_{p^4} e^{-ipx} . \tag{237}$$

One arrives for $g^B_<$ and $g^B_>$ at the momentum-space representations

$$g^B_<(p)_{\zeta\zeta'} = -e^{-\beta p^0}\, g^B_>(p)_{\zeta\zeta'} = -2\pi i\, \Xi^B_{\zeta\zeta'}(p)\, f_+(p^0)\,, \tag{238}$$

$$g^B_>(p)_{\zeta\zeta'} = 2\pi i\, \Xi^B_{\zeta\zeta'}(p)\, \Big(1 - f_+(p^0)\Big)\,, \tag{239}$$

$$f_+(p^0) \equiv \frac{1}{e^{\beta p^0}+1}\,. \tag{240}$$

The first relation of Eq. (238) results from the Fourier representation of $g^B_<(p^0,\boldsymbol{p})$ in combination with Eq. (230), evaluated at $x_0 - i\beta$. The definition of the the spectral function $\Xi^B(p)$ introduced below allows to rewrite the first equation of Eq. (238) in terms of Ξ^B and the Fermi-Dirac distribution function $f_+(p^0)$, defined in Eq. (240). From Eq. (238) and the definition of the spectral function,

$$\Xi^B_{\zeta\zeta'}(p) \equiv \frac{g^B_>(p)_{\zeta\zeta'} - g^B_<(p)_{\zeta\zeta'}}{2\pi i}\,, \tag{241}$$

Eq. (239) for $g^B_>(p)$ follows.

To demonstrate that the structure of $g^B(p)$ is completely determined by $\Xi(p)$, we proceed as follows. From the imaginary-time representation of $g^B(\omega_n,\boldsymbol{p})$ of Eqs. (233) - (234) it follows that $g^B(x_0,\boldsymbol{x})$ can be replaced by $g^B_>(x_0,\boldsymbol{x})$, because of $x_0 \in [0,-i\beta]$ and Eq. (83). Fourier transformation of $g^B_>(x_0,\boldsymbol{x})$ and use of Eq. (239) leads to the final result

$$g^B_{\zeta\zeta'}(\omega_n,\boldsymbol{p}) = \int\limits_{-\infty}^{+\infty} dp^0\, \frac{\Xi^B_{\zeta\zeta'}(p)}{p^0-\omega_n}\,. \tag{242}$$

To determine Ξ^B one extends $g^B(\omega_n,\boldsymbol{p})$ to an analytically continued function (denoted by a tilde) in the complex energy plane,

$$\tilde{g}^B_{\zeta\zeta'}(z,\boldsymbol{p}) = \int\limits_{-\infty}^{+\infty} d\omega\, \frac{\Xi^B_{\zeta\zeta'}(\omega,\boldsymbol{p})}{\omega - z}\,. \tag{243}$$

From Eq. (243) it follows that each baryon spectral function Ξ^B can be expressed by the cut-line of the baryon propagator $\tilde{g}(z,\boldsymbol{p})$ along the real energy axis (i.e. Eq. (103)):

$$\Xi^B_{\zeta\zeta'}(\omega,\boldsymbol{p}) = \frac{\tilde{g}^B_{\zeta\zeta'}(\omega+i\eta,\boldsymbol{p}) - \tilde{g}^B_{\zeta\zeta'}(\omega-i\eta,\boldsymbol{p})}{2\pi i}\,. \tag{244}$$

Th results of Eqs. (243) - (244) are formally identical with those of the non-relativistic Green's functions method [89, 90, 85, 42].

For the subsequent analysis we make use of the identity

$$\Theta(\pm x_0) = \frac{i}{2\pi} \int\limits_{-\infty}^{+\infty} d\omega \, \frac{e^{\mp i\omega x_0}}{\omega + i\eta} \, . \tag{245}$$

The momentum-space representations $g^B(x)$, $g^B_>(x)$ and $g^B_<(x)$ then follow in the form

$$g^B_{\zeta\zeta'}(p) = \frac{i}{2\pi} \int\limits_{-\infty}^{+\infty} d\omega \left[\frac{g^B_>(\omega,\boldsymbol{p})_{\zeta\zeta'}}{p^0 - \omega + i\eta} - \frac{g^B_<(\omega,\boldsymbol{p})_{\zeta\zeta'}}{p^0 - \omega - i\eta} \right] \tag{246}$$

$$= - \int\limits_{-\infty}^{+\infty} d\omega \left[\frac{1 - f_+(\omega)}{p^0 - \omega + i\eta} + \frac{f_+(\omega)}{p^0 - \omega - i\eta} \right] \Xi^B_{\zeta\zeta'}(\omega,\boldsymbol{p}) \tag{247}$$

$$= \int\limits_{-\infty}^{+\infty} d\omega \, \frac{\Xi^B_{\zeta\zeta'}(\omega,\boldsymbol{p})}{\omega - p^0 - i\eta} - 2\pi i \, \Xi^B_{\zeta\zeta'}(p) \, f_+(p^0) \, . \tag{248}$$

To derive the last two expressions use of Eqs. (238) - (240) has been made. Equation (248) can be rewritten in the form

$$g^B_{\zeta\zeta'}(p) = \int\limits_{-\infty}^{+\infty} d\omega \, \frac{\Xi^B_{\zeta\zeta'}(\omega,\boldsymbol{p})}{\omega - p^0\,(1 + i\eta)} - 2\pi \, i \, \mathrm{sgn}(p^0) \, \Xi^B_{\zeta\zeta'}(p) \, f_+(\mid p^0 \mid) \, . \tag{249}$$

In the free-particle case, the spectral representation of Eq. (249) can be evaluated analytically. Substituting $\tilde{g}^B(\omega \pm i\eta, \boldsymbol{p}) \equiv \tilde{g}^{0\,B}(\omega \pm i\eta, \boldsymbol{p})$ of Eq. (235) into Eq. (244) one obtains for the free spectral function (denoted by Ξ^{0B})

$$\Xi^{0B}_{\zeta\zeta'}(p) = \mathrm{sgn}(p^0) \, (\gamma^\mu p_\mu + m_B)_{\zeta\zeta'} \, \delta(p^2 - m_B^2) \, . \tag{250}$$

Substituting Ξ^{0B} in Eq. (249) leads to

$$g^{0B}_{\zeta\zeta'}(p^\mu) = \frac{(\gamma^\mu p_\mu + m_B)_{\zeta\zeta'}}{p_\mu^2 - m_B^2 + i\eta} + i\pi \, f_+(\mid p^0 \mid) \, \frac{(\gamma^\mu p_\mu + m_B)_{\zeta\zeta'}}{E^B(\boldsymbol{p})} \times \left[\delta(p^0 - E^B(\boldsymbol{p})) + \delta(p^0 + E^{\bar{B}}(\boldsymbol{p})) \right] \tag{251}$$

$$= \frac{(\gamma^\mu p_\mu + m_B)_{\zeta\zeta'}}{2 \, E^B(\boldsymbol{p})} \times \left\{ \frac{1 - f^B(\boldsymbol{p})}{p^0 - E^B(\boldsymbol{p}) + i\eta} + \frac{f^B(\boldsymbol{p})}{p^0 - E^B(\boldsymbol{p}) - i\eta} - \frac{1 - f^{\bar{B}}(\boldsymbol{p})}{p^0 + E^B(\boldsymbol{p}) - i\eta} - \frac{f^{\bar{B}}(\boldsymbol{p})}{p^0 + E^B(\boldsymbol{p}) + i\eta} \right\} . \tag{252}$$

The definitions have been introduced:

$$E^B(\boldsymbol{p}) = +\sqrt{m_B^2+\boldsymbol{p}^2} = E^{\bar{B}}(\boldsymbol{p})\,, \tag{253}$$

$$f^B(\boldsymbol{p}) \equiv f_+(E^B(\boldsymbol{p}))\,. \tag{254}$$

The physical interpretation of $g^{0\,B}(p)$ is given in the following [54]: Both particle and anti-particle states occur as in the usual (causal) Feynman propagator. But due to the nuclear medium two new states corresponding to "holes" in the particle Fermi sea (unfilled states in the Fermi sea of particles) and "anti-holes" in the anti-particle Fermi sea (unfilled states in the Fermi sea of anti- particles) result. Thus, the principle effect of finite temperatures on baryon propagation results in states with momenta $\mid \boldsymbol{p} \mid > p_F$ and $\mid \boldsymbol{p} \mid > \bar{p}_F$ (i.e. states outside the Fermi seas of particles and anti-particles become populated) and hole (anti-hole) states in the corresponding Fermi seas of particles (anti-particles).

In the *interacting* particle case the spectral function has a more complicated structure. However, one can keep the single-particle description if the many-particle system is treated in the Hartree, Hartree-Fock, and Λ^{00} approximation [53]. As an example we give the propagator calculated for the Hartree approximation [51, 25]:

$$\begin{aligned} -\,g^{\mathrm{H},B}_{\zeta\zeta'}(p^\mu) = & \frac{\gamma^0_{\zeta\zeta'}\,(p^0-\Sigma^{\mathrm{H},B}_0(\boldsymbol{p}))\,-\,(\gamma\cdot\boldsymbol{p})_{\zeta\zeta'}\,+\,1_{\zeta\zeta'}\,(m_B+\Sigma^{\mathrm{H},B}_S(\boldsymbol{p}))}{2\,\epsilon^B(\boldsymbol{p})} \\ & \times\Bigg\{\frac{1-f^B(\boldsymbol{p})}{p^0-\Sigma^{\mathrm{H},B}_0(\boldsymbol{p})-\epsilon^B(\boldsymbol{p})+i\eta}+\frac{f^B(\boldsymbol{p})}{p^0-\Sigma^{\mathrm{H},B}_0(\boldsymbol{p})-\epsilon^B(\boldsymbol{p})-i\eta} \\ & -\frac{1-f^{\bar{B}}(\boldsymbol{p})}{p^0-\Sigma^{\mathrm{H},B}_0(\boldsymbol{p})+\epsilon^B(\boldsymbol{p})-i\eta}-\frac{f^{\bar{B}}(\boldsymbol{p})}{p^0-\Sigma^{\mathrm{H},B}_0(\boldsymbol{p})+\epsilon^B(\boldsymbol{p})+i\eta}\Bigg\}\,, \end{aligned} \tag{255}$$

with ϵ^B defined in Eq. (154).

C.2 Meson two-point functions

A list of the relevant mesons fields is given in Table 4. The free scalar ones (σ, δ) obey (compar with Eq. (268))

$$\left(\partial^\mu \partial_\mu \, + \, m_\sigma^2\right) \sigma(x) \, = \, 0 \, . \tag{256}$$

The corresponding free propagator $\Delta_\sigma^0(x,x')$ satisfies

$$\left(\partial^\mu \partial_\mu \, + \, m_\sigma^2\right) \Delta_\sigma^0(x,x') \, = \, \delta^4(x-x') \, , \tag{257}$$

which reads in momentum-space representation

$$\Delta_\sigma^0(p) \, = \, \frac{-1}{p^2 - m_\sigma^2 + i\,\eta} \, . \tag{258}$$

In the case of the pseudoscalar π-meson field $\boldsymbol{\pi}(x)$ of isospin one ($\pi \equiv (\pi_1, \pi_2, \pi_3)$ each field component satisfies ($r = 1,2,3$ refer to the three components of the field):

$$\left(\partial^\mu \partial_\mu \, + \, m_{\pi,r}^2\right) \pi_r(x) \, = \, 0 \, , \tag{259}$$

and for the pion two-point Green's function one gets

$$\left(\partial^\mu \partial_\mu \, + \, m_{\pi,r}^2\right) \Delta_\pi^0(x,x';r) \, = \, \delta^4(x-x') \, , \tag{260}$$

$$\Delta_\pi^0(p;r) \, = \, \frac{-1}{p^2 - m_{\pi,r}^2 + i\,\eta} \, . \tag{261}$$

The analog expressions for vector mesons fiels (i.e. ω, ϱ, ϕ) are:

$$\partial^\kappa \, G^r_{\kappa\lambda}(x) \, + \, m_{\varrho,r}^2 \, \varrho^r_\lambda(x) = 0 \, , \tag{262}$$

$$\left(\partial^\kappa \partial_\kappa \, \delta_\lambda{}^\mu - \partial_\lambda \partial^\mu + m_{\varrho,r}^2 \, \delta_\lambda{}^\mu\right) \mathcal{D}^{0\,\varrho}_{\mu\nu}(x,x';r) \, = \, \delta_{\lambda\nu} \, \delta^4(x-x') \, , \tag{263}$$

(the field tensor G is defined in Eq. (221) with

$$\mathcal{D}^{0\,\varrho}_{\mu\nu}(x-x';r) \, = \, \left(g_{\mu\nu} + \frac{\partial_\mu \partial_\nu}{m_{\varrho,r}^2}\right) \Delta^{0\,\varrho}(x-x';r) \, , \tag{264}$$

which reads in momentum space

$$\mathcal{D}^{0\,\varrho}_{\mu\nu}(p;r) \, = \, \left(g_{\mu\nu} - \frac{p_\mu p_\nu}{m_{\varrho,r}^2}\right) \Delta^{0\,\varrho}(p;r) \, , \tag{265}$$

$$\Delta^{0\,M}(p;r) \, = \, \frac{-1}{p^2 - m_{M,r}^2 + i\eta} \, . \tag{266}$$

Equation (266) holds for $M = \sigma, \omega, \pi, \varrho$. In the latter case one has $r = 1,2,3$, otherwise r is without meaning. The propagator of Eq. (266) enters in Eqs. (272) - (282).

D Field equations of the nuclear scalar-vector-isovector theory

From $\mathcal{L}$ of Eqs. (211) - (224) the the equations of motion can be derived. The baryon spinors $\psi_B(x)$ satisfy

$$\begin{aligned}\left(i\gamma^\mu\partial_\mu - m_B\right)\psi_B(x) \;=\; & - \; g_{\sigma B}\,\psi_B(x)\,\sigma(x) \\ & + \; g_{\omega B}\gamma^\mu\omega_\mu(x)\,\psi_B(x) + \frac{f_{\omega B}}{4m_B}\sigma^{\mu\nu}F_{\mu\nu}(x)\,\psi_B(x) \\ & - \; \frac{f_{\pi B}}{m_\pi}\,\gamma^\mu\gamma^5\left(\partial_\mu\,\boldsymbol{\tau}\cdot\boldsymbol{\pi}(x)\right)\psi_B(x) \\ & + \; g_{\varrho B}\,\gamma^\mu\,\boldsymbol{\tau}\cdot\boldsymbol{\varrho}_\mu(x)\,\psi_B(x) \\ & + \; \frac{f_{\varrho B}}{4\,m_B}\,\sigma^{\mu\nu}\,\boldsymbol{\tau}\cdot\boldsymbol{G}_{\mu\nu}(x)\,\psi_B(x)\,. \end{aligned} \tag{267}$$

The σ and ω-mesons couple to the scalar $(\bar\psi\psi)$ and vector $(\bar\psi\gamma_\nu\psi)$ currents, respectively:

$$\begin{aligned}(\partial^\mu\partial_\mu + m_\sigma^2)\,\sigma(x) \;=\; & \sum_B g_{\sigma B}\,\bar\psi_B(x)\psi_B(x) - m_N\,\bar b_N\,g_{\sigma N}\left(g_{\sigma N}\sigma(x)\right)^2 \\ & - \bar c_N\,g_{\sigma N}\left(g_{\sigma N}\sigma(x)\right)^3, \end{aligned} \tag{268}$$

$$\begin{aligned}\partial^\mu F_{\mu\nu}(x) + m_\omega^2\,\omega_\nu(x) \;=\; & \sum_B g_{\omega B}\,\bar\psi_B(x)\gamma_\nu\psi_B(x) \\ & - \sum_B \frac{f_{\omega B}}{2\,m_B}\,\partial^\mu\left(\bar\psi_B(x)\,\sigma_{\mu\nu}\,\psi_B(x)\right). \end{aligned} \tag{269}$$

The equations of motion of the isovector mesons $\boldsymbol{\pi}$ and $\boldsymbol{\varrho}$ are given by

$$\left(\partial^\mu\partial_\mu + m_\pi^2\right)\boldsymbol{\pi}(x) \;=\; \sum_B \frac{f_{\pi B}}{m_\pi}\,\partial^\mu\left(\bar\psi_B(x)\,\gamma_5\,\gamma_\mu\,\boldsymbol{\tau}\,\psi_B(x)\right), \tag{270}$$

$$\begin{aligned}\partial^\mu\boldsymbol{G}_{\mu\nu}(x) + m_\varrho^2\,\boldsymbol{\varrho}_\nu(x) \;=\; & \sum_B g_{\varrho B}\,\bar\psi_B(x)\,\boldsymbol{\tau}\,\gamma_\nu\,\psi_B(x) \\ & - \sum_B \frac{f_{\varrho B}}{2\,m_B}\,\partial^\mu\left(\bar\psi_B(x)\,\boldsymbol{\tau}\,\sigma_{\mu\nu}\,\psi_B(x)\right). \end{aligned} \tag{271}$$

E Self-energies of ω, π, and ϱ-mesons for the Hartree-Fock approximation

In the following we list the set of equations, which determine the self-energy of a baryon of type B, $\Sigma(p) \equiv \Sigma^{\mathrm{H},B}(p) + \Sigma^{\mathrm{F},B}(p)$, in infinite neutron matter. The symbols "H" and "F" refer to Hartree and Fock terms, respectively, given by:

$$\Sigma^{\mathrm{H},B}_{\zeta_1\zeta_1'}(p)\Big|_\omega = i\,\gamma^\mu_{\zeta_1\zeta_1'}\,\Delta^0_{\mu\nu}(0)\,g_{\omega B}\sum_{B'} g_{\omega B'}\int_{q^4} e^{i\eta q^0}\,Tr\left(\gamma^\nu g^{B'}(q)\right), \tag{272}$$

$$\Sigma^{\mathrm{F},B}_{\zeta_1\zeta_1'}(p)\Big|_\omega = -\,i\,g^2_{\omega B}\int_{q^4} e^{i\eta q^0}\gamma^\mu_{\zeta_1\zeta_3}\,\Delta^0(p-q)_{\mu\nu}\,g^B_{\zeta_3\zeta_2}(q)\,\gamma^\nu_{\zeta_2\zeta_1'}, \tag{273}$$

$$\Sigma^{\mathrm{H},B}_{\zeta_1\zeta_1'}(p)\Big|_\pi = 0, \tag{274}$$

$$\begin{aligned}\Sigma^{\mathrm{F},B}_{\zeta_1\zeta_1'}(p)\Big|_\pi = {}& i\left(\frac{f_{\pi B}}{m_\pi}\right)^2\int_{q^4} e^{i\eta q^0}(\gamma_5\gamma_\nu)_{\zeta_1\zeta_3}\\ & \times (p-q)^\mu\,(p-q)^\nu\,\Delta^0(p-q)\,g^B_{\zeta_3\zeta_2}(q)\,(\gamma_5\gamma_\mu)_{\zeta_2\zeta_1'},\end{aligned} \tag{275}$$

$$\begin{aligned}\Sigma^{\mathrm{H},B}_{\zeta_1\zeta_1'}(p)\Big|_\varrho = {}& i\sum_{B'}\int_{q^4} e^{i\eta q^0}\left(g_{\varrho B}\gamma_\mu - i\,\frac{f_{\varrho B}}{2m_B}\,(p-q)^\lambda\,\sigma_{\lambda\mu}\right)_{\zeta_1\zeta_1'}\\ & \times \Delta^0(0)^{\mu\nu}\,Tr\left[\left(g_{\varrho B'}\gamma_\nu + i\,\frac{f_{\varrho B'}}{2m_{B'}}\,(p-q)^\kappa\sigma_{\kappa\nu}\right)g^{B'}(q)\right],\end{aligned} \tag{276}$$

$$\begin{aligned}\Sigma^{\mathrm{F},B}_{\zeta_1\zeta_1'}(p)\Big|_\varrho = {}& -\,i\int_{q^4} e^{i\eta q^0}\left(g_{\varrho B}\gamma_\mu - i\,\frac{f_{\varrho B}}{2m_B}\,(p-q)^\lambda\,\sigma_{\lambda\mu}\right)_{\zeta_1\zeta_3}\\ & \times \Delta^0(p-q)^{\mu\nu}\,g^B_{\zeta_3\zeta_2}(q)\left(g_{\varrho B}\gamma_\nu + i\,\frac{f_{\varrho B}}{2m_B}\,(p-q)^\kappa\sigma_{\kappa\nu}\right)_{\zeta_2\zeta_1'},\end{aligned} \tag{277}$$

One obtains from Eqs. (272) - (277) via contour integration over the variable q^0, and keeping only the medium terms as outlined in Sect. 3.5.1:

$$\Sigma^{\mathrm{H},B}_{\zeta_1\zeta_1'}(p)\Big|_\omega = 2\,\gamma^0_{\zeta_1\zeta_1'}\left(\frac{g_{\omega B}}{m_\omega}\right)^2\sum_{B'}(2J_{B'}+1)\left(\frac{g_{\omega B'}}{g_{\omega B}}\right)\int_{\boldsymbol{q}^3}\Xi^{B'}_0(\boldsymbol{q})\,\Theta^{B'}(\boldsymbol{q}), \tag{278}$$

$$\Sigma^{\mathrm{H},B}_{\zeta_1\zeta_1'}(p)\Big|_\varrho = 2\,\gamma^0_{\zeta_1\zeta_1'}\left(\frac{g_{\varrho B}}{m_\varrho}\right)^2\sum_{B'}(2J_{B'}+1)\,I_{3B'}\left(\frac{g_{\varrho B'}}{g_{\varrho B}}\right)\int_{\boldsymbol{q}^3}\Xi^{B'}_0(\boldsymbol{q})\,\Theta^{B'}(\boldsymbol{q}), \tag{279}$$

$$
\begin{aligned}
\Sigma^{\mathrm{F},B}_{\zeta_1\zeta_1'}(p)\Big|_{\omega} = \quad & g^2_{\omega B}\int_{\boldsymbol{q}^3}\Big\{ -\delta_{\zeta_1\zeta_1'}\left[4-\frac{(p^0-\omega^B(\boldsymbol{q}))^2-(\boldsymbol{p}-\boldsymbol{q})^2}{m^2_\omega}\right]\Xi^B_S(\omega^B(\boldsymbol{q}),\boldsymbol{q}) \\
& +(\boldsymbol{\gamma}\cdot\hat{\boldsymbol{p}})_{\zeta_1\zeta_1'}\left[\left(\hat{\boldsymbol{p}}\cdot\hat{\boldsymbol{q}}\left(2-\frac{\boldsymbol{p}^2+\boldsymbol{q}^2+(p^0-\omega^B(\boldsymbol{q}))^2}{m^2_\omega}\right)\right.\right. \\
& \left.\left.+\frac{2\,|\boldsymbol{p}|\,|\boldsymbol{q}|}{m^2_\omega}\right)\Xi^B_V(\omega^B(\boldsymbol{q}),\boldsymbol{q}) - \frac{2}{m^2_\omega}\,\hat{\boldsymbol{p}}\cdot(\boldsymbol{p}-\boldsymbol{q})\,(p^0-\omega^B(\boldsymbol{q}))\,\Xi^B_0(\omega^B(\boldsymbol{q}),\boldsymbol{q})\right] \\
& +\gamma^0_{\zeta_1\zeta_1'}\left[\frac{2}{m^2_\omega}\,\hat{\boldsymbol{q}}\cdot(\boldsymbol{p}-\boldsymbol{q})\,(p^0-\omega^B(\boldsymbol{q}))\,\Xi^B_V(\omega^B(\boldsymbol{q}),\boldsymbol{q})\right. \\
& \left.+\left(2+\frac{(p^0-\omega^B(\boldsymbol{q}))^2+(\boldsymbol{p}-\boldsymbol{q})^2}{m^2_\omega}\right)\Xi^B_0(\omega^B(\boldsymbol{q}),\boldsymbol{q})\right]\Big\} \\
& \times\Delta^0(p^0-\omega^B(\boldsymbol{q}),\boldsymbol{p}-\boldsymbol{q})\,\Theta^B(|\boldsymbol{q}|)\,,
\end{aligned}
\tag{280}
$$

$$
\begin{aligned}
\Sigma^{\mathrm{F},B}_{\zeta_1\zeta_1'}(p)\Big|_{\pi} = \quad & \left(\frac{f_{\pi B}}{m_\pi}\right)^2\int_{\boldsymbol{q}^3}\Big\{\delta_{\zeta_1\zeta_1'}\left[-(p^0-\omega^B(\boldsymbol{q}))^2+(\boldsymbol{p}-\boldsymbol{q})^2\right]\Xi^B_S(\omega^B(\boldsymbol{q}),\boldsymbol{q}) \\
& +(\boldsymbol{\gamma}\cdot\hat{\boldsymbol{p}})_{\zeta_1\zeta_1'}\left[\left(2(|\boldsymbol{q}|\,\hat{\boldsymbol{p}}\cdot\hat{\boldsymbol{q}}-|\boldsymbol{p}|)\,(|\boldsymbol{p}|\hat{\boldsymbol{p}}\cdot\hat{\boldsymbol{q}}-|\boldsymbol{q}|)\right.\right. \\
& \left.\left.-\left((p^0-\omega^B(\boldsymbol{q}))^2-(\boldsymbol{p}-\boldsymbol{q})^2\right)\hat{\boldsymbol{p}}\cdot\hat{\boldsymbol{q}}\right)\Xi^B_V(\omega^B(\boldsymbol{q}),\boldsymbol{q}) \\
& \left.+2(|\boldsymbol{q}|\hat{\boldsymbol{p}}\cdot\hat{\boldsymbol{q}}-|\boldsymbol{p}|)\,(p^0-\omega^B(\boldsymbol{q}))\,\Xi^B_0(\omega^B(\boldsymbol{q}),\boldsymbol{q})\right] \\
& +\gamma^0_{\zeta_1\zeta_1'}\left[2(|\boldsymbol{p}|\,\hat{\boldsymbol{p}}\cdot\hat{\boldsymbol{q}}-|\boldsymbol{q}|)\,(p^0-\omega^B(\boldsymbol{q}))\,\Xi^B_V(\omega^B(\boldsymbol{q}),\boldsymbol{q})\right. \\
& \left.+\left((p^0-\omega^B(\boldsymbol{q}))^2+(\boldsymbol{p}-\boldsymbol{q})^2\right)\Xi^B_0(\omega^B(\boldsymbol{q}),\boldsymbol{q})\right]\Big\} \\
& \times\Delta^0(p^0-\omega^B(\boldsymbol{q}),\boldsymbol{p}-\boldsymbol{q})\,\Theta^B(|\boldsymbol{q}|)\,,
\end{aligned}
\tag{281}
$$

$$
\begin{aligned}
\Sigma^{\mathrm{F},B}_{\zeta_1\zeta_1'}(p)\Big|_{\varrho} = \quad & g^2_{\varrho B}\int_{\boldsymbol{q}^3}\Big\{\delta_{\zeta_1\zeta_1'}\left[\left(-4+\chi^B_1\left((p^0-\omega^B(\boldsymbol{q}))^2-(\boldsymbol{p}-\boldsymbol{q})^2\right)\right)\Xi^B_S(\omega^B(\boldsymbol{q}),\boldsymbol{q})\right. \\
& \left.+\frac{3f_{\varrho B}}{m_B g_{\varrho B}}\left(\hat{\boldsymbol{q}}\cdot(\boldsymbol{p}-\boldsymbol{q})\,\Xi^B_V(\omega^B(\boldsymbol{q}),\boldsymbol{q})+(p^0-\omega^B(\boldsymbol{q}))\,\Xi^B_0(\omega^B(\boldsymbol{q}),\boldsymbol{q})\right)\right] \\
& +(\boldsymbol{\gamma}\cdot\hat{\boldsymbol{p}})_{\zeta_1\zeta_1'}\left[\frac{3f_{\varrho B}}{m_B g_{\varrho B}}\,(|\boldsymbol{p}|-|\boldsymbol{q}|\,\hat{\boldsymbol{p}}\cdot\hat{\boldsymbol{q}})\,\Xi^B_S(\omega^B(\boldsymbol{q}),\boldsymbol{q})\right. \\
& +\left(2\,\hat{\boldsymbol{p}}\cdot\hat{\boldsymbol{q}}+|\boldsymbol{p}|\,|\boldsymbol{q}|\,(\hat{\boldsymbol{p}}\cdot\hat{\boldsymbol{q}})^2\,(\chi^B_2-2\chi^B_3)+|\boldsymbol{p}|\,|\boldsymbol{q}|\,\chi^B_2\right. \\
& \left.-(\boldsymbol{p}^2+\boldsymbol{q}^2)\,(\hat{\boldsymbol{p}}\cdot\hat{\boldsymbol{q}})\,(\chi^B_2-\chi^B_3)-\chi^B_3\,(p^0-\omega^B(\boldsymbol{q}))^2\,\hat{\boldsymbol{p}}\cdot\hat{\boldsymbol{q}}\right)\Xi^B_V(\omega^B(\boldsymbol{q}),\boldsymbol{q}) \\
& \left.+\chi^B_2\,(p^0-\omega^B(\boldsymbol{q}))\,(|\boldsymbol{q}|\hat{\boldsymbol{p}}\cdot\hat{\boldsymbol{q}}-|\boldsymbol{p}|)\,\Xi^B_0(\omega^B(\boldsymbol{q}),\boldsymbol{q})\right] \\
& +\gamma^0_{\zeta_1\zeta_1'}\left[-\frac{3f_{\varrho B}}{m_B g_{\varrho B}}\,(p^0-\omega^B(\boldsymbol{q}))\,\Xi^B_S(\omega^B(\boldsymbol{q}),\boldsymbol{q})+\chi^B_2\,(p^0-\omega^B(\boldsymbol{q}))\right.
\end{aligned}
$$

$$\times \quad \boldsymbol{q} \cdot (\boldsymbol{p}-\boldsymbol{q})\, \Xi_V^B(\omega^B(\boldsymbol{q}),\boldsymbol{q})$$
$$+\Big((\chi_2^B-\chi_3^B)\,(p^0-\omega^B(\boldsymbol{q}))^2+\chi_3^B\,(\boldsymbol{p}-\boldsymbol{q})^2+2\Big)\,\Xi_0^B(\omega^B(\boldsymbol{q}),\boldsymbol{q})\Big]\Big\}$$
$$\times\, \Delta^0(p^0-\omega^B(\boldsymbol{q}),\boldsymbol{p}-\boldsymbol{q})\,\Theta^B(|\boldsymbol{q}|)\,. \tag{282}$$

The following abbreviations have been introduced in Eq. (282):

$$\chi_1^B \;\equiv\; \frac{1}{m_\varrho^2}-\frac{3}{(2m_B)^2}\Big(\frac{f_{\varrho B}}{g_{\varrho B}}\Big)^2\,, \tag{283}$$

$$\chi_2^B \;\equiv\; \frac{2}{m_\varrho^2}+\frac{1}{m_B^2}\Big(\frac{f_{\varrho B}}{g_{\varrho B}}\Big)^2\,, \tag{284}$$

$$\chi_3^B \;\equiv\; \frac{1}{m_\varrho^2}+\frac{1}{(2m_B)^2}\Big(\frac{f_{\varrho B}}{g_{\varrho B}}\Big)^2\,. \tag{285}$$

F Energy momentum tensor in the $\sigma - \omega$ model

The pressure P and energy density ϵ are determined by the expectation value of the energy-momentum density tensor [14], defined by

$$\mathcal{T}_{\mu\nu}(x) = \sum_B \partial_\nu \psi_B(x) \frac{\partial \mathcal{L}(x)}{\partial\,[\partial^\mu \psi_B(x)]} - g_{\mu\nu}\,\mathcal{L}(x)\,, \tag{286}$$

from which we obtain via the equations of motion of Eqs. (267) - (269)

$$\begin{aligned}
\mathcal{T}_{\mu\nu}(x) \;=\; & \sum_B \bar\psi_B(x)\,\Big(i\gamma_\mu\partial_\nu \;-\; g_{\mu\nu}\,\Big[i\,\gamma^\lambda\partial_\lambda \;-\; m_B + \; g_{\sigma B}\,\sigma(x) \\
& - g_{\omega B}\,\gamma^\lambda\,\omega_\lambda(x)\Big]\Big)\,\psi_B(x) \\
& - g_{\mu\nu}\,\Big(-\frac{1}{2}\,\sigma(x)\,[\partial_\lambda\partial^\lambda \;+\; m_\sigma^2]\,\sigma(x) \;+\; \frac{1}{2}\,\partial_\lambda[\sigma(x)\partial^\lambda\sigma(x)] \\
& - \frac{1}{2}\partial_\lambda[\omega_\kappa(x)\,F^{\lambda\kappa}(x)] \;+\; \frac{1}{2}\,\omega_\lambda(x)\,\Big[\partial_\kappa F^{\kappa\lambda}(x) \;+\; m_\omega^2\,\omega^\lambda(x)\Big]\Big) \\
& + g_{\mu\nu}\Big(\frac{1}{3}\,\bar b_N\,m_N[g_{\sigma N}\sigma(x)]^3 \;+\; \frac{1}{4}\,\bar c_N\,[g_{\sigma N}\sigma(x)]^4\Big)\,.
\end{aligned} \tag{287}$$

By means of the two-point Green's functions g^B, one can express the expectation value of the energy momentum tensor of Eq. (287) as

$$\begin{aligned}
< \Phi_0|\,\mathcal{T}_{\mu\nu}(x)\,|\Phi_0 > = \; & - \lim_{x'\to x^+}\,\partial_\nu \sum_B \mathrm{Tr}\;\gamma_\mu\,g^B(x,x') \\
& - \frac{1}{2}\,g_{\mu\nu}\,\sum_B \int d^4y\;\mathrm{Tr}\;\Sigma^B(x,y)\,g^B(y,x')\,.
\end{aligned} \tag{288}$$

Energy density and pressure are determined by respectively

$$\epsilon \;\equiv\; < \Phi_0|\,\mathcal{T}_{00}(x)\,|\Phi_0 >\,, \tag{289}$$

$$P \;\equiv\; \frac{1}{3}\sum_{i=1}^{3} < \Phi_0|\,\mathcal{T}_{ii}(x)|\Phi_0 >\;. \tag{290}$$

from which one calculates

$$\begin{aligned}
\epsilon = \; & - \lim_{x'\to x^+}\,\sum_B \partial_0 \int_{q^4} e^{-i\,q\,(x-x')}\,\gamma^0_{\zeta\zeta'}\,g^B_{\zeta'\zeta}(q) - \frac{i}{2}\sum_B \int_{q^4} e^{i\,q^0\,\eta}\,\Sigma^B_{\zeta\zeta'}(q) \\
& - \frac{1}{2}\,\Big[\frac{1}{3}\,\bar b_N\,m_N\,[g_{\sigma N}\,\sigma_0]^3 \;+\; \frac{1}{2}\,\bar c_N\,[g_{\sigma N}\,\sigma_0]^4\Big]\,,
\end{aligned} \tag{291}$$

and

$$\begin{aligned}
P \;=\; & \frac{i}{3}\sum_B \int_{q^4} e^{i\,q^0\,\eta}\;(\boldsymbol{\gamma}\cdot\boldsymbol{q})_{\zeta\zeta'}\,g^B_{\zeta'\zeta}(q) + \frac{i}{2}\sum_B \int_{q^4} e^{i\,q^0\,\eta}\,\Sigma^B_{\zeta\zeta'}(q)\,g^B_{\zeta'\zeta}(q) \\
& + \frac{1}{2}\,\Big[\frac{1}{3}\,\bar b_N\,m_N\,[g_{\sigma N}\,\sigma_0]^3 \;+\; \frac{1}{2}\,\bar c_N\,[g_{\sigma N}\,\sigma_0]^4\Big]\,.
\end{aligned} \tag{292}$$

The quantity σ_0 refers to the static limit of the σ-field, obtained from the field equation (268) for $\partial^\mu\partial_\mu \equiv 0$ and replacing $\bar{\psi}_B\psi_B$ by $< \bar{\psi}_B\psi_B >= \bar{\varrho}$ (see Eqs. (172) - (175)). The mean-field value σ_0 is given in terms of $\Sigma_S^{H,N}$ via $-g_{\sigma N}\,\sigma_0 = \Sigma_S^{H,N}$.

By means of inserting the spectral decomposition of Eq. (101) into Eqs. (291) and (292), the energy and pressure densities can be written as

$$\begin{aligned}
\epsilon &= \sum_B (2\,J_B+1)\int_{\boldsymbol{q}^3}\Big\{2\Big[m_B\,\Xi_S^B(\boldsymbol{q}) - |\boldsymbol{q}|\,\Xi_V^B(\boldsymbol{q})\Big] \qquad (293)\\
&+ \Big[\Sigma_S^B(\omega^B(\boldsymbol{q}),\boldsymbol{q})\,\Xi_S^B(\boldsymbol{q}) - \Sigma_V^B(\omega^B(\boldsymbol{q}),\boldsymbol{q})\,\Xi_V^B(\boldsymbol{q}) + \Sigma_0^B(\omega^B(\boldsymbol{q}),\boldsymbol{q})\,\Xi_0^B(\boldsymbol{q})\Big]\Big\}\,\Theta^B(|\boldsymbol{q}|)\\
&- \frac{1}{2}\Big[\frac{1}{3}\,\bar{b}_N\,m_N[g_{\sigma N}\sigma_0]^3 + \frac{1}{2}\,\bar{c}_N\,[g_{\sigma N}\sigma_0]^4\Big]\,,
\end{aligned}$$

and

$$\begin{aligned}
P &= \sum_B (2\,J_B+1)\int_{\boldsymbol{q}^3}\Big\{\Sigma_S^B(\omega^B(\boldsymbol{q}),\boldsymbol{q})\,\Xi_S^B(\boldsymbol{q}) - \Big[\Sigma_V^B(\omega^B(\boldsymbol{q}),\boldsymbol{q}) + \frac{2}{3}\,|\boldsymbol{q}|\Big]\,\Xi_V^B(\boldsymbol{q})\\
&+ \Sigma_0^B(\omega^B(\boldsymbol{q}),\boldsymbol{q})\,\Xi_0^B(\boldsymbol{q})\Big\}\,\Theta^B(|\boldsymbol{q}|) \qquad (294)\\
&+ \frac{1}{2}\Big[\frac{1}{3}\,\bar{b}_N\,m_N\,[g_{\sigma N}\,\sigma_0]^3 + \frac{1}{2}\,\bar{c}_N\,[g_{\sigma N}\,\sigma_0]^4\Big\}\,.
\end{aligned}$$

G γ matrices in the self-consistent nucleon-antinucleon basis

To transform the spectral functions Ξ^B of Eq. (117) and self-energies of Eq. (105) to the self-consistent basis, knowledge of the following matrix elements is useful: Σ^B

$$< \Phi_l(p)|\ \gamma^0\ |\Phi_{l'}(p) > \ = \ \delta_{ll'}\ \frac{W(p)}{m^*(p)}\ , \tag{295}$$

$$< \Theta_l(p)|\ \gamma^0\ |\Theta_{l'}(p) > \ = \ \delta_{ll'}\ \frac{W(p)}{m^*(p)}\ , \tag{296}$$

$$< \Theta_l(p)|\ \gamma^0\ |\Phi_{l'}(p) > = < \Phi_l(p)|\ \gamma^0\ |\Theta_{l'}(p) > \ = \ \delta_{ll'}\ \frac{2\,l\,p^*(p)}{m^*(p)}\ , \tag{297}$$

$$< \Phi_l(p)|\ \boldsymbol{\gamma}\cdot\hat{\boldsymbol{p}}\ |\Phi_{l'}(p) > \ = \ \delta_{ll'}\ \frac{p^*(p)}{m^*(p)}\ , \tag{298}$$

$$< \Theta_l(p)|\ \boldsymbol{\gamma}\cdot\hat{\boldsymbol{p}}\ |\Theta_{l'}(p) > \ = \ \delta_{ll'}\ \frac{p^*(p)}{m^*(p)}\ , \tag{299}$$

$$< \Theta_l(p)|\ \boldsymbol{\gamma}\cdot\hat{\boldsymbol{p}}\ |\Phi_{l'}(p) > = < \Phi_l(p)|\ \boldsymbol{\gamma}\cdot\hat{\boldsymbol{p}}\ |\Theta_{l'}(p) > \ = \ \delta_{ll'}\ \frac{2\,l\,W(p)}{m^*(p)}\ . \tag{300}$$

The spinors Φ, Θ and functions W, m^* are defined in Eqs. (128) and (129) - (131), respectively.

H Integral equations of the T matrix

Use of the relations (138) and (139) and the assumption that the matrix elements of the nucleon spectral function with anti-nucleon spinors are negligible, leads to a suitable decoupling of the T-matrix equations in the self-consistent basis. Introducing the shorthand notation $T_P^{\Phi\Phi\,\Phi\Phi}(p',p) \equiv < \Phi_l(p), \Phi_{l'}(p')|T|\Phi_l(p), \Phi_{l'}(p') >$, $T_P^{\Theta\Phi\,\Phi\Theta}(p',p) \equiv < \Theta_l(p), \Phi_{l'}(p')|T|\Phi_l(p), \Theta_{l'}(p') >$ etc., the integral equations of the various amplitudes read

$$T_P^{\Phi\Phi\,\Phi\Phi}(p',p) = v_P^{\Phi\Phi\,\Phi\Phi}(p',p) + \int_{q^4} v^{\Phi\Phi\,\Phi\Phi}(p,q)\,\Lambda^{\Phi\Phi\,\Phi\Phi}(p_+,p_-)\,T_P^{\Phi\Phi\,\Phi\Phi}(q,p)\,, \quad (301)$$

$$T_P^{\Theta\Phi\,\Phi\Phi}(p',p) = v_P^{\Theta\Phi\,\Phi\Phi}(p',p) + \int_{q^4} v^{\Theta\Phi\,\Phi\Phi}(p,q)\,\Lambda^{\Phi\Phi\,\Phi\Phi}(p_+,p_-)\,T_P^{\Phi\Phi\,\Phi\Phi}(q,p)\,, \quad (302)$$

$$T_P^{\Phi\Phi\,\Theta\Phi}(p',p) = v_P^{\Phi\Phi\,\Phi\Phi}(p',p) + \int_{q^4} v^{\Phi\Phi\,\Phi\Phi}(p,q)\,\Lambda^{\Phi\Phi\,\Phi\Phi}(p_+,p_-)\,T_P^{\Phi\Phi\,\Theta\Phi}(q,p)\,, \quad (303)$$

$$T_P^{\Theta\Phi\,\Theta\Phi}(p',p) = v_P^{\Theta\Phi\,\Theta\Phi}(p',p) + \int_{q^4} v^{\Theta\Phi\,\Phi\Phi}(p,q)\,\Lambda^{\Phi\Phi\,\Phi\Phi}(p_+,p_-)\,T_P^{\Phi\Phi\,\Theta\Phi}(q,p)\,, \quad (304)$$

$$T_P^{\Theta\Phi\,\Phi\Theta}(p',p) = v_P^{\Theta\Phi\,\Phi\Theta}(p',p) + \int_{q^4} v^{\Theta\Phi\,\Phi\Phi}(p,q)\,\Lambda^{\Phi\Phi\,\Phi\Phi}(p_+,p_-)\,T_P^{\Phi\Phi\,\Theta\Phi}(q,p)\,. \quad (305)$$

The four-momenta $p_\pm$ are denfined by $p_\pm = P \pm q$, with $P = (P^0, \boldsymbol{p})$ and $q = (q^0, \boldsymbol{q})$. One sees that Eqs. (301) and (303) represent integral equations for the amplitudes $T^{\Phi\Phi\,\Phi\Phi}$ and $T^{\Phi\Phi\,\Theta\Phi}$, respectively. All remaining amplitudes are obtained by simple integration. According to the possible helicity degrees of freedeom, each of the above amplitudes has 16 components. By exploiting the invarianz properties of the T-matrix, one finally arrives at 6 independent components for $T^{\Phi\Phi\,\Phi\Phi}$ and 8 components for $T^{\Phi\Phi\,\Theta\Phi}$. To make these systems of equations numerically tractable, a partical-wave expansion of the matrix elements of T and v has been performed [60].

The intermediate Λ^{00} nucleon-nucleon propagator in the above equations is given by

$$\begin{aligned}\Lambda^{\Phi\Phi\,\Phi\Phi}(p_+,p_-) &\equiv < \Phi_l(p_+), \Phi_{l'}(p_-)|\,\Lambda^{00}(p_+,p_-)\,|\Phi_l(p_+), \Phi_{l'}(p_-) > \\ &= 2\pi\,\delta\Big(q^0 - \omega^N(|\boldsymbol{p}_+|) + \frac{P^0}{2}\Big) \\ &\quad \times \frac{n(\omega^{0\,N}(|\boldsymbol{p}_+|), |\boldsymbol{p}_+|)\; n(P^0 - \omega^{0\,N}(|\boldsymbol{p}_+|), |\boldsymbol{p}_+|)}{P^0 - \omega^{0\,N}(|\boldsymbol{p}_+|) - \omega^{0\,N}(|\boldsymbol{p}_-|) + i\eta}\,,\end{aligned} \quad (306)$$

with

$$n^N(p) \equiv n(p^0,|\boldsymbol{p}|) \equiv <\bar{\Phi}_l(p)|\,\Xi^N(\boldsymbol{p})\,|\Phi_{l'}(p)> = \Xi^N_S(|\boldsymbol{p}|) + \Xi^N_V(|\boldsymbol{p}|)\,\frac{p^*(p^0,|\boldsymbol{p}|)}{m^*(p^0,|\boldsymbol{p}|)} + \Xi^N_0(|\boldsymbol{p}|)\,\frac{W(p^0,|\boldsymbol{p}|)}{m^*(p^0,|\boldsymbol{p}|)}\,. \quad (307)$$

It is independent of l and l' and can therefore be evaluated for fixed values of l and l'. According to the regularization procedure, the intermediate propagator is restricted to positive-energy spinors.

The mass operator components Σ_S, Σ_V, and Σ_0 can be obtained from those determined in the self-consistent basis (Eqs. (141) - (143)):

$$\Sigma_S(p) = \frac{1}{2}\left[\,\Sigma^{\Phi\Phi}(p) - \Sigma^{\Theta\Theta}(p)\,\right], \quad (308)$$

$$\Sigma_V(p) = \frac{A(p)\,|\boldsymbol{p}| \pm B(p)\sqrt{\boldsymbol{p}^2 + [A(p)^2 - B(p)^2]\,[m^*(p)]^2}}{A(p)^2 - B(p)^2} - |\boldsymbol{p}|\,, \quad (309)$$

$$\Sigma_0(p) = \frac{1}{2}\,\frac{W(p)}{m^*(p)}\left[\,\Sigma^{\Phi\Phi}(p) + \Sigma^{\Theta\Theta}(p)\,\right] - \frac{p^*(p)}{m^*(p)}\,\Sigma^{\Theta\Phi}(p)\,, \quad (310)$$

with the definitions

$$A(p) \equiv 1 + \frac{\Sigma^{\Phi\Phi}(p) + \Sigma^{\Theta\Theta}(p)}{2\,m^*(p)}\,, \quad (311)$$

$$B(p) \equiv \frac{\Sigma^{\Theta\Phi}(p)}{m^*(p)}\,. \quad (312)$$

The energy density and nuclear density of Eqs. (162), (164), and (168), respectively, can be expressed in the self-consistent basis as

$$\epsilon^0_{\rm Bary} = 2\sum_B (2J_B+1)\int_{\boldsymbol{p}^3}\left[\frac{m_B\,m^*_B(p) + |\boldsymbol{p}|\,p^*_B(p)}{m^*_B(p)}\right]_{p^0=\omega^B(|\boldsymbol{p}|)} n^B(|\boldsymbol{p}|)\Theta^B(|\boldsymbol{p}|)\,, \quad (313)$$

$$\epsilon^0_{\rm Mes} + \epsilon_{\rm Int} = \sum_B (2J_B+1)\int_{\boldsymbol{p}^3}\left[\Sigma^{B\,\Phi\Phi}(p)\right]_{p^0=\omega^B(|\boldsymbol{p}|)} n^B(|\boldsymbol{p}|)\;\Theta^B(|\boldsymbol{p}|)\,, \quad (314)$$

$$\varrho = 2\sum_B (2J_B+1)\int_{\boldsymbol{p}^3}\left[\frac{W_B(p)}{m^*_B(p)}\right]_{p^0=\omega^B(|\boldsymbol{p}|)} n^B(|\boldsymbol{p}|)\;\Theta^B(|\boldsymbol{p}|)\,, \quad (315)$$

where n^B is given by Eq. (140).

I Non-relativistic limit

In the non-relativistic treatment the self-energies of Eq. (105) satisfy

$$\Sigma_S(p) \rightarrow 0\,, \qquad \Sigma_V(p) \rightarrow 0\,, \qquad \Sigma_0(p) \rightarrow \Sigma(p)\,, \tag{316}$$

which leads to the replacements

$$m_N^* \rightarrow m_N\,, \qquad p^* \rightarrow p\,, \qquad W \rightarrow \sqrt{m_N^2 + \boldsymbol{p}^2} \approx m_N + \frac{\boldsymbol{p}^2}{2\,m_N}\,. \tag{317}$$

The relativistic energy-momentum relation of Eq. (119) is to be replaced by

$$\omega^N(\boldsymbol{p}) \rightarrow \omega^N(\boldsymbol{p}) - m_N \equiv \epsilon^N(\boldsymbol{p}) = \frac{\boldsymbol{p}^2}{2\,m_N} + \Sigma(\epsilon^N(\boldsymbol{p}) - \mu^N, \boldsymbol{p})\,. \tag{318}$$

The spectral function $\Xi^N(\boldsymbol{p})$ of Eq. (115) plays the role of a momentum-density function, i.e.

$$\Xi^N(p^0, \boldsymbol{p}) = n^N(|\boldsymbol{p}|)\ \delta(p^0 - \epsilon^N(\boldsymbol{p}) + \mu^N)\,, \tag{319}$$

with (cf. Eq. (140))

$$n^N(|\boldsymbol{p}|) \equiv \left| 1 - \frac{\partial \Sigma}{\partial \omega} \right|^{-1}_{\omega^N = \epsilon^N(\boldsymbol{p})}\,. \tag{320}$$

Equations (319), (320) are well-know results of the non-relativistic Green's function theory [42]. For the expressions of energy density and nuclear density follows from Eqs. (162), (164) and (168) (or alternatively from Eqs. (313) - (315))

$$\epsilon = 2 \int_{\boldsymbol{p}^3} \left[\frac{\boldsymbol{p}^2}{2\,m_N} + \frac{1}{2}\,\Sigma(\epsilon^N(\boldsymbol{p}) - \mu^N, \boldsymbol{p})\right] n^N(|\boldsymbol{p}|)\,\Theta^N(|\boldsymbol{p}|)\,, \tag{321}$$

$$\varrho = 2 \int_{\boldsymbol{p}^3} n^N(|\boldsymbol{p}|)\,\Theta^N(|\boldsymbol{p}|)\,. \tag{322}$$

We recall that in the non-relativistic Λ theory the single-particle basis are *a priori* given plane-wave functions. In the relativistic approach the basis consists of self-consistent, effective Dirac spinors. Their density dependence has an important influence on the saturation mechanism of nuclear matter [11] and hence on the nuclear equation of state itself. The integral equation of the T matrix in the plane-wave basis has the form [42]

$$\begin{aligned} &< \boldsymbol{p}|\, T^{ij}_{\boldsymbol{P}}(E) \ - \ 2\,v^{\mathrm{a}}\,|\boldsymbol{p}' > \\ &= \int d^3\boldsymbol{q} < \boldsymbol{p}|\, v^{\mathrm{a}}\,|\boldsymbol{q} > \ \Lambda^{ij}(\frac{\boldsymbol{P}}{2} + \boldsymbol{q}, \frac{\boldsymbol{P}}{2} - \boldsymbol{q}; E) < \boldsymbol{q}|\, T^{ij}_{\boldsymbol{P}}(E)\,|\boldsymbol{p}' >\,, \end{aligned} \tag{323}$$

where $2\,v^{\mathrm{a}} = v - v^{\mathrm{ex}}$ denotes the anti-symmetrized nucleon-nucleon interaction in free space [42]. The non-relstivistic Λ^{00} nuclear matter propagator has the form (compare with Eq. (126))

$$\Lambda^{00}(\frac{\boldsymbol{P}}{2}+\boldsymbol{q},\frac{\boldsymbol{P}}{2}-\boldsymbol{q};E) \;=\; \left[E \;-\; \frac{\left(\frac{1}{2}\boldsymbol{P}+\boldsymbol{q}\right)}{2\,m_N} \;-\; \frac{\left(\frac{1}{2}\boldsymbol{P}-\boldsymbol{q}\right)}{2\,m_N} \;+\; 2\,\mu^N\right]^{-1} . \quad (324)$$

The on-shell mass operator is given by ($\epsilon_1 = \epsilon(\boldsymbol{p}_1) - \mu^N$)

$$\begin{aligned}\Sigma(\epsilon_1,\boldsymbol{p}_1) \;&=\; \frac{1}{2}\int d^3\boldsymbol{p}_2 \left[\left\langle\frac{\boldsymbol{p}_1-\boldsymbol{p}_2}{2}\right| T^{00}_{\boldsymbol{p}_1+\boldsymbol{p}_2}(\epsilon_1+\epsilon^N(\boldsymbol{p}_2)-\mu^N)\left|\frac{\boldsymbol{p}_1-\boldsymbol{p}_2}{2}\right\rangle\right. \quad (325)\\ &\qquad \left. -\left\langle\frac{\boldsymbol{p}_1-\boldsymbol{p}_2}{2}\right| T^{00}_{\boldsymbol{p}_1+\boldsymbol{p}_2}(\epsilon_1+\epsilon^N(\boldsymbol{p}_2)-\mu^N)\left|\frac{\boldsymbol{p}_2-\boldsymbol{p}_1}{2}\right\rangle\right] .\end{aligned}$$

Acknowledgements: One of us (F. W.) would like to thank the President of the Max-Kade Foundation of New York for a grant. This work was supported by the Director, Office of Energy Research, Office of High Energy and Nuclear Physics, Division of Nuclear Physics, of the U.S. Department of Energy under Contract DE-AC03-76SF00098, and by the Max Kade Foundation of New York.

References

[1] T. Gold, Nature **218** (1968) 731.

[2] D. C. Backer and S. R. Kulkarni, Physics Today, **43** (1990) 26.

[3] J. L. Friedman, J. R. Ipser, and L. Parker, Astrophys. J. **304** (1986) 115.

[4] F. Weber, N. K. Glendenning, and M. K. Weigel, Astrophys. J. **373** (1991) 579.

[5] F. Weber and N. K. Glendenning, *Exact versus Approximate Solution of Einstein's Equations for Rotating Neutron Stars*, (1991), (LBL-29785).

[6] F. Weber and N. K. Glendenning, *Applicability of Hartle's Method for the Construction of General Relativistic Rotating Neutron Star Models*, October, 1990 (LBL-29671).

[7] J. B. Hartle, Astrophys. J. **150** (1967) 1005.

[8] J. B. Hartle and K. S. Thorne, Astrophys. J. **153** (1968) 807.

[9] N. K. Glendenning, Phys. Lett. **114B** (1982) 392;
N. K. Glendenning, Astrophys. J. **293** (1985) 470;
N. K. Glendenning, Z. Phys. A **326** (1987) 57;
N. K. Glendenning, Z. Phys. A **327** (1987) 295.

[10] F. Weber and M. K. Weigel, Nucl. Phys. **A505** (1989) 779, and references contained therein.

[11] P. Poschenrieder and M. K. Weigel, Phys. Lett. **200B** (1988) 231;
P. Poschenrieder and M. K. Weigel, Phys. Rev. C **38** (1988) 471.

[12] R. Machleidt, K. Holinde, and Ch. Elster, Phys. Rep. **149** (1987) 1.

[13] K. Holinde, K. Erkelenz, and R. Alzetta, Nucl. Phys. **A194** (1972) 161; **A198** (1972) 598.

[14] B. D. Serot and J. D. Walecka, Adv. Nucl. Phys. **16** (1986) 1.

[15] L. S. Celenza and C. M. Shakin, *Relativistic Nuclear Structure Physics*, World Scientific Lecture Notes in Physics, Vol. 2, World Scientific, Singapore, 1986.

[16] C. J. Horowitz and B. D. Serot, Nucl. Phys. **A464** (1987) 613.

[17] B. ter Haar and R. Malfliet, Phys. Rep. **149** (1987) 208.

[18] L. Wilets, Green's functions method for the relativistic field theory many-body problem, in *Mesons in nuclei*, Vol. III, ed. M. Rho, D. Wilkinson, North-Holland, Amsterdam, 1979.

[19] S. L. Shapiro and S. A. Teukolsky, *Black Holes, White Dwarfs, and Neutron Stars*, John Wiley & sons, N. Y., 1983.

[20] N. K. Glendenning, *Neutron Stars, Fast Pulsars, Supernovae and the Equation of State of Dense Matter*, in: "The Nuclear Equation of State", ed. by W. Greiner and H. Stöcker, NATO ASI Series, Phys. Vol. 216 A, Plenum Press, New York, p. 751.

[21] B. Friedman and V. R. Pandharipande, Nucl. Phys. **A361** (1981) 502.

[22] K. Schwarzschild, *Sitzber. Deut. Akad. Wiss. Berlin, Kl. Math.-Phys. Tech.*, p. 424-434, 1916.

[23] Ch. W. Misner, K. S. Thorne, and J. A. Wheeler, *Gravitation*, W. H. Freeman and Company, San Francisco, 1973.

[24] J. R. Oppenheimer and G. M. Volkoff, Phys. Rev. **55** (1939) 374.

[25] R. L. Bowers, A. M. Gleeson, and R. D. Pedigo, Phys. Rev. D **12** (1975) 3043; 3056.

[26] W. D. Arnett and R. L. Bowers, Astrophys. J. Suppl. **33** (1977) 415.

[27] F. Weber and M. K. Weigel, Nucl. Phys. **A493** (1989) 549.

[28] J. M. Irvine, *Neutron Stars*, Clarendon Press, Oxford, 1978.

[29] E. M. Butterworth and J. R. Ipser, Astrophys. J. **204** (1976) 200.

[30] R. C. Kapoor and B. Datta, Mon. Not. R. Astr. Soc. **209** (1984) 895.

[31] H. Heintzmann, W. Hillebrandt, M. F. Eid, and E. R. Hilf, Z. Naturforsch. **29a** (1974) 933.

[32] G. Baym, C. Pethick, and P. Sutherland, Astrophys. J. **170** (1971) 299.

[33] A. Ray and B. Datta, Astrophys. J. **282** (1984) 542.

[34] J. L. Friedman, J. R. Ipser, and L. Parker, Phys. Rev. Lett. **62** (1989) 3015.

[35] P. Haensel and J. L. Zdunik, Nature **340** (1989) 617.

[36] J. M. Lattimer, M. Prakash, D. Masak and A. Yahil, Astrophys. J. **355** (1990) 241.

[37] B. Datta and A. Ray, Mon. Not. R. Astr. Soc. **204** (1983) 75P.

[38] S. Chandrasekhar, *Ellipsoidal Figures of Equilibrium*, Yale University Press, New Haven, 1969.

[39] J. L. Friedman and B. F. Schutz, Astrophys. J. **222** (1978) 281.

[40] J. L. Friedman, Phys. Rev. Lett. **51** (1983) 11.

[41] V. R. Pandharipande, Nucl. Phys. **A178** (1971) 123.

[42] M. K. Weigel and G. Wegmann, Fortschr. Phys. **19** (1971) 451.

[43] F. Weber and M. K. Weigel, Phys. Rev. C **32** (1985) 2141.

[44] H. Muether, M. Prakash, and T. L. Ainsworth, Phys. Lett. **199B** (1987) 469.

[45] N. K. Glendenning, Astrophys. J. **293** (1985) 470.

[46] R. F. Dashen and R. Rajaraman, Phys. Rev. D **10** (1974) 696; 708.

[47] N. K. Glendenning, Phys. Lett. **185B** (1987) 275;
N. K. Glendenning, Nucl. Phys. **A469** (1987) 600.

[48] D. Lurie, *Particles and Fields*, Wiley, New York, 1968.

[49] S. I. A. Garpman, N. K. Glendenning, and Y. J. Karant, Nucl. Phys. **A322** (1979) 382.

[50] F. Weber and M. K. Weigel, Z. Phys. A**330** (1988) 249.

[51] F. Weber and M. K. Weigel, J. Phys. G **15** (1989) 765.

[52] L. Dolan and R. Jackiw, Phys. Rev. D **9** (1974) 3320.

[53] F. Weber and M. K. Weigel, Europhys. Lett. **12** (1990) 603.

[54] R. L. Bowers and R. L. Zimmerman, Phys. Rev. D **7** (1973) 296.

[55] N. K. Glendenning, Phys. Lett. **114B** (1982) 392; Astrophys. J. **293** (1985) 470; Z. Phys. A **326** (1987) 57; ibid. **327** (1987) 295; Nucl. Phys. **A493** (1989) 521.

[56] N. K. Glendenning, Nucl. Phys. **A493** (1989) 521.

[57] Q. Ho-Kim and F. C. Khanna, Ann. Phys. **86** (1974) 233.

[58] G. Wegmann, Z. Phys. **211** (1968) 235.

[59] G. Wegmann and M. K. Weigel, Phys. Lett. **26B** (1968) 245.

[60] P. Poschenrieder, Dissertation, University of Munich, 1987.

[61] K. Erkelenz, Phys. Rep. C 13 (1974) 191.

[62] J. D. Bjorken and S. D. Drell, *Relativistic Quantum Fields*, Mc Graw-Hill, New York, 1965.

[63] K. Holinde, Phys. Rep. **68** (1981) 121.

[64] H. P. Duerr, Phys. Rev. **103** (1956) 469;.

[65] J. D. Walecka, Ann. Phys. **83** (1974) 491.

[66] M. Jetter, F. Weber, and M. K. Weigel, Europhys. Lett. **14** (1991) 633.

[67] J. Zimanyi and S. A. Moszkowski, Phys. Rev. C **42** (1990) 1416.

[68] N. K. Glendenning, F. Weber, and S. A. Moszkowski, *Neutron and Hybrid Stars in the Derivative Coupling Model*, March, 1991 (LBL-30296).

[69] G. Baym, Nuclear Physics with Heavy Ions and Mesons, Vol. 2, Les Houches Session XXX, ed. R. Balian, M. Rho and G. Ripka (North Holland, Amsterdam, 1978) p. 745.

[70] B. Banerjee, N. K. Glendenning, and M. Gyulassy, Nucl. Phys. **A361** (1981) 326.

[71] N. K. Glendenning, B. Banerjee, and M. Gyulassy, Ann. Phys. (N. Y.) **149** (1983) 1.

[72] N. K. Glendenning, P. Hecking, and V. Ruck, Ann. Phys. (N. Y.) **149** (1983) 22.

[73] D. K. Campbell,*Field Theory, chiral symmetry, and pion-nucleus interaction*, in Nuclear Physics with heavy ions and mesons, vol. 2, Les Houches, North-Holland, Amsterdam, 1977, p. 549.

[74] R. Machleidt, Adv. Nucl. Phys. **19** (1989) 188.

[75] Particle Data Group, Rev. Mod. Phys. **48** (1976) 30.

[76] J. J. Sakurai, Phys. Rev. Lett. **17** (1966) 1021.

[77] A. Bouyssy, S. Marcos, J. F. Mathiot, and N. Van Giai, Phys. Rev. Lett. **55** (1985) 1731.

[78] B. K. Harrison and J. A. Wheeler, cited in B. K. Harrison et al. *Gravitation Theory and Gravitational Collapse*, University of Chicago Press, Chicago, 1965.

[79] J. W. Negele and D. Vautherin, Nucl. Phys. **A178** (1973) 123.

[80] N. K. Glendenning, Phys. Rev. C **37** (1988) 2733.

[81] B. M. Waldhauser, J. A. Maruhn, H. Stöcker, and W. Greiner, Phys. Rev. C **38** (1988) 1003.

[82] H. A. Bethe and M. Johnson, Nucl. Phys. **A230** (1974) 1.

[83] J. B. Hartle and M. W. Munn, Astrophys. J. **198** (1975) 467.

[84] J. L. Friedman, J. R. Ipser, and R. D. Sorkin, Astrophys. J. **325** (1988) 722.

[85] L. P. Kadanoff and G. Baym *Quantum Statistical Mechanics*, Benjamin, New York, 1962.

[86] C. W. Bernard, Phys. Rev. D **9** (1974) 3312.

[87] E. V. Shuryak, Phys. Rep. **61** (1980) 71.

[88] D. J. Gross, R. D. Pisarski, L. G. Yaffe, Rev. Mod. Phys. **53** (1981) 43.

[89] P. C. Martin and J. Schwinger, Phys. Rev. **115** (1959) 1342.

[90] R. D. Puff, Ann. Phys. **13** (1961) 317.

List of Figures

List of Tables

LAWRENCE BERKELEY LABORATORY
UNIVERSITY OF CALIFORNIA
INFORMATION RESOURCES DEPARTMENT
BERKELEY, CALIFORNIA 94720